DISCOVERY OF CD147 MOLECULAR FUNCTION BY PHAGE-DISPLAYED CD147 ECTODOMAIN VIA gpVIII

NUTJEERA INTASAI

A THESIS SUBMITTED IN PARTIAL FULFILLMENT
OF THE REQUIREMENTS FOR
THE DEGREE OF DOCTOR OF PHILOSOPHY
(MEDICAL TECHNOLOGY)
FACULTY OF GRADUATE STUDIES
MAHIDOL UNIVERSITY
2005

ISBN 974-04-6258-8
COPYRIGHT OF MAHIDOL UNIVERSITY

Thesis

Entitled

DISCOVERY OF CD147 MOLECULAR FUNCTION BY PHAGE-DISPLAYED CD147 ECTODOMAIN VIA gpVIII

……...
Miss Nutjeera Intasai
Candidate

……...
Asst. Prof. Chatchai Tayapiwatana, Ph..D.
Major-advisor

……...
Assoc. Prof. Watchara Kasinrerk, Ph.D.
Co-advisor

……...
Assoc. Prof. Virapong Prachayasittikul, Ph.D.
Co-advisor

……...
Assoc. Prof. Rassmidara Hoonsawat, Ph.D.
Dean
Faculty of Graduate Studies

……...
Assoc. Prof. Virapong Prachyasittikul, Ph.D.
Chair
Doctor of Philosophy programme in Medical Technology
Faculty of Medical Technology

Thesis

Entitled

DISCOVERY OF CD147 MOLECULAR FUNCTION BY PHAGE-DISPLAYED CD147 ECTODOMAIN VIA gpVIII

was submitted to the Faculty of Graduate Studies, Mahidol University
For the degree of Doctor of Philosophy (Medical Technology)
on
June 2, 2005

……...
Miss Nutjeera Intasai
Candidate

……...
Asst. Prof. Chatchai Tayapiwatana, Ph..D.
Chair

……...
Assoc. Prof. Watchara Kasinrerk, Ph.D.
Member

……...
Assoc. Prof. Virapong Prachyasittikul, Ph.D.
Member

……...
Assoc. Prof. Surasakdi Wongratanacheewin, Ph.D.
Member

……...
Assoc. Prof. Rassmidara Hoonsawat, Ph.D.
Dean
Faculty of Graduate Studies
Mahidol University

……...
Assoc. Prof. Chatchai Sornchai, M.D.
Dean
Faculty of Medical Technology
Mahidol University

ACKNOWLEDGEMENTS

I would like to express my deepest attitude and sincere appreciation to my supervisor, Assist. Prof. Dr. Chatchai Tayapiwatana, for his excellent guidance, valuable suggestions, advice, enthusiastic, continuous support, and encouragement throughout my study, and for the revision of this thesis and manuscripts

I am extremely grateful to Assoc. Prof. Dr. Watchara Kasinrerk, for kindly gift the CD147 cDNA and monoclonal antibodies, and cell lines throughout my study, his constructive suggestions and comments, kind supports, revision the manuscripts and supervisory thesis committee. My grateful appreciation is also extended to Assoc. Prof. Dr. Virapong Prachayasittikul and Assoc. Prof. Dr. Surasakdi Wongratanacheewin for their constructive comments, suggestions and kindness in serving on the thesis defense committee.

A part of my research was performed at Manitoba Institute of Cell Biology (MICB) and the Genomic Centre of Cancer Research and Diagnosis (GCCRD), the University of Manitoba, Canada. I am eternally grateful to Prof. Dr. Sabine Mai for giving me a great opportunity to work in her lab, invaluable advice, kind help, continuous support and encouragement during I was in her lab. I also especially thank to Dr. Fabien Kuttle for his excellent advice, consultant, kindness and sharing his knowledge; Dr. Alice Ya-Chun Chuang and Amanda Guffei for their technical training, help, kindness, and wonderful friend during working in Dr. Mai's lab. I would like to thanks all staffs in Dr. Mai's lab for providing me a technical training, warm helpful and friendly atmosphere. In addition, my gratitude is extended to Dr. Edward Rector for his excellent advice and technical support.

I am greatly indebted Faculty of Associated Medical Sciences, Chiang Mai University, for providing the scholarship from the Thai Staff Development Project of Ministry of University Affair; the Canadian Institutes of Health Research (CIHR) Strategic Training Program "Innovative Technologies in Multidisciplinary Health Research Training" Canada for financial supporting during my research in Canada; and The Thailand Research Fund and the National Center for Genetic Engineering and Biotechnology (BIOTEC) for additional support.

I would like to specially acknowledge all staffs in Dr. Chatchai's lab and Dr. Watchara's lab for their kindness and contributions for technical training throughout the work. I am grateful to all personnel and faculty members for their assistance in using the equipment at Faculty of Associated Medical Sciences, Chiang Mai University. I am also thankful to all my friends and all staffs at Faculty of Medical Technology, Mahidol University for their endless help and sharing a good time together.

Finally, I would like to express my deepest gratitude to my parents for their infinite love, constant trust and great support. In addition, I would like to extend my gracious thanks to the Mendoza family for their love, support and encouragement throughout my study in Canada.

Nutjeera Intasai

DISCOVERY OF CD147 MOLECULAR FUNCTION BY PHAGE-DISPLAYED CD147 ECTODOMAIN VIA gpVIII

NUTJEERA INTASAI 4437274 MTMT/D

Ph.D. (MEDICAL TECHNOLOGY)

THESIS ADVISORS: CHATCHAI TAYAPIWATANA, Ph.D., WATCHARA KASINRERK, Ph.D., VIRAPONG PRACHAYASITTIKUL, Ph.D.

ABSTRACT

CD147 is a broadly expressed cell surface molecule which is important for the immunological function. However, its function is hitherto largely unclear. Phage display technology is applied in production of multivalent CD147 extracellular domain (CD147Ex) on phage particle to enhance the functional affinity of CD147 and used for functional study of CD147. A phagemid expressing CD147Ex was constructed and used to produce phage display CD147Ex-gpVIII fusion protein in TG1 *Escherichia coli*. Displaying of CD147Ex via gpVIII was successfully increased when growing the transformed TG1 at 25 ^{o}C with simultaneous IPTG-stimulation and helper phage. By sandwich ELISA, incorporation of the CD147Ex into phage particle was confirmed. The correct size of the CD147Ex-gpVIII fusion protein at 28 kDa was demonstrated by Western immunoblotting. Cellular morphological change in the monocytic cell line, U937, incubated with multivalent CD147 phages was observed after 24 h of cultivation and cell propagation ceased after 48 h of incubation. Cytotoxicity of CD147 phage on U937 cells was further analyzed by EthD-1/calcein double staining. In contrast to wild-type phage, dual-colour fluorescence in U937 cells induced with recombinant phage, which correlated with the apoptotic appearance, was observed. The level of cleaved caspase-3 in U937 cells incubated with multivalent CD147 phage was also measured, but was not as high as in U937 cells stimulated with cisplatin when evaluated by flow cytometry. When quantified by immunocytochemistry, 12.8% of multivalent CD147-activated U937 cells with apoptotic nucleus harbored substantial amount of cleaved caspase-3, in contrast to 41% of cisplatin-induced U937 cells. These results suggest that the CD147-induced cell death program may partially involve a caspase dependent pathway. The binding of multivalent CD147 phage on cell surface of U937 cells was confirmed by ELISA and immunocytochemistry. In addition, apoptotic nuclei were found to coordinate with U937-bound phage. This function of CD147 in triggering apoptosis implies the existence of CD147 counter-receptor (s) on the U937 cell membrane.

KEY WORDS: PHAGE DISPLAY, gpVIII, CD147, CELL SURFACE MOLECULES, APOPTOSIS

109 p ISBN 974-04-6258-8

การค้นพบหน้าที่ในระดับโมเลกุลของ CD147 โดยใช้เฟจที่แสดงบริเวณภายนอกของโมเลกุล CD147 ผ่านจีพีแปด (DISCOVERY OF CD147 MOLECULAR FUNCTION BY PHAGE-DISPLAYED CD147 ECTODOMAIN VIA gpVIII)

ณัฐจีรา อินต๊ะใส 4437274 MTMT/D

ปร.ด. (เทคนิคการแพทย์)

คณะกรรมการควบคุมวิทยานิพนธ์ : ชัชชัย ตะยาภิวัฒนา, ปร.ด., วัชระ กสิณฤกษ์, ปร.ด., วีระพงศ์ ปรัชชญาสิทธิกุล, ปร.ด.

บทคัดย่อ

CD147 เป็นโมเลกุลบนผิวเซลล์ทั่วไปที่ความสำคัญต่อการทำงานของระบบภูมิคุ้มกัน อย่างไรก็ตามหน้าที่ของโมเลกุล CD147 ยังไม่เป็นที่ทราบแน่ชัด การศึกษานี้มีวัตถุประสงค์ที่จะใช้ phage display technology มาประยุกต์ใช้ในการผลิตบริเวณภายนอกของโมเลกุล CD147 (CD147Ex) หลายโมเลกุลบนเฟจเพื่อใช้ในการเพิ่ม functional affinity ของ CD147 และใช้สำหรับศึกษาหน้าที่ของ CD147 การผลิตเฟจที่แสดงบริเวณภายนอกของ CD147 หลายโมเลกุล (phage-displayed CD147ExgpVIII) ประสบผลสำเร็จดียิ่งขึ้นเมื่อเพาะเลี้ยงแบคทีเรีย TG1 ที่มีเฟจมิดที่แสดง CD147Ex ที่ 25 องศาเซลเซียสและกระตุ้นด้วย IPTG ในเวลาเดียวกับ helper phage infection เมื่อนำ phage-displayed CD147ExgpVIII มาเลี้ยงร่วมกับเซลล์ไลน์ต่างๆ พบว่าสามารถทำให้เซลล์ U937 เปลี่ยนแปลงสัณฐานวิทยาและยับยั้งการเพิ่มจำนวนของเซลล์เมื่อเวลาผ่านไป 24 ชั่วโมงและ 48 ชั่วโมงตามลำดับ โดยพบว่าเซลล์มีลักษณะการตายแบบอะพอพโตสิส โดยที่ระดับของ cleaved caspase-3 ในเซลล์ U937 ที่ถูกกระตุ้นด้วย phage-displayed CD147ExgpVIII ไม่สูงเท่ากับเซลล์ U937 ที่ถูกกระตุ้นด้วย cisplatin ซึ่งแสดงให้เห็นว่าการตายของเซลล์ที่ถูกกระตุ้นด้วย phage-displayed CD147ExgpVIII นี้อาจมี caspase dependent pathway เกี่ยวข้องเพียงบางส่วนเท่านั้น นอกจากนี้ได้พบว่า phage-displayed CD147ExgpVIII เกาะอยู่บนผิวของเซลล์ U937 โดยเซลล์เหล่านี้มีนิวเคลียสแบบอะพอพโตสิสร่วมด้วย งานวิจัยนี้ได้พบหน้าที่ใหม่ของ CD147 ในการกระตุ้นให้เซลล์ U937 ตายแบบอะพอพโตสิส และแสดงโดยนัยว่ามีตัวรับของโมเลกุล CD147 บนผิวเซลล์ U937

109 หน้า ISBN 974-04-6258-8

CONTENTS

CONTENTS (CONTINUED)

CONTENTS (CONTINUED)

CONTENTS (CONTINUED)

CONTENTS (CONTINUED)

LIST OF TABLES

LIST OF FIGURES

LIST OF FIGURES (CONTINUED)

LIST OF ABBREVIATIONS

Ab	Antibody
bp	Base pair
BSA	Bovine serum albumin
$CaCl_2$	Calcium chloride
cfu	Colony forming unit
E. coli	*Escherichia coli*
EDTA	Ethylenediaminetetra-acetic acid
ELISA	Enzyme linked immunosorbent assay
FACS	Fluorescence-activated cell sorter
FBS	Fetal bovine serum
g	Gram
h	Hour
HBSS	Hank’s balanced salt solution
HCl	Hydrochloric acid
HRP	Horseradish peroxidase
IgG	Immunoglobulin G
IgM	Immunoglobulin M
Igs	Immunoglobulins
IPTG	Isopropyl-β-D-thiogalactopyranoside
KCl	Potassium chloride
kDa	Kilodalton

LIST OF ABBREVIATIONS (CONTINUED)

KH_2PO_4	Potassium phosphate monobasic
LB	Luria-Bertani
mAbs	Monoclonal antibodies
mg	Milligram
MgCl2	Magnesium chloride
min	Minute
ml	Milliliter
MW	Molecular weight
Na_2CO_3	Sodium carbonate
Na_2HPO_4	Sodium phosphate dibasic
NaCl	Sodium chloride
ng	Nanogram
OD	Optical density
PBS	Phosphate buffer saline
PAGE	Polyacrylamide gel electrophoresis
PCR	Polymerase chain reaction
PEG	Polyethylene glycol
pfu	Plaque forming unit
rpm	Round per minute
SDS	Sodium dodecyl sufate
sec	Second
TAE	Tris-acetate/EDTA electrophoresis buffer

LIST OF ABBREVIATIONS (CONTINUED)

μg	Microgram
μl	Microliter

Available online at www.sciencedirect.com
SCIENCE DIRECT®
Protein Expression and Purification 32 (2003) 323–331
Protein Expression & Purification
www.elsevier.com/locate/yprep

Construction of high-density display of CD147 ectodomain on VCSM13 phage via gpVIII: effects of temperature, IPTG, and helper phage infection-period

Nutjeera Intasai,[a] Pramoon Arooncharus,[b] Watchara Kasinrerk,[b,c] and Chatchai Tayapiwatana[b,*]

[a] *Department of Clinical Microscopy, Faculty of Associated Medical Sciences, Chiang Mai University, Chiang Mai 50200, Thailand*
[b] *Department of Clinical Immunology, Faculty of Associated Medical Sciences, Chiang Mai University, Chiang Mai 50200, Thailand*
[c] *Medical Biotechnology Unit, The National Center for Genetic Engineering and Biotechnology, The National Science and Technology Development Agency, Chiang Mai University, Chiang Mai 50200, Thailand*

Received 28 June 2003, and in revised form 25 August 2003

Abstract

Production of VCSM13 phage displaying a high density of CD147 ectodomain (CD147Ex) was achieved when culturing conditions were modulated. A phagemid expressing CD147Ex was constructed and used to produce phage display CD147Ex gpVIII fusion protein in TG1 *Escherichia coli*. Displaying of CD147Ex via gpVIII was successfully increased when growing the transformed TG1 at 25 °C with IPTG-stimulation. In addition to temperature and IPTG-stimulation, the VCSM13 helper phage infection-period particularly affected the insertion of CD147Ex into phage progeny. By sandwich ELISA, incorporation of the CD147Ex into phage particle was confirmed. The correct size of the CD147Ex-gpVIII fusion protein at 28 kDa was demonstrated by Western immunoblotting. Multivalent display of CD147Ex on phage particles will be valuable in discovering its ligand partner.
© 2003 Elsevier Inc. All rights reserved.

Keywords: Phage display; CD147; gpVIII; Expression

The human leukocyte surface molecule CD147 is a 50–60 kDa-glycoprotein of the immunoglobulin superfamily that is broadly expressed on human peripheral blood cells, hematopoietic, and non-hematopoietic cell lines [1]. Within peripheral blood cells, CD147 expressed on all leukocytes, red blood cells, platelets, and endothelial cells. It has the typical feature of a type I integral membrane glycoprotein. CD147 is also known as human basigin [2], M6 antigen [3], and extracellular matrix metalloproteinase inducer (EMMPRIN) [4]. CD147 expression in T-cells depends on the differentiation state. Thymocytes are more strongly positive than mature T-cells [5]. CD147 is up-regulated upon activation in T cells [3,6]. Significant expression of CD147 in neoplasm of bladder, liver, and lung has been reported [7,8]. CD147 is enriched on the surface of tumor cells and stimulates adjacent stromal cells to produce several matrix metalloproteinases (MMPs) [9–13]. CD147 molecules seem to be responsible for the induction of expression of the matrix metalloproteinases (MMPs), interstitial collagenase (MMP-1), gelatinase A (MMP-2), and stromelysin-1 (MMP-3), when CD147 interacts with fibroblasts [2–4,14]. Furthermore, N-linked glycosylation of CD147 is essential for MMP-1 and MMP-2 production [15].

The function of human leukocyte surface molecule CD147 is not fully understood. However, CD147 as a potential adhesion molecule with an unknown counter–receptor was suggested [1]. CD147 may be involved in signal transduction and cell adhesion function, either directly as a signal transmitting adhesion molecule or

* Corresponding author. Fax: +66-53-946042.
E-mail address: asimi002@chiangmai.ac.th (C. Tayapiwatana).

1046-5928/$ - see front matter © 2003 Elsevier Inc. All rights reserved.
doi:10.1016/j.pep.2003.08.019

as a regulator of adhesion [16]. Furthermore, CD147 was found to be involved in T cell regulation [17]. Thus production of the CD147 ectodomain (CD147Ex) is important for studying the immunological function of CD147.

Phage display is a powerful technique for engineering proteins or peptides [18–22]. Proteins or peptides of interest are expressed as fusion to phage minor (gpIII) or major (gpVIII) coat proteins. To identify the CD147 counter–receptor, we recently applied phage display technology to construct phage-displayed CD147 on gpIII [23]. However, by using the constructed recombinant phages, we could not demonstrate the binding of phage-displayed CD147 to any cell types by the immunofluorescence technique (unpublished observation). The weak binding affinity between CD147 and its ligand partner was suspected. Increasing the copy number of CD147 molecule per phage particle may enhance the bonding forces by multivalent ligand–receptor anchoring and serve the purpose of ligand–receptor study.

Displaying the heterologous protein on phage gpIII limited the level of display to less than one molecule per phage particle [24]. In contrast, high level of heterologous protein display could be achieved on the gpVIII, which contains approximately 2000 copies per phage particle [25,26]. It has been reported that the filamentous phage usually displayed the fusion protein at lower level than expected as a result of proteolysis of the polypeptide [27–30]. In general, phage is propagated at the optimal temperature for bacterial growth, 37 °C. This temperature, concurrently, is suitable for the enzymatic activity of proteases produced by *Escherichia coli* host. The produced fusion proteins could, then, be degraded by these proteases and result in low amount of fusion proteins for packaging on phage particles. One strategy to prevent the degradation of the heterologous protein was to culture *E. coli* at low temperature, i.e., 25 °C [31–33]. Lowering the temperature of phage propagation was formerly applied to overcome this problem [31,34]. However, the rate of protein production was also significantly decreased at low temperature. To compensate this, isopropyl thio-β-D-galactopyranoside (IPTG) was commonly added to up-regulate the expression level when a leaky inducible promoter such as *Lac* is provided [31,35–38].

In an attempt to generate high density of phage expressing CD147, pComb8 phagemid vector was employed to display the ectodomain of human CD147 (CD147Ex) on gpVIII in the present study. The optimization of culturing conditions, i.e., temperature and IPTG for incorporating the CD147ExgpVIII into VCSM13 particle, was investigated. Since the packaging process involves a competition between wild-type gpVIII and CD147ExgpVIII, we also demonstrated the effect of helper phage infection period following the IPTG induction. The influences of these combinatorial factors on displaying of the heterologous protein on phage particle via gpVIII have never been reported elsewhere.

Materials and methods

CD147Ex gene amplification by PCR

Two oligonucleotides, CD147ExgpVIIIFw (5′-GAG GAG GAG GTc tcg agG CTG CCG GCA CAG TCT TC-3′, the *Xho*I restriction site at 5′ overhang is designated in small letters) and CD147ExgpVIIIRev (5′-GAG GAG GAG CTa cta gtG TGG CTG CGC ACG CGG AG-3′, the *Spe*I restriction site at 5′ overhang is designated in small letters), were used as primers for amplifying the CD147Ex fragment.

PCR was used to amplify the CD147Ex from the mammalian expressing vector, pCDM8-CD147 [3]. Fifty nanograms of pCDM8-CD147 was annealed with 250 ng of each described primer in the 100 μl of a PCR mixture containing 5 U ProofStart DNA polymerase (Qiagen, Hilden, Germany). The PCR cycling condition was one cycle at 95 °C for 5 min followed by 34 cycles of 94 °C for 50 s, 50 °C for 50 s, and 72 °C for 1 min. After 35 amplification cycles, the mixture was incubated at 72 °C for 10 min. The resulting 550 bp PCR product was subsequently treated with *Xho*I and *Spe*I at 37 °C for 18 h and purified by QIAquick PCR purification Kit (Qiagen, Hilden, Germany).

Construction of phagemid expressing CD147Ex

The pComb8 phagemid (a gift from Dr. C.F. Barbas, Scripps Institute, USA) was digested with *Xho*I and *Spe*I at 37 °C for 18 h. The DNA fragment of digested pComb8, 3300 bp, was further purified and ligated with digested CD147Ex PCR product by using T_4 ligase enzyme (Roche Molecular Biochemicals, Mannheim, Germany). The ligated product was transformed into TG1 *E. coli* host strain {*supE hsd*Δ5 *thi*Δ(*lac-proAB*) F′[*traD*36*proAB*+, *lacI*^{q} *lacZ*ΔM15]} (kindly provided by Dr. A.D. Griffiths, MRC Cambridge, UK). The transformed *E. coli* were selected on LB agar containing ampicillin (100 μg/ml). The ampicillin-resistant colonies were selected and cultured at 37 °C for 18 h in LB broth containing ampicillin (100 μg/ml) for Plasmid Mini Kit (Qiagen, Hilden, Germany). The inserted CD147Ex gene in the purified phagemid was checked by restriction fragment analysis with *Xho*I and *Spe*I, and reamplification by PCR. The complete nucleotide sequence of inserted fragment was determined according to dideoxychain terminator procedure using BigDye Terminator v3.1 Cycle Sequencing Kit (PE Applied Biosystems,

CA, USA). CD147ExgpVIIIFw and CD147ExgpVIII-Rev were applied as the sequencing primers. The sequencing data was analyzed further by ABI PRISM 3100 DNA Analyzer (PE Applied Biosystems). The newly constructed phagemid was named pComb8-CD147Ex.

Phage-displayed CD147ExgpVIII

Transformed bacteria were grown in 10 ml of 2× TY broth (1.6% [w/v] tryptone, 1% [w/v] yeast extract, and 0.5% [w/v] sodium chloride) containing ampicillin (100 μg/ml) at 37 °C until the absorption at 600 nm was 0.8. The precultured bacteria were subsequently transferred to 100 ml of the same medium containing 1% [w/v] glucose and cultivated until the absorption at 600 nm of 0.5 was reached at either 25 or 37 °C. If the bacterial cultures were to be induced, IPTG was added to the culture at a final concentration of 1 mM. After induction, the cells were grown at the desired temperature for 0 or 2 h. Each bacterial culture was infected further with 10^{12} t.u.[1] of the VCSM13 helper phages and left at 37 °C for 30 min without shaking. Phage-infected TG1 were pelleted by centrifugation at 3000 rpm for 10 min at 4 °C. The pellets were resuspended in 2× TY broth containing ampicillin (100 μg/ml) and kanamycin (70 μg/ml). Fifteen milliliters of bacterial cultures was transferred to 250 ml of the same medium and shaken at 180 rpm for 16 h at the desired temperature. The recombinant phages were harvested by PEG 8000 precipitation and centrifugation as described previously [39]. Finally, the phages were reconstituted with 2.5 ml of 0.15 M PBS, pH 7.2, and centrifuged at 11,600 rpm for 10 min at 4 °C. The supernatant was stored at −70 °C.

Immunoassay for phage-displayed CD147ExgpVIII by sandwich ELISA

Fifty microliters of 10 μg/ml CD147 mAbs (M6-1B9; IgG_3, M6-1E9; IgG_{2a}, M6-1D4; IgM, and M6-2F9; IgM) [6,16] in carbonate/bicarbonate buffer, pH 9.6, was coated on a microtiter plate (NUNC, Roskilde, Denmark) at 4 °C for 18 h. Blocking was performed by addition of 2% skim milk in PBS, pH 7.2, and incubated for 1 h at room temperature. After washing 5 times with 0.05% Tween 20 in PBS, pH 7.2, phage-displayed CD147ExgpVIII produced under different conditions were diluted to 10^{10} t.u./ml in 2% skim milk in PBS, pH 7.2 and 50 μl of recombinant phage was added to the wells. After incubation at room temperature for 1 h, the plate was washed to remove unbound phages. Binding of phage particles was monitored by using two alternative sets of anti-M13 mAb. One was HRP-conjugated anti-gpVIII mAb (Amersham–Pharmacia Biotech, Buckinghamshire, UK) and the other was biotinylated anti-gpIII mAb (Exalpha Biologicals, Watertown, MA). HRP-conjugated streptavidin (ZYMED Laboratories, San Francisco, CA) was applied to trace the biotinylated anti-gpIII mAb. Following washing, the 3,3′,5,5′-tetramethylbenzidine (TMB) substrate was added and incubated at room temperature for signal development. Optical density at 450 nm was determined after adding 1 N HCl to stop the reaction.

SDS–PAGE and Western immunoblotting

Phage-displayed CD147ExgpVIII was separated by SDS–PAGE under reducing conditions on a 15% polyacrylamide gel. For Western immunoblotting, the separated proteins were electroblotted onto polyvinylidene fluoride (PVDF) membrane. Blotted membrane was blocked at 4 °C for 18 h in 5% skim milk in PBS, pH 7.2, and then incubated with the pooled CD147 mAbs (M6-1B9, M6-1E9, and M6-1D4 at 10 μg/ml each) for 1 h at room temperature on a shaking platform. Following washing with 0.05% Tween 20 in PBS, pH 7.2, HRP-conjugated rabbit-anti-mouse immunoglobulins (DAKO A/S, Copenhagen, Denmark) was added to the membranes and incubated at room temperature for 1 h. The immunoreactive bands were then visualized by chemiluminescent detection system (Amersham–Pharmacia Biotech, Buckinghamshire, UK).

Results

Construction of pComb8-CD147Ex phagemid

The ectodomain of CD147 cDNA was amplified from pCDM8-CD147 by PCR using primers CD147ExgpVIIIFw and CD147ExgpVIIIRev. The PCR product of 552 bp was obtained (Fig. 1A). The amplified product was subsequently cleaved with *Xho*I and *Spe*I, and ligated into the pComb8 phagemid treated with the same enzymes. The ampicillin-resistant *E. coli* TG1 colonies transformed with the ligated product were grown at 37 °C for plasmid minipreps. The inserted fragment of CD147Ex with the molecular weight of approximately 550 bp was retrieved from the isolated plasmid DNA after checking by restriction fragment analysis with *Xho*I and *Spe*I (Fig. 1B), and reamplification by PCR

[1] *Abbreviations:* t.u., transforming unit; ELISA, enzyme-linked immunosorbent assay; SDS–PAGE, sodium dodecyl sulfate–polyacrylamide gel electrophoresis; PCR, polymerase chain reaction; RBS, ribosome binding site; *Pel*B, pectate lyase B signal peptide from *Erwinia carotovora*.

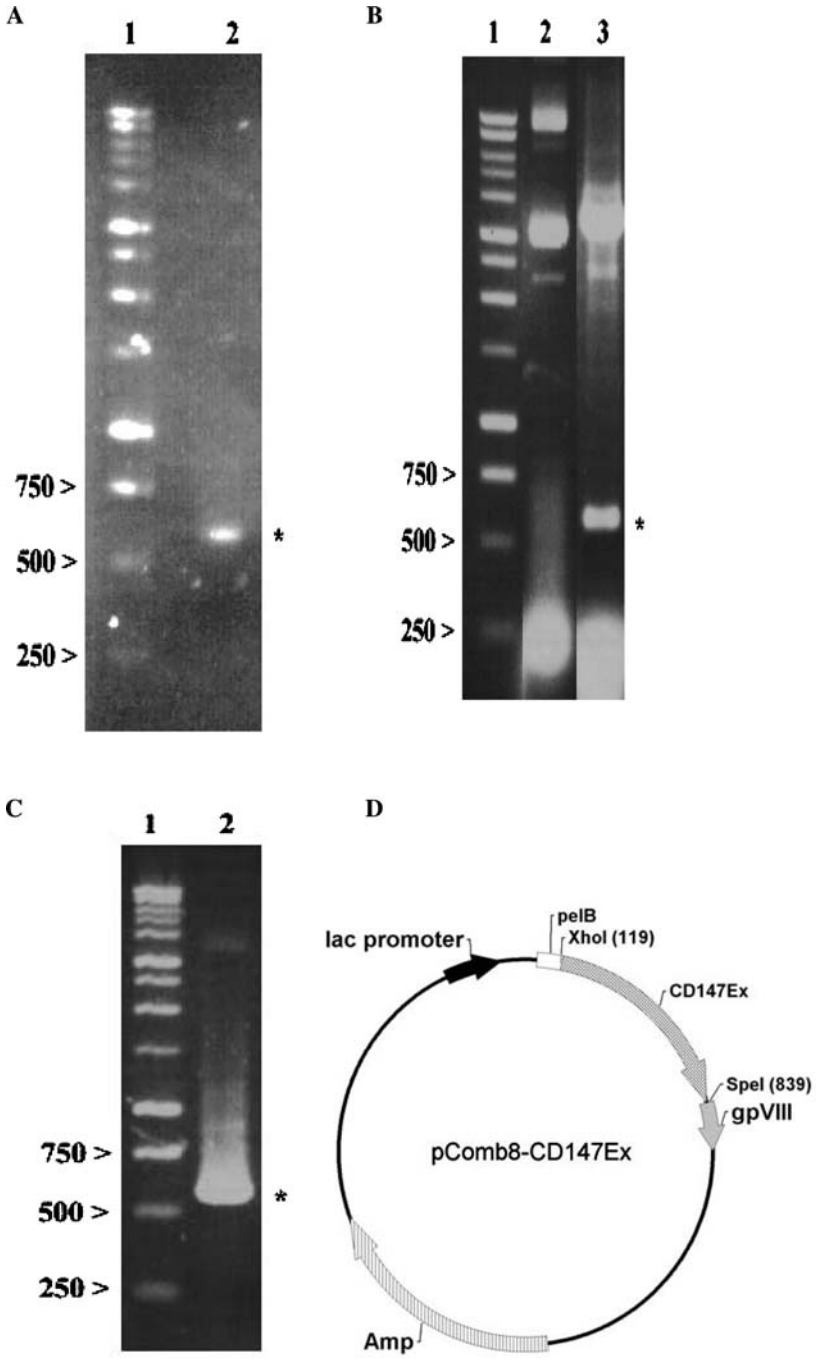

Fig. 1. Construction of phagemid expressing CD147Ex. (A) Analysis of PCR product, 552 bp (*), of the CD147Ex amplified from pCDM8-CD147 vector using CD147ExgpVIIIFw and CD147ExgpVIIIRev primers. Samples were electrophoresed in a 1% agarose gel. Lane 1, 1 kb DNA marker; lane 2, amplified product. (B) Restriction fragment analysis of pComb8-CD147Ex with *Xho*I and *Spe*I. The constructed pComb8-CD147Ex was cleaved with *Xho*I and *Spe*I. The inserted fragment of CD147Ex with the molecular weight of approximately 552 bp (*) was retrieved from the pComb8-CD147Ex (lane 3). Lane 1, 1 kb DNA marker; lane 2, pComb8-CD147Ex; and lane 3, *Xho*I- and *Spe*I-digested pComb8-CD147Ex. (C) Amplified product of CD147Ex from pComb8-CD147Ex. The 552 bp amplified product (*) from pComb8-CD147Ex template using CD147Ex-gpVIIIFw and CD147ExgpVIIIRev primers is shown (lane 2). Lane 1, 1 kb DNA marker; lane 2, amplified product of CD147Ex. (D) Construction of pComb8-CD147Ex phagemid. *Xho*I- and *Spe*I-cloning sites where the CD147Ex gene was inserted; *lac* promoter, the signal sequence (*PelB*) and gpVIII gene is shown. STOP represents the stop codon for CD147ExgpVIII translation.

(Fig. 1C). The nucleotide sequence of inserted fragment is identical to CD147 ectodomain (data not shown). The engineered phagemid bearing CD147 ectodomain gene, flanked upstream by *Pel*B signal sequence and downstream by gpVIII (Fig. 1D), was designated as pComb8-CD147Ex.

Detection of phage-displayed CD147ExgpVIII by sandwich ELISA

To study the culturing conditions for efficiently displaying of CD147Ex molecules on the phage particle, the pComb8-CD147Ex-transformed TG1 was cultured and infected with the VCSM13 helper phages under five different conditions (Fig. 2). The phage-displayed CD147ExgpVIII in culture supernatants obtained from various culturing conditions were compared by sandwich ELISA using a panel of anti-CD147 mAb as capture antibody. By using HRP-conjugated anti-gpVIII mAb, production of phage-displayed CD147ExgpVIII at 25 °C with IPTG-stimulation showed the highest signal with all anti-CD147 mAbs (M6-1B9, M6-1E9, M6-1D4, and M6-2F9) used (Fig. 3A). The second order was phage harvested from 37 °C without IPTG-, followed by 25 °C without IPTG-, and 37 °C with IPTG-stimulation when mAb M6-1B9 was used as a capture antibody. However, the second and the third ranks were switched when the precipitated phages were captured by other three mAbs (M6-1E9, M6-1D4, and M6-2F9). In contrast, the recombinant phages were not recognized by an irrelevant capture antibody, mouse anti-GFP mAb (data not shown).

The binding of the phage-displayed CD147ExgpVIII under 25 °C with IPTG-stimulation onto the CD147 mAb-coated wells was also demonstrated by biotinylated

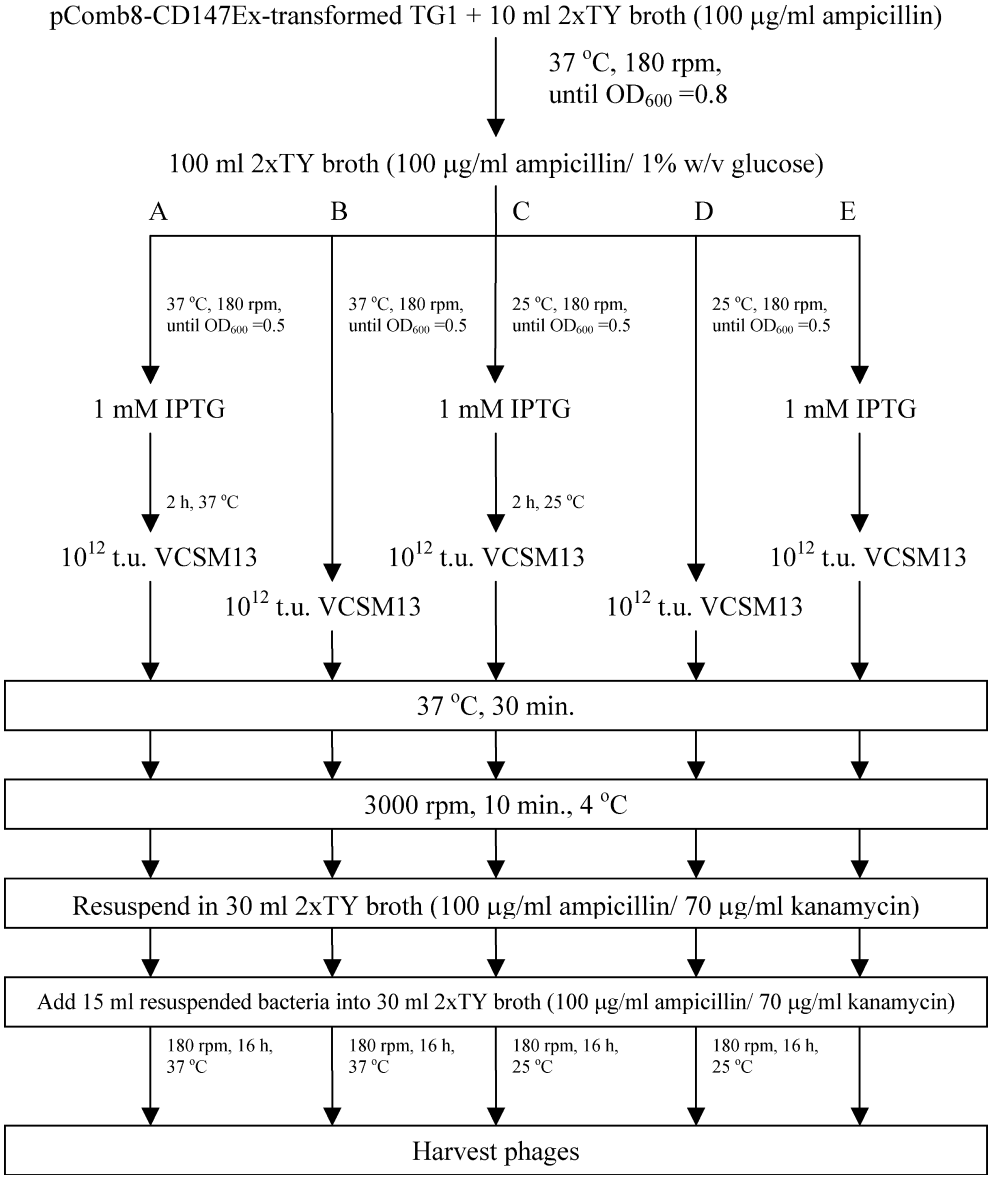

Fig. 2. Schematic diagram of the cultivating conditions for displaying CD147ExgpVIII on phage particles. The culture was divided into five experiments. The first set (A,B) was grown at 37 °C. The second set (C–E) was cultivated at 25 °C. (A,C) were stimulated with IPTG for 2 h before helper phage infection. (E) was stimulated with IPTG for 0 h before helper phage infection.

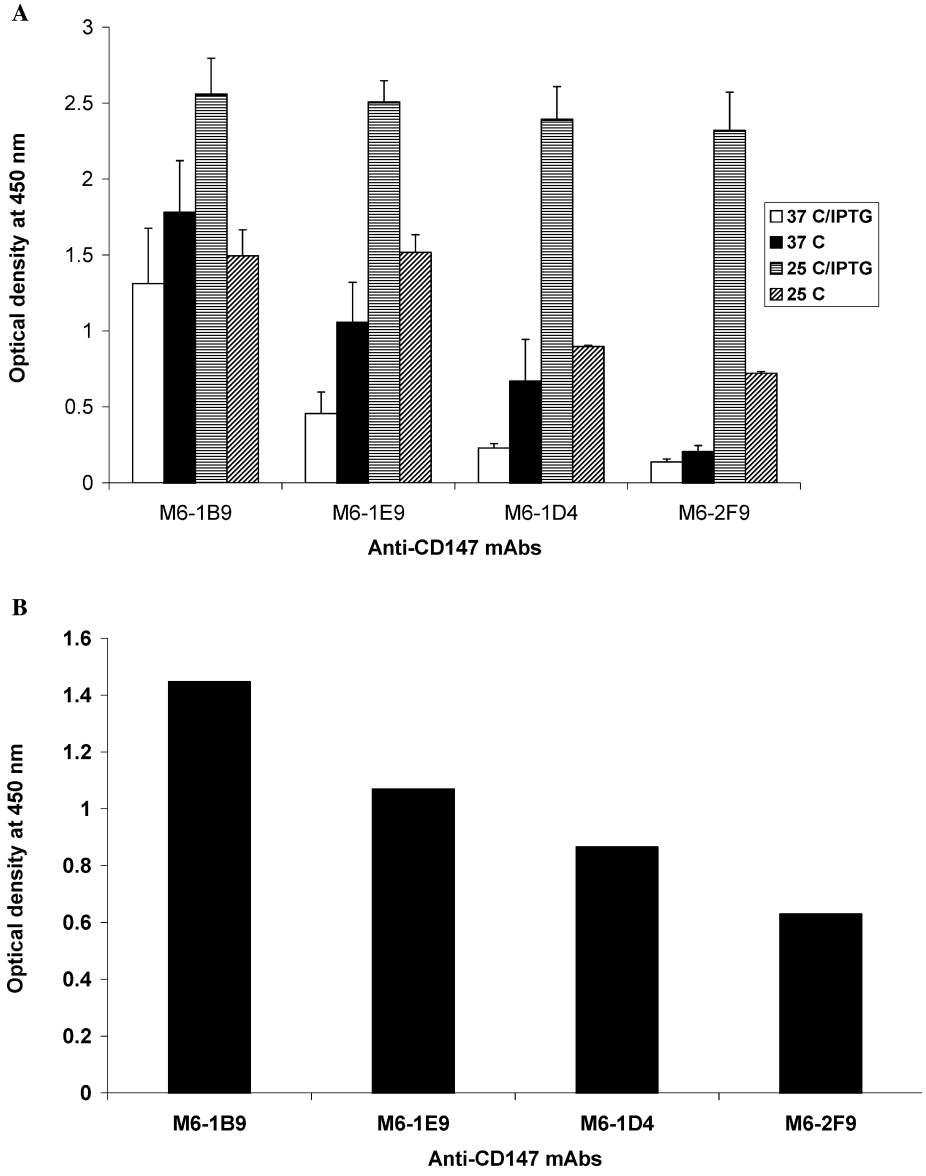

Fig. 3. Comparison of different expression levels of phage-displayed CD147ExgpVIII. (A) Sandwich ELISA analysis of phage-displayed CD147ExgpVIII under different growth conditions using four anti-CD147 mAbs (M6-1B9, M6-1E9, M6-1D4, and M6-2F9) as a capture and HRP/anti-gpVIII monoclonal conjugate as a tracer. Phage-displayed CD147Ex under 37 °C with IPTG-stimulation (no fill), 37 °C (solid bars), 25 °C with IPTG-stimulation (horizontals), and 25 °C (diagonals) were demonstrated. This experiment was done in duplicate. Fifty microliters of 10^{10} t.u./ml phage was used in this experiment. (B) Sandwich ELISA analysis of phage-displayed CD147ExgpVIII under 25 °C with IPTG-stimulation using four anti-CD147 mAbs (M6-1B9, M6-1E9, M6-1D4, and M6-2F9) as a capture and biotinylated monoclonal anti-gpIII/streptavidin conjugated to HRP as a tracer. Fifty microliters of 10^{10} t.u./ml phage was used in this experiment.

anti-gpIII mAb/HRP-conjugated streptavidin detection system (Fig. 3B). The signaling pattern of all capture-mAbs used corresponded to the HRP-conjugated anti-gpVIII mAb detection system.

To determine the effect of helper phage-infection period, the phage-displayed CD147ExgpVIII were produced under 25 °C with IPTG-stimulation for 0 and 2 h before helper phage infection. The produced phages from both conditions were compared by sandwich ELISA. The recombinant phages harvested from simultaneous IPTG-stimulation and helper phage infection (0 h) were 6–11-fold higher than those harvested from which inoculation of helper phage 2 h after IPTG-stimulation (Table 1).

Western immunoblotting

The protein components of the recombinant phages prepared under 25 °C with IPTG-stimulation were fractionated by SDS–PAGE under reducing conditions, blotted, and probed with pooled CD147 mAbs (M6-1B9, M6-1E9, and M6-1D4). An immunoreactive

Table 1
Comparison of helper phage infection periods on the production of phage-displayed CD147ExgpVIII under 25 °C with IPTG-stimulation

CD147 mAbs	Optical density at 450 nm	
	0 h after IPTG-stimulation	2 h after IPTG-stimulation
M6-1B9	1.68	0.28
M6-1E9	1.47	0.13
M6-1D4	1.67	0.19
M6-2F9	1.24	0.20

Sandwich ELISA using a panel of CD147 mAbs as a capture and tracing by biotinylated anti-gpIII mAb/HRP-conjugated streptavidin system was employed.

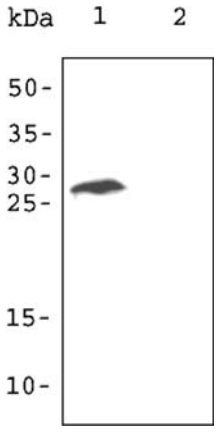

Fig. 4. Western immunoblotting of phage-displayed CD147ExgpVIII separated by reducing SDS–PAGE . Immunological assay was performed by probing with the combination of three anti-CD147 mAbs (M6-1B9, M6-1E9, and M6-1D4). Lane 1, phage-displayed CD147ExgpVIII; lane 2, phage-displayed Fo protein of respiratory syncytial virus. The immunoreactive bands were visualized by chemiluminescence substrate detection system. Molecular weight markers in kDa were indicated.

protein band with the molecular weight of 28 kDa was obtained (Fig. 4). This band was regarded as the fusion protein of CD147Ex, 20 kDa and gpVIII, 6 kDa. No reactive band was detected in the control lane to which with phage-displayed Fo protein of respiratory syncytial virus had been applied.

Discussions

In an attempt to characterize the counter–receptor of CD147 molecule, we recently generated phage-displayed ectodomain of CD147 via gpIII [23]. However, by indirect immunofluorescence, the binding of these recombinant phages could not be demonstrated on any cells. Since the majority of the generated phages possessed less than one copy of CD147 molecule, the low ligand-binding affinity of the CD147 to its ligands was presumed. Multimeric display of CD147-on phage particles is therefore required and will be valuable in further discovering its ligand-partner on cell surface. Furthermore, multivalent CD147 on the 930 nm-length filamentous phage might overwhelm the limitation in the binding of CD147 to the low-level expression of its ligands. The multivalent phage carrying CD147 may be valuable in functional study. Signal transferring by individual pairing with monovalent CD147 may differ from the cross-linking of cell-surface ligands with phage-displayed multivalent CD147 via gpVIII. It has recently been demonstrated that CD147 appears to be a cofactor that mediates activity of virus-associated cyclophilin A and is required for efficient infection [24]. Phage-displayed CD147 might be used to define the novel targets for anti-HIV interventions.

The gpVIII of VCSM13 was previously applied for achieving the multimeric polypeptide libraries [25,26]. The absolute binding force of these phage libraries to a certain ligand was enhanced according to the increasing copy number of each polypeptide. The display of CD147 ectodomain on phage particles via gpVIII was, thus, proposed in this study. However, the multivalent display of fusion protein on phage particles had been hindered because of a limitation on the fusion length [40]. Culturing conditions during phage preparation such as temperature, IPTG-stimulation, and helper phage infection-period are important factors for production of the phage expressing interested protein. In the present study, the factors mentioned were investigated to optimize the quantity of display. Filamentous phage was used to display CD147EXgpVIII in TG1 *E. coli* host. By sandwich ELISA using a panel of anti-CD147 monoclonal antibodies as a capture and HRP-conjugated anti-gpVIII mAb as a tracer, the generated phages showed strong positive reactivity. The correct size of the CD147Ex-gpVIII fusion protein at 28 kDa from the generated phages was also demonstrated by Western immunoblotting. This result indicated that the expression of fusion CD147-gpVIII proteins was occurred. However, we raised a question whether the positive signal was due to the secreted or the phage-bound CD147Ex-gpVIII fusion protein. To address this question, the expression of CD147 on the surface of complete phage particles was subsequently confirmed by using the biotinylated anti-gpIII mAb/HRP-conjugated streptavidin as a tracer in sandwich ELISA. As predicted, the generated phages showed also strong positive reactivity. Our ELISA experiments indicated that the generated phages harbored CD147 ectodomain on their surfaces.

Production of phage-displayed CD147ExgpVIII at 25 °C with IPTG-stimulation was demonstrated as the most suitable condition. Reducing growth temperature, from 37 to 25 °C, may facilitate the correct folding and stability of the displayed protein [41–43]. Although the rate of protein synthesis was low at 25 °C comparing to

37 °C, IPTG seemed to compensate for this disadvantage. The reduction in cultivating temperature and addition of IPTG may have a complementary effect on phage propagation and on the fusion protein incorporation, resulting in the high density display per phage particle.

Phage harvested from 37 °C without IPTG-stimulation was demonstrated to be the second effective order when M6-1B9 mAb was used as a capture antibody. In surprising contrast, when other three mAbs (M6-1E9, M6-1D4, and M6-2F9) were used as capture antibodies, the second rank was changed to phage harvested from 25 °C without IPTG-stimulation. We speculated that the folding of CD147 epitope recognized by M6-1B9 mAb on recombinant phage produced at 37 °C without IPTG-stimulation was more proper than phages produced at 25 °C without IPTG-stimulation. Regarding our previous study [23], the epitopes recognized by M6-1B9 and M6-1E9 mAbs were overlapping. The variation in exposing of these epitopes in the different culturing conditions indicated the proximate but non-identical epitopes recognized by M6-1B9 and M6-1E9 mAbs. The recombinant phage harvested from 37 °C with IPTG-stimulation was given the lowest signal in all capture CD147 mAbs used. This result was consistent with the experiment of antibody-gpVIII phage production [36]. Insoluble protein accumulation and degradation of the recombinant protein in the periplasm by host proteases might be facilitated at higher growth temperatures [42]. Apparently, high expression level of fusion protein by IPTG-stimulation rendered the formation of inclusion bodies which decreased the incorporating efficiency of CD147Ex-gpVIII into phage particles [41–43].

One proposed strategy for increasing the amount of recombinant protein displayed on phage particles via gpVIII was delaying the infection-period of helper phage after IPTG-stimulation [35]. However, the controversial result was obtained in this study. The phage-displayed CD147ExgpVIII produced at 25 °C with IPTG-stimulation at the same time of helper phage infection were higher than those obtained by infection of helper phages 2 h later. We suggested that after 2-h induction, *E. coli* produced an excess amount of CD147ExgpVIII, which was prone to form aggregates before the phage packaging components were synthesized.

To produce high density phages, various sophisticated techniques have been developed. Sidhu increased the display of human growth hormone by mutating the amino acid residues on the gpVIII fusion partner [44]. More recently, a novel gpVIII display system, in which every copy of gpVIII was modified, was reported [38]. The gpVIII was expressed from the phagemid and the helper phage was used to rescue the phagemid deficient in gpVIII production. In contrast, we established here a simple method for increasing of the multimeric CD147Ex expression on phage particles. Apart from the major parameters, i.e., temperature and IPTG-stimulation, which were formerly investigated [31,36], the influence of helper phage infection-period after IPTG-stimulation on enhancing the CD147Ex displaying demonstrated a high impact on this study.

Acknowledgments

This work was supported by The Thailand Research Fund and The National Center for Genetic Engineering and Biotechnology (BIOTEC) of the National Science and Technology Development Agency, Thailand. We are thankful to Dr. Nicole Ngo (The Perinatal HIV Prevention Trial Group, Chiang Mai, Thailand) for cooperation in determining the inserted fragment in pComb8-CD147Ex and Miss Nattika Nuntachit for technical assistance.

References

[1] H. Stockinger, T. Ebel, C. Hansmann, C. Koch, O. Majdic, E. Prager, D.D. Patel, D.A. Fox, V. Horejsi, K. Sagawa, D.C. Shen, CD147 (neurothelin/basigin) workshop panel report, In: T. Kishimoto, H. Kikutani, A.E.G.K. von dem Borne, S.M. Goyert, D.Y. Mason, M. Miyasaka, L. Moretta, K. Okumura, S. Shaw, T.A. Springer, K. Sugamura, H. Zola (Eds.), Leukocyte Typing VI, Garland Publishing, New York, 1997, p. 760.

[2] T. Miyauchi, Y. Masuzawa, T. Mutamatsu, The basigin group of the immunoglobulin superfamily: complete conservation of a segment in and around transmembrane domains of human and mouse basigin and chicken HT7 antigen, J. Biochem. (Tokyo) 110 (1991) 770–774.

[3] W. Kasinrerk, E. Fiebiger, I. Stefanova, T. Baumruker, W. Knapp, H. Stockinger, Human leukocyte activation antigen M6, a member of the Ig superfamily, is the species homologue of rat OX-47, mouse basigin, and chicken HT7 molecule, J. Immunol. 149 (1992) 847–854.

[4] C. Biswas, Y. Zhang, R. DeCastro, H. Gou, T. Nakamura, H. Kataoka, K. Kabeshima, The human cell-derived collagenase stimulatory factor (renamed EMMPRIN) is a member of the immunoglobulin superfamily, Cancer Res. 55 (1995) 434–435.

[5] A.H. Kirsch, L.A. Diaz, B. Bonish Jr., P.A. Anthony, D.A. Fox, The pattern of expression of CD147/neurothelin during human T-cell ontogeny as defined by the monoclonal antibody 8D6, Tissue Antigens 50 (1997) 147–152.

[6] W. Kasinrerk, N. Tokrasinwit, P. Phunpae, CD147 monoclonal antibodies induce homotypic cell aggregation of monocytic cell line U937 via LFA-1/ICAM-1 pathway, Immunology 96 (1999) 184–192.

[7] K. Muraoka, K. Nabeshima, T. Murayama, C. Biswas, M. Koono, Enhanced expression of a tumor-cell-derived collagenase-stimulatory factor in urothelial carcinoma: its usefulness as a tumor marker for bladder cancers, Int. J. Cancer 55 (1993) 19–26.

[8] A. Rizzo, E. Aragona, O. Dino, R. Pisa, M. Vignola, F. Guddo, M. Albanese, D. Guerrera, A. Orlando, R. Simonetti, F. Raiata, A. Realmuto, G. Bonsignore, L. Pagliaro, G. Malizia, Expression of CD147 (neurothelin) in liver and lung cancer, in: T. Kishimoto, H. Kikutani, A.E.G.K. von dem Borne, S.M. Goyert, D.Y. Mason, M. Miyasaka, L. Moretta, K. Okumura, S. Shaw, T.A. Springer, K. Sugamura, H. Zola (Eds.), Leukocyte Typing VI, Garland Publishing, New York, 1997, p. 763.

[9] P. Basset, J.P. Bellocq, C. Wolf, I. Stoll, P. Hutin, J.M. Limacher, O.L. Podhajcer, M.P. Chenard, M.C. Rio, P. Chambon, A novel metalloproteinase specifically expressed in stromal cells of breast carcinoma, Nature 348 (1990) 699–704.
[10] G. Majmudar, B.R. Nelson, T.C. Jensen, T.M. Johnson, Increased expression of matrix metalloproteinase-3 (stromyelin-1) in cultured fibroblasts and basal cell carcinomas of nevoid basal cell carcinoma syndrome, Mol. Carcinog. 11 (1994) 29–33.
[11] K.J. Heppner, L.M. Matrisian, R.A. Jensen, W.H. Williams, Expression of most matrix metalloproteinase family members in breast cancer represents a tumor-induced host response, Am. J. Pathol. 149 (1996) 273–282.
[12] M. Polette, C. Gilles, V. Marchand, M. Lorenzato, B.P. Toole, J.M. Tournier, S. Zucker, P. Birembaut, Tumor collagenase stimulatory factor (TCSF) expression and localization in human lung and breast cancers, J. Histochem. Cytochem. 45 (1997) 703–709.
[13] M. Lim, T. Martinez, D. Jablons, R. Cemeron, H. Guo, B.P. Toole, J.D. Li, C. Basbaum, Tumor-derived EMMPRIN stimulates collagenase transcription through MAPK p38, FEBS Lett. 441 (1998) 88–92.
[14] M.M. Cesario, J.R. Bartels, Compartmentalization processing and redistribution of the plasma membrane protein CE9 on rodent spermatozoa, J. Cell Sci. 107 (1994) 561–570.
[15] J. Sun, M.E. Hemler, Regulation of MMP-1 and MMP-2 production through CD147/extracellular matrix metalloproteinase inducer interactions, Cancer Res. 61 (2001) 2276–2281.
[16] P. Khunkeawla, S. Moonsom, G. Staffler, P. Kongtawelert, W. Kasinrerk, Engagement of CD147 molecule-induced cell aggregation through the activation of protein kinases and reorganization of the cytoskeleton, Immunobiology 203 (2001) 659–669.
[17] C. Koch, G. Staffler, R. Huttinger, I. Hilgert, E. Prager, J. Cerny, P. Steinlein, O. Majdic, V. Horejsi, H. Stockinger, T cell activation-associated epitopes of CD147 in regulation of the T cell response, and their definition by antibody affinity and antigen density, Int. Immunol. 11 (1999) 777–786.
[18] G.P. Smith, Filamentous fusion phage: novel expression vectors that display cloned antigens on the virion surface, Science 228 (1985) 1315–1317.
[19] J.K. Scott, G.P. Smith, Searching for peptide ligands with an epitope library, Science 249 (1990) 386–390.
[20] S.E. Cwirla, E.A. Peters, R.W. Barrett, W.J. Dower, Peptides on phage: a vast library of peptides for identifying ligands, Proc. Natl. Acad. Sci. USA 87 (1990) 6378–6382.
[21] N.C. Wrighton, F.X. Farrell, R. Chang, A.K. Kashyap, F.P. Barbone, L.S. Mulcahy, D.L. Johnson, R.W. Barrett, L.K. Jolliffe, W.J. Dower, Small peptides as potent mimetics of the protein hormone erythropoietin, Science 273 (1996) 458–463.
[22] W.J. Fairbrother, H.W. Christinger, A.G. Cochran, G. Fuh, C.J. Keenan, C. Quan, S.K. Shriver, J.Y.K. Tom, J.A. Wells, B.C. Cunningham, Novel peptides selected to bind vascular endothelial growth factor target the receptor-binding site, Biochemistry 37 (1998) 3111–3115.
[23] C. Tayapiwatana, P. Arooncharus, W. Kasinrerk, Displaying and epitope mapping of CD147 on VCSM13 phages: influence of *Escherichia coli* strains, J. Immunol. Methods 281 (2003) 177–185.
[24] S. Bass, R. Greene, J.A. Wells, Hormone phage: an enrichment method for variant proteins with altered binding properties, Proteins 8 (1990) 309–314.
[25] V.A. Petrenko, G.P. Smith, X. Gong, T. Quinn, A library of organic landscapes on filamentous phage, Protein Eng. 9 (1996) 797–801.
[26] G. Iannolo, O. Minenkova, S. Gonfloni, L. Castagnoli, G. Cesareni, Construction, exploitation and evolution of a new peptide library displayed at high density by fusion to the major coat protein of filamentous phage, Biol. Chem. 378 (1997) 517–521.
[27] D. Larocca, P.D. Kassner, A. Witte, R.C. Ladner, G.F. Pierce, A. Baird, Gene transfer to mammalian cells using genetically targeted filamentous bacteriophage, FASEB J. 13 (1999) 727–734.
[28] D. Legendre, P. Soumillion, J. Fastrez, Engineering a regulatable enzyme for homogeneous immunoassays, Nat. Biotechnol. 17 (1999) 67–72.
[29] D. Legendre, N. Laraki, T. Graslund, M.E. Bjornvad, M. Bouchet, P.A. Nygren, T.V. Borchert, J. Fastrez, Display of active subtilisin 309 on phage: analysis of parameters influencing the selection of subtilisin variants with changed substrate specificity from libraries using phosphonylating inhibitors, J. Mol. Biol. 296 (2000) 87–102.
[30] I. Ponsard, M. Galleni, P. Soumillion, J. Fastrez, Selection of metalloenzymes by catalytic activity using phage display and catalytic elution, Chembiochemistry 2 (2001) 253–259.
[31] J.A. Chappel, M. He, A.S. Kang, Modulation of antibody display on M13 filamentous phage, J. Immunol. Methods 221 (1998) 25–34.
[32] F.B. Nygaard, K.W. Harlow, Heterologous expression of soluble, active proteins in *Escherichia coli*: the human estrogen receptor hormone-binding domain as paradigm, Protein Expr. Purif. 21 (2001) 500–509.
[33] P.M. O'Brien, G. Maxwell, M.S. Campo, Bacterial expression and purification of recombinant bovine Fab fragments, Protein Expr. Purif. 24 (2002) 43–50.
[34] G. Soltes, H. Barker, K. Marmai, E. Pun, A. Yuen, E.J. Wiersma, A new helper phage and phagemid vector system improves viral display of antibody Fab fragments and avoids propagation of insert-less virions, J. Immunol. Methods 274 (2003) 233–244.
[35] A.S. Kang, C.F. Barbas, K.D. Janda, S.J. Benkovic, R.A. Lerner, Linkage of recognition and replication functions by assembling combinatorial antibody Fab libraries along phage surfaces, Proc. Natl. Acad. Sci. USA 88 (1991) 4363–4366.
[36] T. Kretzschmar, M. Geiser, Evaluation of antibodies fused to minor coat protein III and major coat protein VIII of bacteriophage M13, Gene 155 (1995) 61–65.
[37] L. Wang, M.Z. Radic, D. Siegel, T. Chang, J. Bracy, U. Galili, Cloning of anti-Gal Fabs from combinatorial phage display libraries: structural analysis and comparison of Fab expression in pComb3H and pComb8 phage, Mol. Immunol. 34 (1997) 609–618.
[38] D. Legendre, J. Fastrez, Construction and exploitation in model experiments of functional selection of a landscape library expressed from a phagemid, Gene 290 (2002) 203–215.
[39] C. Tayapiwatana, W. Kasinrerk, Construction and characterization of phage-displayed leukocyte surface molecule CD99, Appl. Microbiol. Biotechnol. 60 (2002) 336–341.
[40] P. Malik, T.D. Tery, L.R. Gowda, A. Langara, S.A. Petukhov, M.F. Symmons, L.C. Welsh, D.A. Marvin, R.N. Perham, Role of capsid structure and membrane protein processing in determining the size and copy number of peptides displayed on the major coat protein of filamentous bacteriophage, J. Mol. Biol. 260 (1996) 9–21.
[41] A. Knappik, C. Krebber, A. Pluckthun, The effect of folding catalysts on the in vivo folding process of different antibody fragments express in *Escherichia coli*, Biotechnology 11 (1993) 77–83.
[42] J.G. Wall, A. Pluckthun, Effects of overexpressing folding modulators on the in vivo folding of heterologous protein in *Escherichia coli*, Curr. Opin. Biotechnol. 6 (1995) 507–516.
[43] H. Bothmann, A. Pluckthun, Selection for a periplasmic factor improving phage display and functional periplasmic expression, Nat. Biotechnol. 16 (1998) 376–380.
[44] S.S. Sidhu, G.A. Weiss, J.A. Well, High copy display of large proteins on phage for functional selections, J. Mol. Biol. 296 (2000) 487–495.

CHAPTER 1

INTRODUCTION

Leukocyte cell surface molecules are important for cellular functions especially for immune-response. Some of them have been identified and characterized, but a number still waiting for the characterization. The function of human leukocyte surface molecule CD147 is not fully understood. However, CD147 may be involved in signal transduction and cell adhesion function, either directly as a signal transmitting adhesion molecules or as a regulator of adhesion. Thus production of the CD147 extracellular domain or ectodomain (CD147Ex) is important for studying the molecular function of CD147.

A major tool for characterizing the structure and function of the surface molecules is antibodies which are raised against these molecules. In addition to specific antibodies, the isolated cell surface molecules themselves have been broadly used for identification and functional characterization of their counter receptors or specific ligand (1-5). However, to prepare these molecules from cell membranes, complicated techniques are required. In addition, contamination of undesired proteins normally occurs. Molecular techniques in mammalian cell expression system have been employed to overcome this problem. The Fc of immunoglobulin was employed as a fusion partner of certain CD molecules, e.g. CD31 (6), and CD147 (1, 7). The recombinant protein was then secreted into the culture medium and purified using a protein A column. Although the recombinant proteins obtained have an almost native conformation, mammalian cell expression systems are more expensive and time-consuming in comparison to prokaryotic expression systems. Phage display is a powerful technique for engineering proteins or peptides (8-12). Proteins or peptides are expressed as fusions to phage minor (gpIII) or major (gpVIII) coat proteins. Displaying of CD147Ex on phage particles should be used as bait for studying the immunological function of CD147. Displaying of the heterologous proteins on phage

gpIII limited the level of display to less than one molecule per phage particle (13). In contrast, high level of heterologous protein display could be achieved on the gpVIII, which contains approximately 2,000 copies per phage particle (14, 15). The filamentous phage usually displayed the fusion protein at lower level than expected as a result of proteolysis of polypeptide was reported (16-19). In general, phage is propagated at the optimal temperature for bacterial growth, 37 ^{o}C. This temperature, concurrently, is suitable for the enzymatic activity of proteases produced by *E. coli* host. The produced fusion proteins could be, then, degraded by these proteases and resulted in low amount of fusion proteins for packaging on phage particles. One strategy to prevent the degradation of the heterologous protein was to culture *E. coli* at low temperature i.e. 25 ^{o}C (20-22). Lowering the temperature of phage propagation was formerly applied to overcome this problem (20, 23). However, the rate of protein production was also significantly decreased at low temperature. To compensate this, isopropyl thio-β-D-galactopyranoside (IPTG) was commonly added to up-regulate the expression level when a leaky inducible promoter such as *Lac* is provided (17, 20, 24-27).

Phage display technology had been introduced to construct phage-displayed CD147 on the gpIII (28). However, the binding of phage-displayed CD147 to any cell types could not be demonstrated by immunofluorescence technique. The weakness of binding affinity of the CD147 to its ligand-partner was presumed. Increasing the copy number of CD147 molecule per phage particle may enhance the bonding forces by multivalent ligand-receptor interaction.

Nowadays, the precise molecular function of CD147 is still largely unclear. It motivates the scientists for further investigations. Construction of high density display of CD147 ectodomain (CD147Ex) on VCSM13 phage via gpVIII for studying the interaction of CD147Ex and its counter-receptor on cell lines and studying the molecular function of CD147 using the constructed phage would be provide more detail of the CD147 molecule in the human immune system. Understanding of CD147 function would be invaluable for prevention of cancer invasion and metastasis, and might define the novel targets for anti-HIV interventions in the future.

CHAPTER 2

OBJECTIVES

The ultimate goal of this study is to produce the multivalent display of CD147 ectodomain (CD147Ex) on phage particles and using as a tool for studying the molecular function of CD147Ex molecule. The studies provide insight into a better understanding of CD147 molecule.

The specific aims of this study were as follows:

1) Determining the factors influencing on displaying of CD147Ex via gpVIII on VCSM13 particles.
2) Investigating the effect of phage-displayed CD147ExgpVIII on various cell lines.
3) Investigating the molecular function of CD147Ex using multivalent phage-displayed CD147EX via gpVIII.

CHAPTER 3

LITERATURE REVIEW

3.1 Leukocyte Surface Molecules

3.1.1 Nomenclature of leukocyte surface molecules

Leukocytes express a huge number of proteins on their cell surfaces. These molecules are called leukocyte surface molecules which play key roles in all aspects of leukocyte functions. The major tool for identifying and discovery the new leukocyte surface molecules is monoclonal antibodies raised against leukocytes. The abbreviations used for identifying different leukocyte cell surface molecules are complex because three historically conventions have been used. Firstly, cell surface molecules are named according to a particular function affected by an anti-leukocyte mAb. For example, the lymphocyte function-associated antigen 1, or LFA-1, was named because antibodies recognizing this structure interfere with lymphocyte cell adhesion events and optimal lymphocyte function. The second convention is effectively no convention at all. Molecules are named arbitrarily according to individual laboratory preferences. For example, no obvious logic follows in the designations B7 and B220, except that the leading "B" reminds us that these antigens are typically expressed on B lymphocytes. To date, leukocyte cell surface molecules are named systematically by assigning them as cluster of differentiation (CD) antigen number (29, 30). This approach is developed by The Human Leukocyte Differentiation Antigen (HLDA) workshops, which is organized by immunologists around the world. Once the cell surface molecule of all immune cell types including endothelial cells is identified, this new cell surface molecule is given a tentative label which begins "CDw". The "w" stands for "workshop" and indicates the label has not yet been confirmed. It may be that the researcher has found a cell surface molecule that someone else already found so a few years must lapse before the CDw label is

changed to a true CD designation that confirmed by an international committee. The CD numbering was extended to endothelial antigens. The CD nomenclature is used for both the human antigens and their homologues.

3.1.2 General structure of membrane proteins

Cell is a single unit or compartment enclosed by cell membrane or plasma membrane which defines the boundary of the cell and separates its internal contents from the environment. The structure and function of cells are critically dependent on membranes. The biological membranes are composed of lipids and proteins. All cell membranes share a common structural organization, phospholipid bilayers with associated proteins, which are responsible for many specialized functions (**Figure 3.1**). Some proteins are responsible for the selective traffic of molecules into and out of the cell. Other proteins of the plasma membrane control the interactions between cells of multicellular organism and serve as sensors through which the cell receives signals from its environment.

Proteins constitute 25 to 75% of the mass of various membranes of the cell. Membrane associated proteins can be classified into 2 classes, peripheral and integral membrane proteins. Peripheral membrane proteins are noncovalently bonded to the polar head groups of the phospholipid bilayer or to the integral membrane protein. These membrane proteins dissociate from the membrane after treatment with polar reagents that do not disrupt the lipid bilayer. In contrast to peripheral membrane proteins, integral membrane proteins contain one or more transmembrane helices. Peripheral membrane proteins are loosely associated with the integral membrane proteins or the lipid polar head. Many of integral membrane proteins are transmembrane proteins, which pass entirely through the lipid bilayer with portions protrude from both extracellular and cytoplasmic sides of membrane.

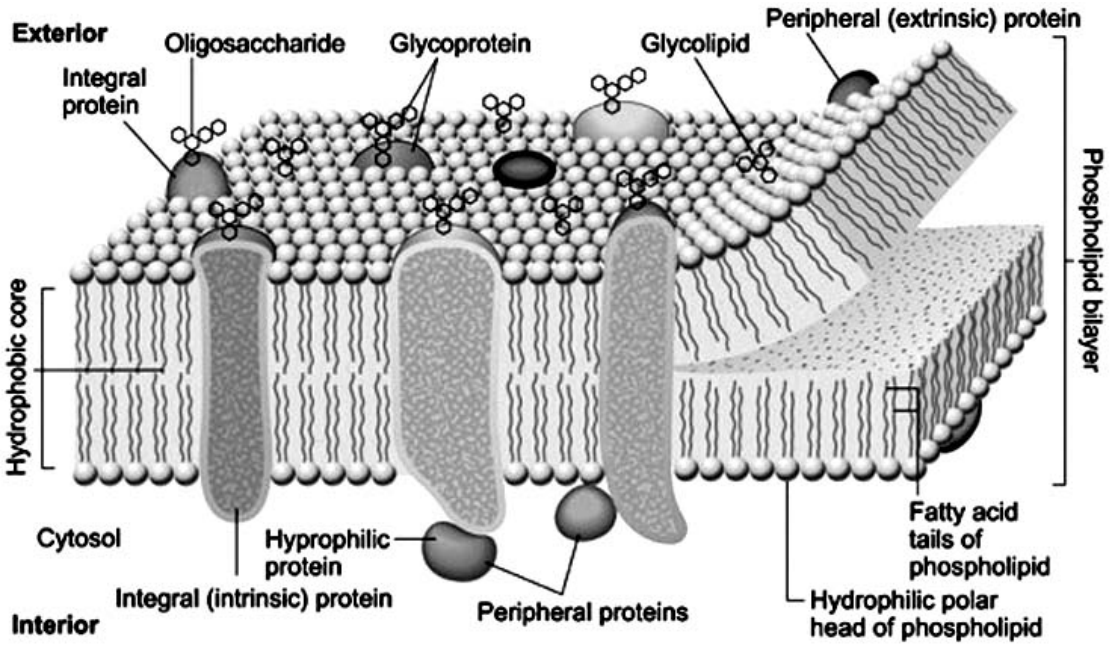

Figure 3.1 Schematic representation of biological membranes. Cell membranes are composed of lipids and proteins. All cell membranes share a common structural organization, phospholipid bilayers with associated proteins, which are responsible for many specialized functions (http://www.che.vt.edu/Sum/images/cell-membrane.gif).

Membrane proteins can be classified into different groups relied on the orientation and anchoring on the plasma membrane (**Figure 3.2**).

1. *Type I transmembrane proteins.* Type I transmembrane proteins retain the COOH-termini in the cytoplasm and protrude the NH_2-termini outside the cell. These molecules generally have a signal sequence at the NH_2-termius which is cleaved off after the molecules passed into the endoplasmic recticulum and have a single transmembrane region. These proteins may be glycosylated in the Golgi apparatus and then exported to express on the cell surface. These molecules commonly serve as cell surface receptor and/or ligand. The membrane spanning portion of type I transmembrane protein are usually α helices of 25 hydrophobic amino acids followed by a cluster of basic amino acid that bind to the phospholipids head group inside the surface membrane bilayer.
2. *Type II transmembrane proteins.* Type II single-pass transmembrane proteins have an opposite orientation to type I transmembrane protein. The NH_2-terminus is located inside the cell and the COOH-terminus is outward. These protein often have uncleaved signal sequences for transmembrane domains, allowing for their cleavage and release from the cell surface. Type II transmembrane proteins have a single transmembrane domain.
3. *Type III transmembrane proteins.* Type III transmembrane proteins have more than one membrane spanning portions. The example of these transmembrane proteins is the multidrug resistance transporter protein, MDR1 (31). These multiple spanning transmembrane portions can form channels for transporting ions or small molecules through the lipid bilayer. On leukocytes, members of this group have usually been identified functionally rather than by antigenicity.
4. *Type IV transmembrane proteins*. Type IV proteins can be distinguished from type III protein in the presence of a water-filled transmembrane channel. None of the current CD antigens is type IV transmembrane proteins.

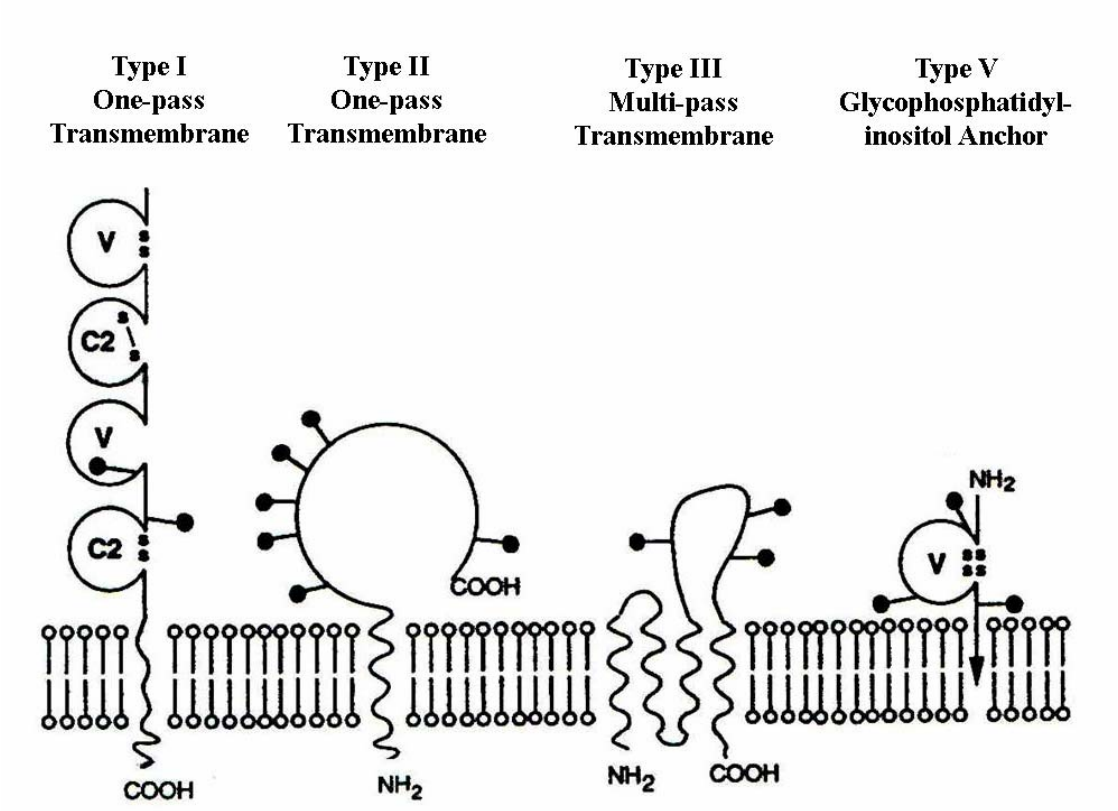

Figure 3.2 Leukocyte surface proteins (CD antigens). The leukocyte surface proteins (CD antigens) can be divided into four types which respects to the orientation and anchoring on the plasma membrane.

5. *Type V glycosyl-phophatidylinositol (GPI)-anchored proteins.* Type V proteins contain multiple transmembrane regions. These proteins utilize a glycosyl-posphateidylinositol (GPI) anchor attached to the C-terminal residue of the protein.

3.1.3 Cell communications

In a multicellular organism the cells must be communicate to each other in order to coordinate and integrate functions. The interaction between cells can range from cooperative to antagonistic. Signaling molecules in cell cooperation are as follows.

Cytokines: Cytokines are low molecular weight, soluble proteins that function as chemical messengers for regulating the immune system. Cytokines are produced by the cells of innate and adaptive immunity, especially by T helper (T_H) lymphocytes. The activation of cytokine-producing cells triggers them to synthesize and secrete the cytokines. These cytokines are able to bind to specific cytokine receptors on other cells of the immune system and influence their activities in some manners. The nomenclature of cytokines is often based on their cellular sources. Cytokines that are produced by mononuclear phagocytes are sometimes called monokines, and those produced by lymphocytes are commonly called lymphokines (32). Because many cytokines are made by leukocytes and act on other leukocytes, they are also called interleukins (IL). Examples of cytokines are IL-4, IL-5 and IL-10 which are produced by $CD4^+$ T lymphocytes (T_H2).

Chemokines: Chemokines are a large family of structurally homologous cytokines that mobilize white blood cells (WBCs) to sites of inflammation (32). They drive the WBCs out of the blood circulation and chemotactically attract them to the inflammatory site, trigger some WBCs to release their killing agents for extracellular killing, and induce some WBCs to ingest the remains of damaged tissue.

Interferons (IFN): Interferons modulate the activity of virtually every component of the immune system. Type I IFNs is composed of distinct groups of proteins called IFN-α which has more than 20 types, IFN-β, IFN Ω, and IFN τ. There

is only one type II IFN, IFN-γ. Type I IFNs, which can be produced by virtually any virus-infected cell, provide an early innate immune response against viruses. Type II IFN is produced by activated T-lymphocytes as part of an immune response and functions mainly to promote activity of the components of cell-mediated immune system such as CTLs, macrophages, and NK cells (32).

Tumor necrosis factors (TNF): TNF is the principle mediator of the acute inflammatory response to infectious microbes and is responsible for many of the systemic complications of severe infection (32). TNF-α is produced by monocytes/macrophages, T_H1 cells, and other cells. TNF-β is produced by T_H1 cells and $CD8^+$ T lymphocytes.

Hormone: Hormone is a chemical or protein product. It can be separated into three broad categories. The first category is composed of small lipophilic molecules that diffuse across the plasma membrane and interact with intracellular receptors. The second category includes hydrophilic molecules that bind to cell-surface receptors and lipophilic that binds to cell-surface receptors are classified as the third group.

Membrane-bound signal molecules: The membrane-bound signal molecules are membrane proteins on cell surface that function as ligand. They are synthesized within the cell via mRNA, ER membrane, and presented on the cell plasma membrane. The synthesis depends by three ways. First, it is constitutively synthesized and it functions when combined with other protein. Example of this molecule is MHC molecule, which function as ligand when peptide antigen is inserted in to this molecule. Second, also constitutively synthesized and is ready to function. Examples of these molecules are CD28, B7, ICAM-1, which function as co-stimulatory molecules. Third, it is induced to synthesize dependable on signaling requirement. Examples of the third type are Fas ligand, which is produced by CTL and CD40L, which is produced by $CD4^+$ helper T lymphocytes (33, 34).

3.1.4 Biological function of leukocyte surface molecules

As the other cell types, leukocytes express a variety of molecules on their cell surface. The leukocyte surface molecules or CD antigens are vital in a whole range of leukocyte functions including cell activation, cell-cell signaling and cytokine-receptor signaling. These biological functions of leukocyte surface molecule are mediated by membrane proteins which are categorized as follows.

Transport of small molecules. Cell must be constantly supplied with nutrients and the metabolic waste products must be withdrawn. Most biological molecules are unable to diffuse through the phospholipid bilayer. Therefore the plasma membrane forms a barrier that block the free exchange of molecules between intracellular and extracellular environments. The plasma membrane of leukocytes contain specific transport proteins including carrier proteins and channel proteins (35) that mediate the selective passage of necessary molecules across the membrane and allowing the cell to control the composition of its cytoplasm.

Enzymatic activities. Some leukocyte surface molecules are enzymes such as CD10 and CD13. These enzymes provide a powerful way in modifying the activity of cytokines in the vicinity of cell surfaces. The cytoplasmic region of some leukocyte surface molecules such as CD45, CD115, CD117 and CD148 has kinase and phosphatase activity which are important in signal transduction (36-38).

Signal transduction. Interactions of some cell surface molecules with soluble proteins or glycoproteins as well as with the cell surface molecules on other cells and extracellular matrix lead to intracellular signal transductions (39, 40). These signals conduct cell activation, differentiation, and finally initiate cell functions. Some cell surface molecules interact with soluble proteins or glycoproteins as well as with the surface of other cells and extracellular matrix (39, 40) and lead to intracellular signal transductions. These signals conduct cell activation, differentiation and finally initiate cell functions. The signal transduction would occur by an event outside the cell somehow being transmitted to the interior via a surface molecule. The binding of ligand to a receptor on the cell surface such as antigen receptor, G protein-coupled receptors or cytokine receptors initiates a cascade of intracellular reactions, ultimately reaching the target cell nucleus and resulting in programmed changes in gene

expression. Although the plasma membrane constitutes the boundary between a living cell and its nonliving environment, materials present outside the plasma membrane play an important role in the life of the cell. Most cells in a multicellular plant or animal are organized into clearly defined tissues in which the component cells maintain a defined relationship with one another and with the extracellular materials that lie between cells. These interactions regulate such diverse activities as cell migration, cell growth and cell differentiation. The outer surface of the plasma membrane contains receptors that mediate interactions between the cell and the components of its environment. These cell surface receptors interact not only with the external surrounding, but are connected at their internal end to various cytoplasmic proteins. Receptors with this type of dual attachment are well suited to transmit messages between the cell and its environment.

Interactions with cells or extracellular matrix. Direct interactions between cells as well as the extracellular matrix, are critical to the development and function of multicellular organisms. Some cell-to-cell interactions are transient, such as the interactions that direct white blood cells to the site of tissue inflammation (41). Cell-cell interaction is a selective process, such that cells adhere only to other cells of specific types. Most of these involve heterophilic interactions although there are some homophilic interactions. A family of cell surface proteins, termed cell adhesion molecules, mediates such selective cell-cell interactions (42-45). The adhesion molecules can be divided into four major groups which are the selectin, the integrin, the immunoglobulin (Ig) superfamily, and the cadherins (**Figure 3.3**).

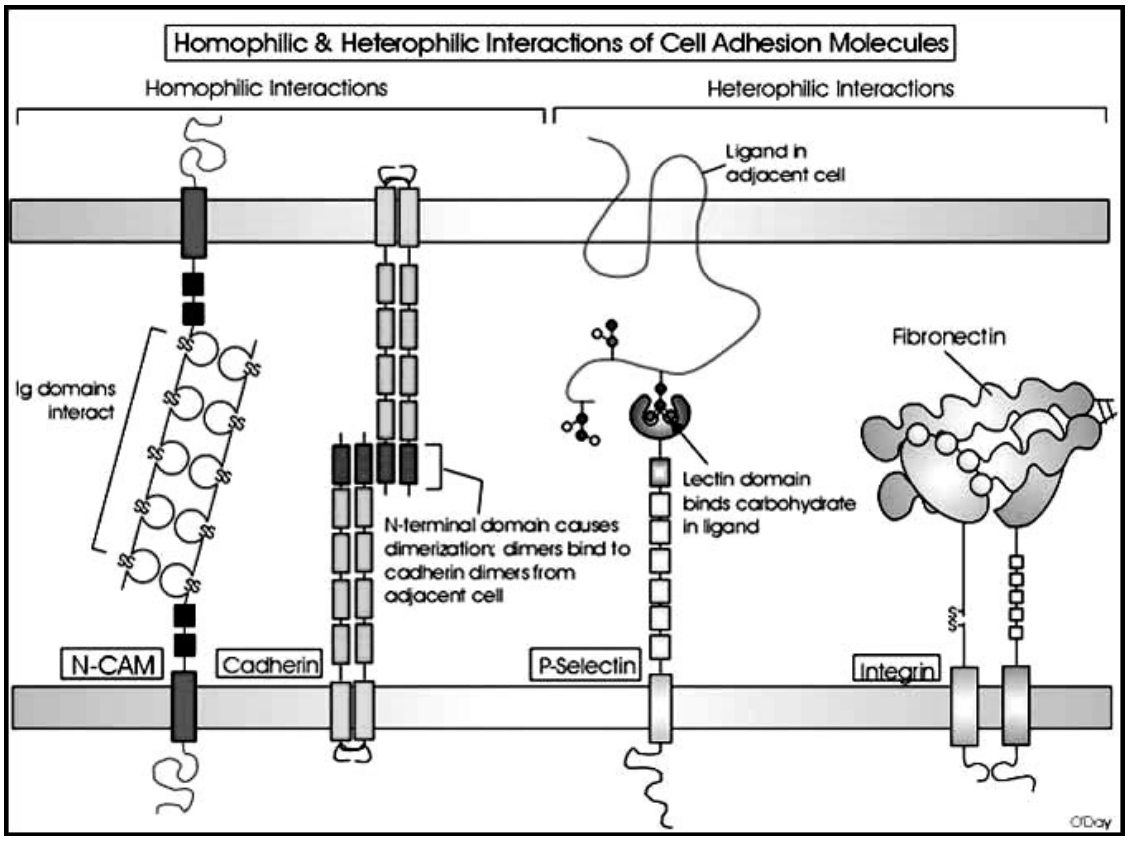

Figure 3.3 A family of cell adhesion molecules. The cell adhesion molecules can be divided into 4 major groups which are the selectins, the integrins, the cadherins and the immunoglobulin (Ig) superfamily (http://www.erin.utoronto.ca/~w3bio315/Lectures/CAMS2/CellAdhesionTypes1.jpg).

Adhesion molecules are surface-bound molecules involved in cell-to-cell interactions (46). Their main function is in facilitation processes where close contact of cells is required such as in cell migration (41), phagocytosis (47, 48) and cellular cytotoxicity (47, 49, 50). Signal transduction after ligation of the cell adhesion molecules lead to cell activation, alteration in receptor expression, cytokine production and effect on cell survival. Some adhesion molecules are expressed mainly on leukocytes, other endothelial cells enabling interaction between the two (51).

Selectins, integrins, and member of the Ig superfamily mediate transient cell-cell adhesions by the interactions between leukocytes and endothelial cells during the migration of leukocytes from the circulation to sites of tissue inflammations (41). In addition, some of these molecules are also costimulatory during intercellular signaling (52). Selectins are found on all leukocytes and functions as lectins, which bind to carbohydrate moieties expressed by endothelial cells or other leukocytes. The three members of the selectin family are L-selectin, E-selectin, and P-selectin. Each of the selectins participates in the process of leukocyte rolling along vascular endothelium. The integrins and Ig superfamily adhesion molecules bind through protein-protein interactions and are important for stopping leukocyte rolling and mediating leukocyte aggregation and transendothelial migrations (41, 46, 53). The integrins are heterodimers and include the very late antigen (VLA) molecules (CD49a-CD49f), leukocyte function-associated antigen (LFA-1 or CD11a) and Mac1 (CD11b). The immunoglobulin superfamily is the most abundant family of cell surface molecules, accounting for 50% of leukocyte surface glycoprotein. Their structures are characterized repeated domains, similar to those found in immunoglobulins, built from a tightly packed barrel of β strands. The Ig superfamily adhesion molecules include the intercellular adhesion molecules (ICAMs), vascular cell adhesion molecules (VCAMs), LFA-2 (CD2) and LFA-3 (CD58). The biological importance of these molecules for host defense is exemplified by the impairment of T-cell cytotoxic function with inhibition of either LFA-1/ICAM-1 (CD54) interactions or LFA-2/LFA-3 interactions. Clinically, mutations in CD18 (the b chain in the integrin LFA-1 and Mac-1) are manifest as recurrent bacterial infections due to an inability to mobilize leukocytes in the sites of inflammation. Interaction of VLA-4 (CD49d)/VCAM-1

(CD106) are especially important for eosinophil adhesion to endothelial cells during allergic late-phase immune responses.

The frequency of different type of functions mediated by leukocyte surface molecules is shown in **Table 3.1**. This data indicates that approximately 48% of identified leukocyte surface molecules act as receptors for cytokines, other soluble proteins or other cell surface proteins and act as receptors for extracellular matrix. Whereas about 50% of leukocyte surface molecule function are still unknown.

Table 3.1 Frequency of the roles of leukocyte surface molecules

Functional roles of leukocyte surface molecules	Frequency
Enzymatic activity in extracellular domains	3%
Receptors for cytokines	13%
Receptors for other soluble proteins	10%
Receptors for cell surface proteins or extracellular matrix	25%
Other (e.g. ion channels and transporters)	1%
Unknown function	49%

3.2 CD147

Human leukocyte surface molecule CD147 is also known as M6 Ag (54), basigin (55) and EMMPRIN (56) which is broadly expressed on both hematopoietic and non-hematopoietic cells. Expression of CD147 on T cells depends on the differentiation state (57). CD147 is strongly expressed on cell surface of thymocytes than mature peripheral T cells (57). Peripheral lymphocytes is not significantly express CD147 however its expression is up regulated on activated T-cells which is observed on the surface of lymphoblasts after 3 days of PHA stimulation (55, 56). cDNA coding M6 proteins was cloned using COS cell expression system (54). Comparison of the M6 sequences with other molecules indicated that M6 is the species homologue of rat OX-47 antigen (58), a mouse molecule termed gp42 (59) or mouse basigin (60) or CE9 antigen (61), and a chicken antigen HT7 (62), 5A11 antigen (63) or neurothelin (64). In addition, the CD147 bears high-frequency Oka blood group antigen (65).

The CD147 gene has been mapped to band p13.3 of chromosome 19 (66). Cloning and sequencing analysis of the CD147 molecule showed that the human CD147 molecule codes for 269 amino acid residues and have a typical feature of a type I integral membrane protein. CD147 belongs to the immunoglobulin superfamily with an approximate molecular weight of 50-60 kDa (67, 68) and contains two extracellular Ig domains, a single transmembrane domain and a short cytoplasmic domain (58, 69) **(Figure 3.4)**. The extracellular domain consists of two Ig-like domains most probably of the C_2 type when determined by comparison with other Ig domains. Domain 1 of the molecule is homologous to domain 3 of IL-1 receptor and domain 2 was found to be significantly related to domain 5 of a chain of CD22 (54). Endoglycosidase F treatment of immunoprecipitates resulted in a mobility shift from 54 kDa to 28 kDa showed that the majority of the oligosaccharide chains are N-linked (54). The 21 amino acid of the putative transmembrane region are absolutely identical in the human, rat and chicken homologues and, with the exception of one amino acid, also in the mouse and rabbit forms (54, 70). Interestingly, the hydrophobic stretch of the transmembrane region of M6 is interrupted by a charged residue, a glutamic acid, and contains a leucine-zipper that is potential protein-protein interaction motifs. The strong conservation of the molecule suggest an important functional role for this region

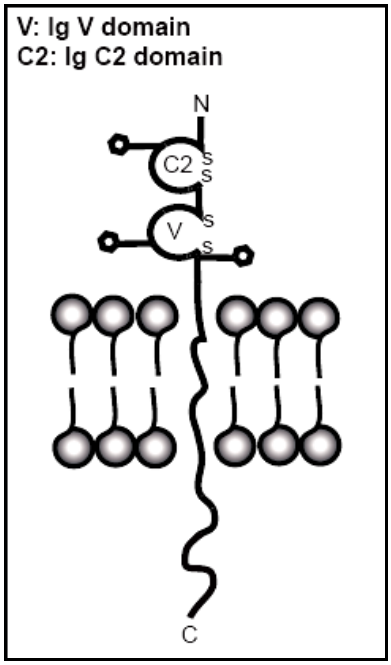

Figure 3.4 Schematic represents the structure of CD147**.**

perhaps involved in interactions with other proteins within the plasma membrane or signal transduction. The transmembrane regions show a very high degree of cross-species conservation. This evidence suggests that the transmembrane domain of CD147 may have an important functional role superior to anchoring the protein in the membrane. Another shared feature of the transmembrane regions of members of the CD147 homologues is a centrally positioned glutamic residue (58). A charged amino acid immerse in the transmembrane domain is a common characteristic of proteins with multiple transmembrane domains, but unusual for a protein with single transmembrane domain protein. This feature is crucial for lateral association of CD147 with MCT1 and MCT4 (71). The physical association between CD147 and β1 integrin in the membrane has been reported (72, 73). Berditchevski *et al*. (72) suggested that association of $\alpha^3\beta_1$ integrin and $\alpha^6\beta_1$ integrin with CD147 is in lateral fashion, similar to interaction of β_3 integrins with CD47, another immunoglobulin superfamily proteins (74, 75). CD147 also serves as a signaling receptor for extracellular cyclophilin A (76-78) and cyclophilin B (77).

Highly expression of CD147 is also observed on human carcinoma cells than normal cells (79-81). Normal oral mucosa showed localized keratinocyte membrane-staining of CD147, whereas oral carcinoma cells showed staining diffusely through the entire tumor specimen (82). Previous studies showed that CD147 seems to directly bind to interstitial collagen (5) suggesting the involvement of CD147 in regulating stromal matrix metalloproteases (MMPs) and leading to extracellular matrix (ECM) degradation which resulted in tumor invasion and metastasis (83-85). Therefore, CD147 was termed EMMPRIN (Extracellular Matrix Metalloproteinase Inducer) (56). The CD147 monoclonal antibodies (mAbs) AAA6 and UM-8D6 inhibited homotypic aggregation of the estrogen-dependent breast cancer cell line, MCF-7, as well as MCF-7 cell adhesion to type IV collagen, fibronectin and laminin (69). Regarding to multidrug resistant (MDR) cancer cells overexpressing P-glycoprotein (P-gp) display variations in invasive and metastatic behavior, expression of CD147 in MDR cell lines seems to be responsible for the increased activity of MMP during the development of MDR cell lines (86). CD147 is also play a role in neoangiogenesis (85), reproduction, neural function and inflammation (87). Since CD147 participates in the breakdown of

the extracellular matrix (ECM) by augmenting matrix metalloproteinase (MMP) expression, the menstrual cycle-dependent expression of EMMPRIN in human endometrium in vivo was identified and characterized (88). This study reported that CD147 may be involved in ECM breakdown at interface between endometrial cells and ECM by using EMMPRIN-bound MMP-1 (88). Mice lacking the gene for CD147/EMMPRIN/basigin showed defects in embryogenesis, spermatogenesis, and female fertilization (89, 90), as well as an altered mixed lymphocyte reaction and loss of an aversive response to a strong odor (91).

The molecular function of CD147 molecule in immune system is not clearly understood. The ligation of CD147 molecule on immature fetal thymocytes which inhibited their further development into mature T-cells was triggered by CD147 mAbs (92). Certain CD147 mAbs induced homotypic cell aggregation of monocytic cell line, U937, by LFA-1/ICAM-1 dependent pathway (67). This activation depended upon the activation of protein kinase and reorganization of cytoskeleton (93). Enhancing mixed lymphocyte responses in CD147 knockout mice indicates a negative regulatory function of CD147 in T cell regulation (90). Triggering of CD147 molecules on T cells by the inhibitory mAb resulted in modulation of lipid rafts, which associated with impaired signaling for expression of the IL-2R α chain CD25 (94).

Most functional studies of CD147 molecules relied on using specific mAbs to induce the cells of interest (67, 71, 83, 84, 90, 92-94). The interaction of mAbs and their targets mimicked the native ligand-receptor signalings, however, was not always relevant to the indigenous communications. In addition, the results obtained did not verify the role of CD147 in binding to membrane receptor (s) and transferring the signal to the cells. Recently, purified native CD147 was used to induce the production of secreted MMP-1 by human dermal fibroblasts and also MMP-2 by breast carcinoma cell line (MDA-435). This study suggested that homophilic CD147-binding may occur in the context of both heterotypic and homotypic cell-cell interaction (1). There was no following reports demonstrated the function of CD147 molecule, especially on hematopoietic cell lines. The binding affinity of CD147 to its receptor was presumably weak, as is seen typically for immunoglobulin superfamily proteins (1). Hence, construction of the multimeric molecule should assist the discovery of CD147 function.

3.3 Phage display technology

Phage display technology is the most widely affiliated molecular display techniques. It has a major impact on immunology, cell biology, drug discovery and pharmacology. Phage display is an extremely powerful tool to generate antibodies, peptides and proteins at the surface of phage particles (8, 95, 96). Display of epitopes, including peptides and genes fragments, facilitates analyses of protein-protein interactions, such as structural mapping of epitopes, characterization of receptor-ligand interactions, and modulation of functional pathway. This technique is accomplished by the incorporation of the nucleotide sequence encoding the protein of interested into a phage or phagemid genome as a fusion to a gene encoding a phage coat protein. This fusion warrants the protein to be displayed is presented at the surface of phage particle, while is coding sequence is contained within the same phage particle. This establishes a physical linkage between phenotype and genotype of the expressed protein.

3.3.1 M13 filamentous bacteriophage structure

The Ff bacteriophages are a group of bacterial viruses that contain a circular single-stranded DNA genome encapsulated in a long protein capsid cylinder. The filamentous bacteriophage of the Ff type (f1, fd and M13) is the main component in phage display technology. These bacteriophages use the tip of the F conjugative pilus as a receptor and thus are specific for *E. coli* containing the F plasmid. The Ff phages replicate within the host cell and do not kill their host during productive infection. M13 is an *E. coli*-specific filamentous bacteriophage about 900 to 2000 nm in length and less than 10 nm in diameter. This flexible cylinder is covered by 2700 copies of gpVIII major coated protein. Each end of the particle is capped by 5 copies each of two minor coated proteins, gpIII and gpVI, at one end and gpVII and gpIX at the other end (**Figure 3.5 and Table 3.2**). All five coat proteins contribute to the structural stability of the phage particle. gpVII and gpIX are required for efficient particle assembly, while gpVI and gpIII are crucial for host recognition and phage infectivity.

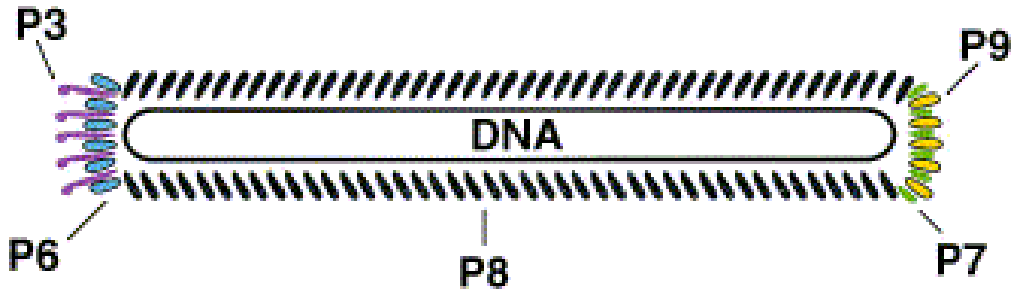

Figure 3.5 Structure of a filamentous bacteriophage. Schematic representation of the bactriphage particle shows the single-stranded DNA (ssDNA) genome surrounded by the phage coat proteins (97).

Table 3.2 Phage coat proteins

Coat protein	Number of amino acids	Molecular weight	Copies per phage
gpIII	406	42,500	5
gpVI	112	12,300	5
gpVII	33	3,600	5
gpVIII	50	5,200	2700
gpIX	32	3,600	5

3.3.2 M13 filamentous bacteriophage infection process

Infection of *E. coli* by the Ff phage is initiated by the specific interaction of gpIII with the tip of the F conjugative pilus. gpIII is sufficient to mediate the phage infection, and has been intensive intensively studied to help the understanding of the infection process (98). gpIII is divided into three domains separated by glycine-rich regions. The N-terminal domain (D1) is thought to be responsible for membrane penetration, the middle domain (D2) for adsorption to the F-pilus tip and the C-terminal domain (D3) for anchoring the gpIII in the phage particle. It also contains a short C-terminal transmembrane segment for anchoring in the bacterial inner membrane. The F pilus consists of a protein tube made up of pilin subunits which are assembled and dissembled by a polymerization and depolymerization process in the bacterial inner membrane. Pilus retraction (by depolymerization) draws the donor and recipient bacteria together thus the end of the phage attached to the F pilus is brought to the membrane surface. gpVIII integrates into the inner membrane, and the phage DNA is translocated into the cytoplasm. The translocation process requires the produce of the *tolQRA* genes. The tolQRA proteins are located in the inner membrane. They may form complex which can communicate between the inner and outer membranes. One of the normal functions of these Tol proteins may be to maintain the integrity of the outer membrane, to avoid a leak of periplasmic proteins into the culture medium. After the phage DNA translocation, bacterial enzymes convert the infecting single ssDNA into a supercoiled, double strand replicative form (RF). gpII binds and introduces a specific cleavage on the (+) strand of the RF molecule. The host enzymes use the resulting 3′ end as a primer to synthesize a new (+) strand which is then converted in a new RF DNA by bacterial enzymes. The gpX is crucial for the proper replication of the phage DNA and functions as an inhibitor of gpII (99). All phage proteins are synthesized from the RF molecule, and their production increases with the accumulation of the RF molecules. All phage proteins involved in the assembly of the particle become integrated in the phage envelope while proteins involved in DNA replication remain in the bacterial cytoplasm. The binding of the phage specific ssDNA binding protein, gpV, to the newly synthesized ssDNA prevents the conversion of ssDNA to RF. When gpV reaches the proper concentration, it sequesters the ssDNA into a complex.

3.3.3 M13 filamentous bacteriophage assembly

The M13 genome contains 11 genes; five of these genes encode the coat proteins as mentioned above while the others encode proteins necessary for viral replication and assembly. The assembly of the bacteriophage is a membrane-associated event. The assembly process of M13 requires the integrated interaction of multiple copies of the five structural proteins, two non-structural proteins (gpI in the inner host cell membrane and gpIV in the outer membrane) and at least one host protein (thioredoxin). M13 replication is triggered when gpIII binds to the F pilus on the surface of an *E. coli* cell, and then promotes the translocation of the viral DNA into the *E. coli* cytoplasm. The single-stranded DNA is then converted to the double-stranded DNA, which is further duplicated and used as the template for the production of all phage proteins in bacterial host cell. This double strand form is also served as the template for the production of new single-stranded viral DNA.

Assembly occurs at sites corresponding to bacterial adhesion zone, where the inner and outer membranes are in close contact. Before assembly into phage particles, the coat proteins are embedded in the bacterial inner membrane with their N-termini in the periplasm and their C-termini in the cytoplasm. Interaction of the gpV-phage complex with proteins in the assembly site is the initiating event for assembly of the particle. Assembly proteins, gpI, gpIV, and gpIX, form a gated pore complex that spans the inner and outer membranes. The gpV are displaced from, and the gpVIII and gpIX added to, the ssDNA as it is extruded through this pore and simultaneously surround by gpVIII and other phage proteins which subsequently transition from the inner membrane into the assembling phage particle (**Figure 3.6**). The elongation process then follows in which thousand of gpVIII molecules are assembled along the length of the particle. This process is terminated by the addition of gpVI and gpIII at the other end of the particle. The assemble phage particle is then released into the culture supernatant. M13 assembly is a non-lytic process. The newly assembled phage particles are continuously extruded from the infected cells which continue to grow and divide, although at a reduced rate.

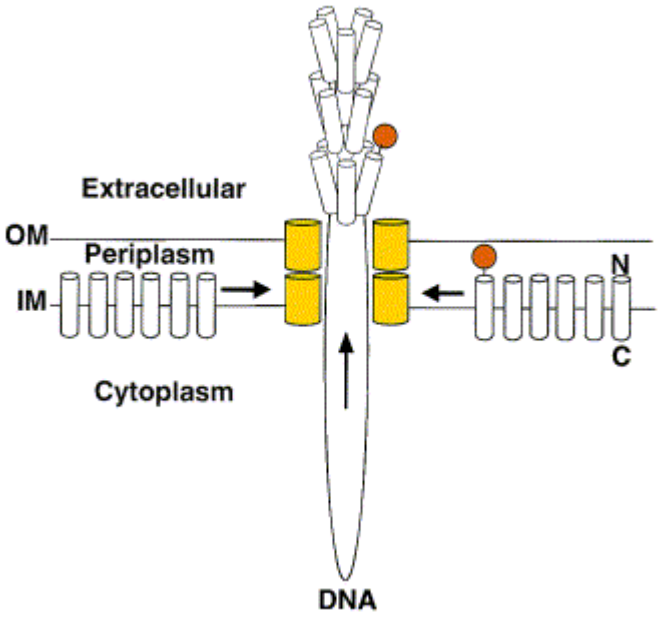

Figure 3.6 A simplified diagram of M13 bacteriophage assembly. Newly- synthesized coat proteins are embedded in the inner membrane (IM) with their N termini in the periplasm and their C termini in the cytoplasm. The single-stranded viral DNA is extruded through a pore complex that span through the inner membrane and the outer membrane (OM). The DNA is concomitantly surrounded by phage coat proteins and transferred into the assembling phage coats. The assembled phage particle is then extruded to the extracellular environment with non-lytic process. A heterologous protein (red circle) will be displayed on the surface of phage particle if it is successfully fused to the coat protein that can successfully incorporate into the phage (97).

3.3.4 Phage display: Historical development

Phage display is first developed with the *E. coli*-specific bacteriophage M13 by Goerge P. Smith in 1985 (8). Smith demonstrated a short peptide sequence fused with the pIII coat protein could be displayed on the surface of the phage. In early example of phage display, the foreign DNA was cloned directly to the amino terminus of either gpIII or gpVIII in the viral genome (97). Before phage assembly, gpIII and gpVIII reside in the inner membrane with their amino terminal in the periplasm and their carboxy terminal in the cytoplasm. By this strategy, multivalent display is obtained which mean every single copy of gpIII or gpVIII will carry a fusion partner on the surface of phage particle. These phage systems were limited because large polypeptides (>10 residues for pVIII display) compromised coat protein function especially since no wild type of coat protein are retained. Alternative strategies have been introduced to overcome this limitation.

This hybrid phage based on the additional element of gene fusion in the complete phage genome, thus the expanded genome encodes two versions of on of the coat protein. Both wild type and fusion proteins are expressed on phage particle (100). Alternatively, a phagemid display system has been introduced and this approach has been widely adopted (13, 101). Sequences encoding fusion protein are conducted by phagemid while the majority of the gene required for the formation of phage particle are carried by helper phage that are co-infected together with phagemids into host bacteria. A mixture of wild type and fusion protein is produced in the bacterial and the progeny contained a mixture of wild type and fusion protein on phage particle. In general, large numbers of smaller proteins may be display if gpVIII is chosen as a fusion partner, while gpIII is suitable for smaller numbers of larger proteins. Normally, less than 10% of gpIII display the fusion protein. The majority is only one copy per phage particle.

3.3.5 Phage display: Application

The experimental goals behind the display of proteins or random peptides can be divided into 2 categories; identification of any protein or peptide that possesses a particular desired property and the selection of a natural protein or peptide mimic. An important application of phage display technology is receptor/ligand research (11). The display of proteins on the surface of phage particles is one of the most effective methods for identifying cell surface proteins that recognize specific baits. Phage display has been successfully applied in signal transduction research, new drug development and screening, production of clinical diagnostic tools and antibody engineering. For example, the strictly binding of an assortment of phage clones to one organ or cell type have been reported (102). The long term goal of this strategy is to develop a new class of targeted drug-delivery systems. Similar work has been done on targeting the tumor-specific antigens on tumor cell surface (103). In addition, recombinant phage particles have been developed to serve as the molecular sponges. The main purpose of this category is to bind as many targets per unit weight as possible. These include phage acting as protein purification agents or as toxic waste removers (14, 104, 105). Furthermore, the displayed protein or peptide is either acting as a "stand-in" for a natural protein or protein fragment or has purposely been engineered to carry variant of a particular protein or peptide to facilitate the coupling of in vitro manipulation of that protein with a rapid functional assay. Numerous groups have carried out directed molecular carried out directed molecular evaluation studies on a broad variety of proteins. These proteins are including hormones (101, 106), antibodies (107, 108), growth factors (109) and enzymes (110-112).

CHAPTER 4

MATERIALS AND METHODS

4.1 Chemicals and instruments

Chemicals and instruments used in this study were shown in Appendix.

4.2 CD147Ex gene amplification by PCR

4.2.1 CD147 extracellular domain gene amplification by PCR

The CD147 extracellular domain (CD147Ex) gene was amplified from the mammalian expressing vector containing CD147Ex, pCDM8-CD147. The pCDM8-CD147 was kindly provided by Associated Professor Dr. Watchara Kasinrerk, Clinical Immunology Unit, Department of Medical Technology, Faculty of Associated Medical Sciences, Chiang Mai University, Chiang Mai, Thailand (54). Two oligonucleotides, CD147ExgpVIIIFw (5′-GAG GAG GAG GTc tcg agG CTG CCG GCA CAG TCT TC-3′, the *Xho*I restriction site is designated in small letters) and CD147ExgpVIIIRev (5′-GAG GAG GAG CTa cta gtG TGG CTG CGC ACG CGG AG-3′, the *Spe*I restriction site is designated in small letters), was used as primers for annealing to the 5′ and 3′ end of the CD147Ex fragment, respectively. PCR was used to amplify the CD147Ex from pCDM8-CD147 (54). Fifty nanograms of pCDM8-CD147 was annealed with 250 ng of each described primer in the 100 µl of a PCR mixture containing 5 U of ProofStart DNA polymerase (QIAGEN, Hilden, Germany). The PCR cycling condition was one cycle at 95 ^{o}C for 5 min followed by 34 cycles of 94 ^{o}C for 50 sec, 50 ^{o}C for 50 sec, and 72 ^{o}C for 1 min. After 35 amplification cycles, the mixture was incubated at 72 ^{o}C for 10 min.

4.2.2 Agarose gel electrophoresis

Agarose gel (1% for DNA fragments and 2% for phagemid vector) was prepared by dissolving 1 or 2 g of agarose in 100 ml of TAE buffer, pH 8.0. The agarose suspension was melted in microwave oven until completely dissolved, and allowed to be cooled to approximately 50 ^{o}C prior to pouring into a casting chamber equipped with comb. After allowing the agarose to be harden at room temperature, it was placed in the electrophoretic chamber and electrophoresis buffer (1x TAE) was added so that the gel surface is submerged. The DNA samples were mixed with 1/5 volume of 6x gel-loading dye (0.25% bromphenol blue and 30% glycerol) and loaded into the well. The DNA marker was also loaded in parallel in the same gel as markers for DNA molecular size. Electrophoresis was carried out by applying constant voltage at 100 volts until the bromphenol blue migrated to about 3/4 of the gel, at which time of the electrophoresis was stopped. The gel was stained with ethidium bromide solution (0.5 μg/ml) for 20 min and subsequently destained with distilled water until the background was clear. The DNA pattern was visualized under UV transilluminator and the size of DNA fragment was estimated by comparing to the size of the DNA markers. The DNA bands were photographed using FOTODYNE transilluminator and camera systems (FOTODYNE Incorporated, Hartland, WI, USA).

4.2.3 Digestion of PCR product with restriction enzymes

The resulting 550 bp PCR product was digested with *Xho*I (Promega, Medison, WI, USA) and *Spe*I (Promega). Approximately 100 μg DNA was digested with restriction enzymes using 5 U of each enzyme/μg DNA in 1x buffer and the total volume of should contain <5% glycerol. The buffer for specific restriction enzymes was followed the commercial recommendation. The digestion reaction was incubated at 37 ^{o}C for 18 h.

4.2.4 Purification of PCR products for sub-cloning into phagemid vector

To purify the PCR product after restriction enzyme digestion, the digested PCR product was firstly analyzed by agarose gel electrophoresis in 2% agarose gel. After ethidium bromide staining, the digested PCR product was visualized under a FLUO-LINK UV transilluminator (Vilber Lourmat, Marne-la-Vallée Cedex, France). The desired band of digested PCR product, 550 bp, was purified by QIAquick PCR purification Kit (QIAGEN) according to the manufacturer's protocol prior to sub-cloning into phagemid vector.

4.3 Construction of phagemid expressing CD147Ex

4.3.1 Preparation of pComb8 phagemid by QIAGEN kit

This method is used for extraction the high purity of pComb8 phagemid using QIAprep spin Miniprep kit (QIAGEN). A single colony of *E. coli* harboring pComb8 phagemid was selected and grown in 3 ml of Luria-Bertini (LB) broth (1% w/v tryptone, 0.5% w/v yeast extract and 1% w/v NaCl) supplement with 100 μg/ml ampicillin. After overnight (14-16 h) growth at 37 ^{o}C with shaking, the bacterial culture was harvested by centrifugation at 12,000 rpm for 5 min in a microcentrifuge tube. The isolation of phagemid was preformed according to the standard protocol by the manufacturer.

4.3.2 Digestion of pComb8 phagemid with restriction enzymes

The pComb8 phagemid was digested with *Xho*I (Promega) and *Spe*I (Promega). Approximately 100 μg DNA was digested with restriction enzymes using 5 U of each enzyme/μg DNA in 1x buffer and the total volume of should be contained <5% glycerol. The buffer for specific restriction enzymes was followed the commercial recommendation. The digestion reaction was incubated at 37 ^{o}C for 18 h.

4.3.3 Purification of digested pComb8 phagemid vector from agarose gel

To purify the digested pComb8 phagemid after restriction enzyme digestion, the phagemid was firstly analyzed by agarose gel electrophoresis in 1% agarose gel. After ethidium bromide staining, the DNA fragments were visualized under a FLUO-LINK UV transilluminator (Vilber Lourmat, Marne-la-Vallée Cedex, France). The DNA fragment of digested pComb8, 3,300 bp, was excised from the gel using a clean razor blade. The digested pComb8 phagemid was recovered using QIAquick Gel Extraction kit (QIAGEN) according to the manufacturer's protocol.

4.3.4 Ligation of DNA fragments

After digestion with the restriction enzymes, the digested pComb8 phagemid vector was ligated with digested CD147Ex PCR product using T_4 DNA ligase. The standard ligation reaction composed of the digested vector and the DNA fragment in 1:3 molar ratio, 1 U of T_4 ligase enzyme (Roche Molecular Biochemicals, Manheim, Germany), 1x ligation buffer (66 mM Tris-HCL, 5 mM $MgCl_2$, 5 mM DTT, 1 mM ATP, pH 7.5) and sterile distilled water in a final volume of 20 µl. The ligation reaction was incubated at 4 ^oC for 16-18 h. The ligated product was used to transformed into TG1 *E. coli* host strain {*supE hsd*Δ5 *thi*Δ(*lac-proAB*) F'[*traD36proAB+, lac*I^q *lacZ*ΔM15]} (kindly provided by Dr. A.D. Griffiths, MRC Cambridge, UK).

4.3.5 Preparation of TG1 *E. coli* competent cells

The competent TG1 *E. coli* were prepared by $CaCl_2$ treatment. A single colony of TG1 *E. coli* was inoculated into 10 ml LB broth at 37 ^oC overnight (14-16 h). The overnight culture was harvested by centrifugation at 2,500 rpm for 10 min at 4 ^oC. After removing the supernatant, the cell pellet was resuspended with 10 ml of ice-cold 100 mM $CaCl_2$. The cell suspension was centrifuged at 2,500 rpm for 10 min at 4 ^oC. After discarding the supernatant, the bacterial pellet was resuspended with 10 ml of ice-cold 100 mM $CaCl_2$ and allowed to be on ice for 1 h. After removing the supernatant the bacterial pellet was gently resuspended with 2 ml of ice-cold 100 mM

$CaCl_2$. Sterile glycerol was added to the cell suspension at 15% of final concentration of glycerol with gently swirling. The resulting competent TG1 *E. coli* was stored in 100 μl-aliquots in pre-chilled sterile microcentrifuge tubes and followed by freezing at -80 ^oC until use. The known concentration of standard plasmid DNA was used to test the transformation efficiency of the competent cells.

4.3.6 Transformation of recombinant phagemid into competent TG1 *E. coli* cells

The 100 μl of frozen $CaCl_2$-treated competent cells prepared as described in the previous section were thawed on ice for 15 min. The ligation reaction or purified plasmid DNA (100 ng) was gently mixed with competent TG1 *E. coli* cells and incubated on ice for 1 h. the mixture were transferred to the pre-chilled 10 ml screw-cap glass tube. The tube was transferred to a 42 ^oC waterbath with gently agitation for 90 sec. The tube was immediately chilled on ice for additional 1 min. One milliliter of LB medium was added into the tube. The transformed cells were then shaken at 37 ^oC for 3 h to allow the cells to recover. The appropriate fractions of the transformation reaction were plated onto LB agar supplemented with 100 μg/ml ampicillin. The plates were then incubated at 37 ^oC overnight (14-16 h).

4.3.7 Characterization of recombinant clones

The isolated colonies of transformed TG1 *E. coli* were randomly picked on LB agar containing 100 μg/ml ampicillin and grown in LB broth containing 100 μg/ml ampicillin at 37 ^oC for 18 h. The phagemid was extracted using Plasmid Mini Kit (QIAGEN) according to the manufacturer's protocol. To analyze the recombinant clones containing the inserted CD147Ex gene, the CD147Ex fragment was characterized by digestion with *Xho*I (Promega) and *Spe*I (Promega), and reamplification by PCR in the purified phagemid. The samples were analyzed by agarose gel electrophoresis. The newly constructed phagemid was named pComb8-CD147Ex.

4.4 Preparation of VCSM13 phage for helper phage infection

4.4.1 VCSM13 phage preparation

A single colony of TG1 *E. coli* was inoculated into 10 ml 2xTY broth (16% w/v tryptone, 10% w/v yeast extract and 5% w/v NaCl) until the absorption at 600 nm of 0.8 was reached. The cultured bacteria were transferred to 100 ml 2xTY and grown at 37 ^{o}C until the absorption at 600 nm reached 0.5. The bacterial culture was further infected with 10^{12} pfu of the VCSM13 helper phages and incubated at 37 ^{o}C for 3 h. Kanamicin was added to phage-infected TG1 to final concentration of 70 μg/ml kanamycin. Bacterial cultures were shaken at 180 rpm for 16 h at 37 ^{o}C. The helper phages were harvested by centrifugation at 3000 rpm for 10 min at 4 ^{o}C. Finally, the supernatant containing phage was aliquot and stored at -70 ^{o}C.

4.4.2 Titration of VCSM13 phage by *E. coli* infection

Titration of VCSM13 phage was performed by infection of 1 ml of TG1 *E. coli* culture (OD_{600} of 0.6) with 1 μl of VCSM13 phage. Fifty microliters of the infected culture and 50 μl of its dilutions 1:10^{6}, 1:10^{8} and 1:10^{10} with TYE were plated on solid TYE medium and 1% glucose. Phage plaques were counted after overnight incubation at 37 ^{o}C.

4.5 Preparation of phage-displayed CD147ExgpVIII

4.5.1 Phage-displayed CD147ExgpVIII preparation

The TG1 *E. coli* harboring pComb8-CD147Ex were grown in 10 ml of 2xTY broth (1.6%w/v tryptone, 1% w/v yeast extract, and 0.5% w/v NaCl) containing 100 μg/ml ampicillin at 37 ^{o}C until the absorption at 600 nm was 0.8. The cultured bacteria were subsequently transferred to 100 ml of the same medium containing 1%w/v glucose and cultivated until the absorption at 600 nm of 0.5 was reached at

two temperatures, 25 and 37 ^{o}C. If the bacteria were cultured under IPTG induction, IPTG was added to the culture at a final concentration of 1 mM. After induction, the cells were grown at the desired temperature for 0 or 2 h. Each bacterial culture was further infected with 10^{12} pfu of the VCSM13 helper phages and left at 37 ^{o}C for 30 min without shaking. Phage-infected TG1 was pelleted by centrifugation at 1,100 g for 10 min at 4 ^{o}C. The pellets were resuspended in 2xTY broth containing 100 μg/ml ampicillin and 70 μg/ml kanamycin. Fifteen milliliters of bacterial cultures were transferred to 250 ml of the same medium and shaken at 180 rpm for 16 h at the desired temperature. The recombinant phages were harvested by PEG 8000 precipitation and centrifugation as described previously (24). Finally, the phage was reconstituted with 2.5 ml of PBS pH 7.2 and centrifuged at 11,600 rpm for 10 min at 4 ^{o}C. The supernatant was stored at -70 ^{o}C. This experiment was simplified by the diagram (**Figure 4.1**).

4.5.2 Titration of phage-displayed CD147ExgpVIII by *E. coli* infection

A single colony of TG1 *E. coli* was inoculated into 10 ml 2xTY broth (16% w/v tryptone, 10% w/v yeast extract and 5% w/v NaCl) and grown at 37 ^{o}C until the absorption at 600 nm of 0.6 was reached. One microliter of phage-displayed CD147ExgpVIII was added into 999 ml of PBS pH 7.2 (1:10^{3}) and then added into 1 ml culture bacteria (1:10^{6}) and incubated for 15 min. The infected TG1 *E. coli* was further diluted into 10^{8} and 10^{10} in PBS pH 7.2. Fifty microliters of each dilution was plated onto LB agar supplemented with 100 μg/ml ampicillin and incubated at 37 ^{o}C overnight (16-18 h). The ampicillin resistant colonies were counted and calculated for the phage concentration.

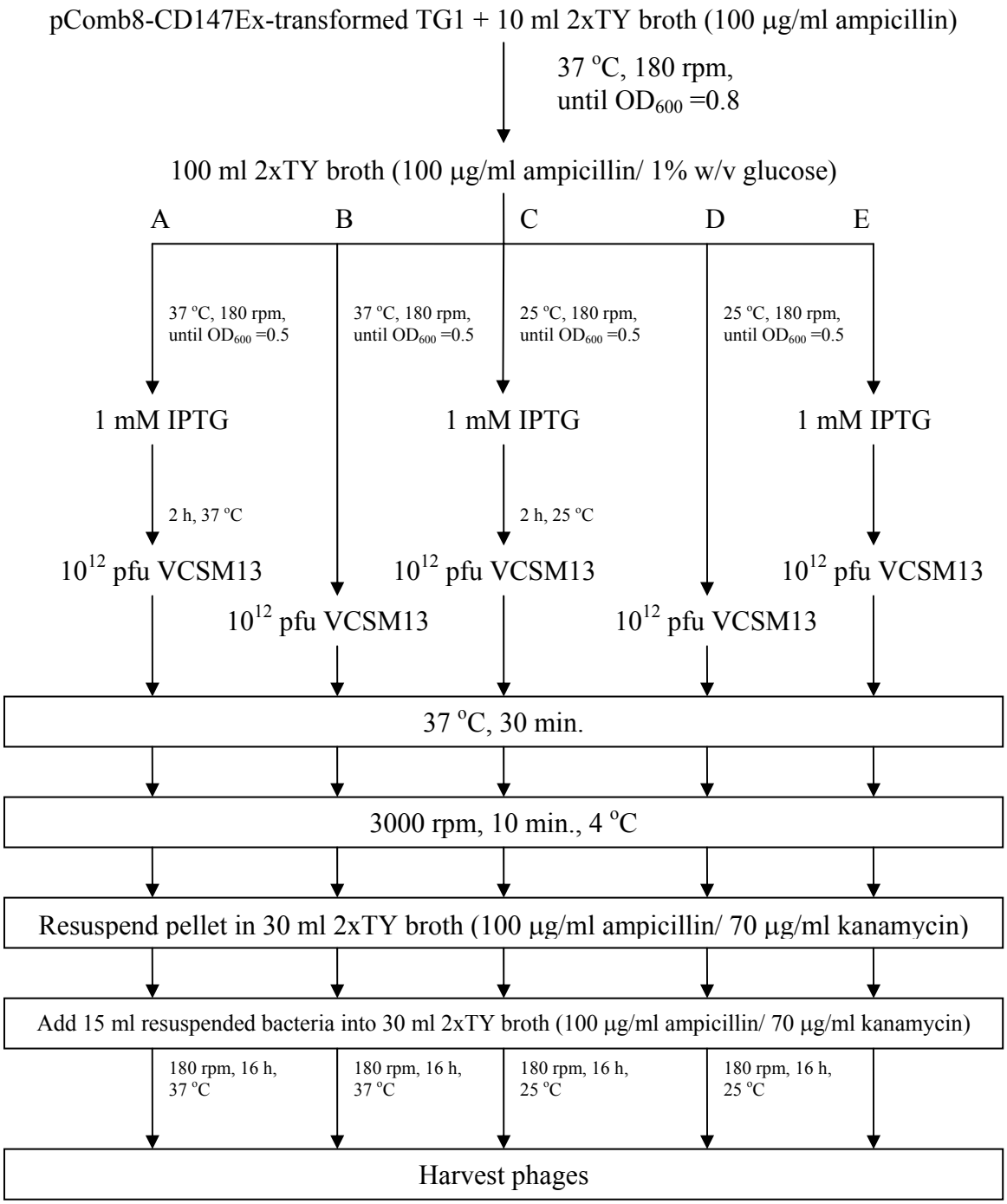

Figure 4.1 Schematic diagrams of the cultivating conditions for production of phage-displayed CD147ExgpVIII.

4.6 Preparation of VCSM13 phage for control phage

4.6.1 VCSM13 phage preparation

A single colony of TG1 *E. coli* was inoculated into 10 ml 2xTY broth (16% w/v tryptone, 10% w/v yeast extract and 5% w/v NaCl) until the absorption at 600 nm of 0.8 was reached. The cultured bacteria were transferred to 100 ml 2xTY and grown at desired temperature until the absorption at 600 nm reached 0.5. The bacterial culture was further infected with 10^{12} pfu of the VCSM13 helper phages and left at 37 ^{o}C for 30 min without shaking. Phage-infected TG1 was pelleted by centrifugation at 1,100 g for 10 min at 4 ^{o}C. The pellets were resuspended in 2xTY broth containing 70 μg/ml kanamycin. Fifteen milliliters of bacterial cultures were transferred to 250 ml of

the same medium and shaken at 180 rpm for 16 h at the desired temperature. The phages were harvested by PEG 8000 precipitation and centrifugation as described previously (24). Finally, the phage was reconstituted with 2.5 ml of PBS pH 7.2 and centrifuged at 11,600 rpm for 10 min at 4 ^{o}C. The supernatant was stored at -70 ^{o}C. Phage titration was performed by *E. coli* infection as in **section 4.4.2**.

4.7 Phage titration by ELISA

The phages are usually tittered by *E. coli* infection with serial dilutions of phage, however, immunotitration by ELISA is an alternative method to determine the relative number of phage particles. Fifty microliters of the phage dilutions 1:10^4, 1:10^5 and 1:2 × 10^5 in 50 mM carbonate/bicarbonate buffer pH 9.6 were coated on microtiter plate (NUNC, Roskilde, Denmark) at 4 ^{o}C for 18 h. Blocking was performed by addition of 2% skimmed milk in PBS pH 7.2 and incubated for 1 h at room temperature. Plate was then washed 5 times with 0.05% Tween20 in PBS pH 7.2. Anti-gpVIII-HRP mAbs (Amersham Pharmacia Biotech, Buckinghamshire, UK) were diluted in 1:5000 with 2% skimmed milk in PBS pH 7.2. One hundred microlitters of mAbs was added to each well and incubated for 1 h at room temperature. Plate was then washed 5 times with 0.05% Tween20 in PBS pH 7.2.

Following washing, the 3,3′,5,5′-tetramethylbenzidine (TMB) substrate (Sigma-Aldrich, St. Louis, MO, USA) was added and incubated at room temperature for signal development. Optical density at 450 nm was determined after adding 1 N HCl to stop the reaction using BIO-KINETICS READER EL 340 MICROPLATE (Bio-Tek Instruments, Winooski, WT, USA).

4.8 Immunoassay for phage-displayed CD147ExgpVIII by sandwich ELISA

The CD147 mAbs (M6-1B9; IgG_3, M6-1E9; IgG_{2a}, M6-1D4; IgM, and M6-2F9; IgM) was used to characterized the CD147Ex displayed on phage particle. These mAbs were kindly provided by Associated Professor Dr. Watchara Kasinrerk, Clinical Immunology Unit, Department of Medical Technology, Faculty of Associated Medical Sciences, Chiang Mai University, Chiang Mai, Thailand (67, 93). Fifty microliters of 10 μg/ml CD147 mAbs in 50 mM carbonate/bicarbonate buffer pH 9.6 was coated on microtiter plate (NUNC) at 4 ^{o}C for 18 h. Blocking was performed by addition of 2% skimmed milk in PBS pH 7.2 and incubated for 1 h at room temperature. Plate was then washed 5 times with 0.05% Tween20 in PBS pH 7.2, 10^{10} cfu of phage-displayed CD147ExgpVIII produced under different conditions were added to the wells. After incubation at room temperature for 1 h, the plate was washed to remove unbound phages. Binding of phage particles was monitored by using two alternative sets of anti-M13 antibodies. One was anti-gpVIII-HRP mAbs (Amersham Pharmacia Biotech). The mAbs were diluted in 1:5000 with 2% skimmed milk in PBS pH 7.2. One hundred microlitters of mAbs was added to each well and incubated for 1 h at room temperature. Plate was then washed 5 times with 0.05% Tween20 in PBS pH 7.2. The other was biotinylated anti-gpIII mAbs (Exalpha Biologicals, Watertown, MA). The mAbs were diluted in 1:2000 with 2% skimmed milk in PBS pH 7.2. One hundred microlitters of mAbs was added to each well and incubated for 1 h at room temperature. After washing, streptavidin conjugated to HRP (ZYMED Laboratories, San Francisco, CA) (1:2500 in 2% skimmed milk in PBS pH 7.2) was applied to trace the biotinylated anti-gpIII mAbs. Following washing, TMB substrate (Sigma-Aldrich) was added and incubated at room temperature for signal development. Optical density

at 450 nm was determined after adding 1 N HCl to stop the reaction using BIO-KINETICS READER EL 340 MICROPLATE (Bio-Tek Instruments).

4.9 CD147-gpVIII fusion protein analysis by SDS-PAGE

4.9.1 SDS-PAGE

Sodium dodecyl sulfate-polyacrylamide gel electrophoresis (SDS-PAGE) was employed for analysis of CD147EX-gpVIII fusion protein. A slab gel (15% separating gel and 5% stacking gel) composed of the components shown in **Table 4.1**. The 10^{11} cfu phage-displayed CD147ExgpVIII was solubilized with reducing buffer solution (62.5 mM Tris-HCl, pH 6.8, 0.01% bromophenol blue, 2% SDS, 5% β-mercaptoethanol, 20% glycerol). The sample were boiled for 5 min and loaded onto the well of SDS-PAGE. Electrophoresis was carried out by applying constant voltage at 100 Volts using 0.025 M Tris/0.192 glycine, pH 8.5 containing 0.1% SDS as a electrophoretic buffer. The size of protein band was estimated by comparing to the band of the Rainbow Marker (Amersham Pharmacia Biotech). After electrophoresis, the separated proteins were electroblotted onto the polyvinylidene-fluoride (PVDF) membrane using 0.025 M Tris/0.192 glycine, pH 8.5 containing 0.05% SDS and 20% methanol as a blotting buffer. Blotting was carried out by apply constant voltage at 25 Volts for 2 h. After blotting, blotted membrane was blocked at 4 ^{o}C for 18 h in 5% skimmed milk in PBS pH 7.2 and then incubated with the pooled CD147 mAbs (M6-1B9, M6-1E9, M6-1D4 at 10 μg/ml each) for 1 h at room temperature on a shaking platform. Following 5 times washing with 0.05% Tween20 in PBS pH 7.2, HRP-conjugated rabbit-anti-mouse IgG (Dako, Dakopatts, High Wycombe, United Kingdom) in 5% skimmed milk in PBS pH7.2 was added to the membranes and incubated at room temperature for 1 h on a shaking platform. The immunoreactive bands were then visualized by chemiluminescent detection system (Amersham Pharmacia Biotech) according to the manufacturer's protocol.

Table 4.1 Composition of reagents for SDS-polyacrylamide gel

Reagents	15% Separating gel (ml)	5% Stacking gel (ml)
Acrylamide:Bis (30:0.8)	5	0.665
1.5 M Tris HCl, pH 8.8	2.5	-
0.5 M Tris HCl, pH 6.8	-	1.25
10% SDS	0.1	0.05
10% Ammonium persulfate	0.15	0.10
TEMED	0.03	0.03
Distilled water	2.3	3

4.10 Cell lines

A human monocytic cell line (U937), T-cell lines (Jurkat, Molt4 and Sup T1) and a B-cell line (Daudi) were used in this study. These hematopoietic cell lines were kindly provided by Associated Professor Dr. Watchara Kasinrerk, Clinical Immunology Unit, Department of Medical Technology, Faculty of Associated Medical Sciences, Chiang Mai University, Chiang Mai, Thailand. All cell lines were maintained in RPMI-1640 medium (Gibco, Grand Island, NY, USA) supplemented with 10% fetal bovine serum (FBS) (Gibco), 40 μg/ml gentamicin and 2.5 μg/ml amphotericin B in a humidified atmosphere of 5% CO_2 at 37 ^{o}C.

4.11 Validation of bioactive domain on phage-displayed CD147ExgpVIII by aggregation inhibition assay

Since the CD147 mAbs, M6-1D4 and M6-2F9, induced the homotypic aggregation of the human monocytic cell line, U937, has been reported (67, 93), these mAbs were used for validation the bioactive domain of CD147 on phage particle using aggregation inhibition assay. Fifty microliters of 2 x 10^9 cfu/ml phage-displayed CD147ExgpVIII in RPMI 1640 was preincubated with 50 μl of 20 μg/ml anti-CD147 mAbs in RPMI 1640 for 1 h at 37 ^{o}C waterbath. One hundred microliters of multivalent phage-incubated mAbs were added to 100 μl of 3 x 10^5 U937 cells/ml in 20% FBS-RPMI 1640 in 96-well flat-bottom tissue culture plate (NUNC). The culture was then maintained at 37 ^{o}C in a humidified atmosphere with 5% CO_2. VCSM13 was used in place of phage-displayed CD147ExgpVIII as a negative inhibition control system. Cell aggregation was monitored at 1, 2, 4, 8, 12 and 24 h and the image was taken using inverted microscope (Carl Zeiss Canada Ltd., Toronto, ON, Canada). The degree of cell aggregation was scored as followed; no aggregation (-), 1-5 cells/aggregate (1+), 6-10 cells/aggregate (2+), 10-15 cells/aggregate (3+), greater than 15 cells/aggregate (4+) (67).

4.12 Biological activity of phage-displayed CD147ExgpVIII on various cell lines

To verify the biological activity of CD147EX displayed on phage particles, these recombinant phages were incubated with various hematopoietic cell lines and the morphological of these cell lines were observed under inverted microscope. One hundred microliters of 10^{10} cfu./ml phage-displayed CD147ExgpVIII in RPMI 1640 medium was added to 100 μl of 3 x 10^5 cells/ml of various cell lines in RPMI 1640 medium supplemented with 20% FBS and antibiotics in 96-well flat-bottom tissue culture plate (NUNC) and incubated at 37 ^oC in a 5% CO_2 atmosphere. VCSM13 phage was used as a control. The culture was observed at 1, 2, 3, 4, 8, 24 and 48 h of incubation under inverted microscope to visualize morphological changes. Images were taken by Live Cell Imaging microscope (Zeiss).

4.13 Cytotoxicity Assay

Phage-displayed CD147ExgpVIII-induced U937 cell death was investigated by LIVE/DEAD Viability/Cytotoxicity Kit (Molecular Probes). VCSM13 phage was used as a negative control. Three milliliters of 10^{10} cfu/ml phage-displayed CD147ExgpVIII in RPMI 1640 medium was incubated with 3 ml of 3 x 10^5 U937 cells/ml in RPMI 1640 supplemented with 20% FBS and antibiotics for 48 h at 37 ^oC in a 5% CO_2 atmosphere. After washing, cells were stained using the LIVE/DEAD Viability/Cytotoxicity Kit (Molecular Probes) according to the manufacturer's instructions. Stained cells were washed twice and cytospun onto microscope slide at a density of 10^5 cells/slide. Nuclei were counterstained with DAPI (Molecular Probes). Images were taken by fluorescence microscope (Zeiss). The fluorescence intensity was analyzed by Northern Eclipse 5.0 (Empix Imaging Inc., Missisauga, ON, Canada) using NucDen function.

4.14 Examination of cleaved caspase-3 by flow cytometry

Incubation of U937 cells with phage-displayed CD147ExgpVIII was performed as described previously in **section 4.12** (cytotoxicity assay). VCSM13

phage and cisplatin (Sigma-Aldrich) were used as controls. After incubation, U937 cells were harvested, washed and resuspended in PBS pH 7.2. Methanol-free formaldehyde was then added to resuspended cells to a final concentration of 0.25%. Cells were fixed at 37 ^{o}C for 10 min and subsequently chilled on ice for 1 min. The cells were then permeabilized with ice-cold 90% methanol and incubated on ice for 30 min. one million permeabilized cells were washed with 0.5% BSA in PBS twice and then resuspended in the same buffer. Cells were subsequently incubated with rabbit anti-cleaved caspase-3 (ASP175) (5A1) mAbs (Cell Signaling, Beverly, MA, USA) at room temperature for 30 min. Cells were then stained with Alexa488-conjugated anti-rabbit immunoglobulins (Molecular Probes) at room temperature for 30 min. After incubation, cells were washed and resuspended with 500 μl of 0.5% BSA in PBS. Flow cytometric analysis was performed on Beckman Coulter EPICS ALTRA (Beckman Coulter, Fullerton, CA, USA).

4.15 Detection of cleaved caspase-3 by immunocytochemistry

U937 cells were incubated with phage-displayed CD147ExgpVIII for 48 h as described in **section 4.12**. VCSM13 phage and cisplatin (Sigma-Aldrich) were used as negative and positive controls, respectively. After incubation, cells were then fixed with 3.7% formaldehyde in PBS containing 50 mM $MgCl_2$ for 10 min. Fifty microliters of 1 x 10^6 cells/ml fixed cells were dropped onto a silane-coated slide and air-dried. Dropped cells on slide were fixed with 3.7% formaldehyde in PBS pH 7.2 containing 50 mM $MgCl_2$ for 10 min. Following washing, cells were permeabilized with 0.2% Triton-X 100 for 12 min. Slides were then washed in PBS containing 50 mM $MgCl_2$. After blocking with FBS (Gibco), the fixed cells were incubated with rabbit anti-cleaved caspase-3 (ASP175) (5A1) mAbs (Cell Signaling) at 4 ^{o}C overnight. After washing, cells were blocked and then incubated with Alexa680-conjugated goat anti-rabbit Immunoglobulin G (Molecular Probes) at room temperature for 30 min. Then, U937 nuclei were counterstained with DAPI. Image analysis was carried out using the Spectra Cube (Applied Spectral Imaging, Carlsbad, CA, USA) on a Zeiss Axiophot 2 microscope (Zeiss) and the SKYVIEW software (Applied Spectral Imaging).

4.16 Determination of cleaved caspase-3 by SDS-PAGE and Western blot analysis

U937 cells were incubated with phage-displayed CD147ExgpVIII for 48 h as described in **section 4.12**. VCSM13 phage and cisplatin were used as controls. After incubation, U937 cells were harvested and washed with cold PBS. Cells pellets were lysed in radioimmunoprecipitation (RIPA) buffer on ice for 10 min. Lysates were centrifuged at 13,000 rpm for 5 min at 4 ^{o}C. Protein concentration was measured using Bradford's reagent (113). One hundred micrograms of proteins from lysates were separated by SDS-PAGE under reducing conditions on a 15% polyacrylamide gel. The sample preparation and electrophoresis was carried out as in **section 4.8.1**. After electrophoresis, the separated proteins were electroblotted onto Hybond-C membrane (Amersham Pharmacia Biotech) using 0.025 M Tris/0.192 glycine, pH 8.5 containing 0.05% SDS and 20% methanol as a blotting buffer. Blotting was carried out by apply constant voltage at 15 volts, 4 ^{o}C overnight. Blotted membrane was blocked at room temperature for 2 h in 10% skimmed milk in PBS pH 7.2 then incubated with rabbit anti-caspase-3 (8G10) mAbs (Cell Signaling) at 4 ^{o}C overnight on a shaking platform. Following washing with 0.1% Tween20 in TBS pH 7.6, goat anti-rabbit immunoglobulins-HRP was added to the membranes and incubated at room temperature for 1 h. After washing, the immunoreactive bands were then visualized by chemiluminescent detection system (Amersham Pharmacia Biotech) according to the manufacturer's protocol. To confirm the equal loading of proteins, membranes were probed with anti-beta-actin mAb (Sigma-Aldrich).

4.17 Investigation of phage-displayed CD147ExgpVIII binding on U937 cells by ELISA

To verify the biological activity of CD147Ex on phage particles cause by the interaction of CD147Ex and cell surface molecule (s) on U937 cells, binding of phage-displayed CD147ExgpVIII on effected cells was analyzed by ELISA. One hundred microliters of 10^6 U937 cells/ml in Hanks Balanced Salt Solution (HBSS) were added to wells of 96-well plate and incubated at room temperature for 30 min. After gentle washing with PBS pH 7.2, plate wells were blocked with 2% skim milk in HBSS pH 7.4 at room temperature for 1 h. One hundred microliters of 10^9 cfu/ml

phage-displayed CD147ExgpVIII or VCSM13 in HBSS pH 7.4 was added to each well and incubated at room temperature for 20 min. Unbound phages were removed by gentle washing with HBSS. Bound phages were fixed to U937 cells by addition of 3.7 % formaldehyde in HBSS pH 7.4 for 10 min. Wells were washed 3 times with HBSS and blocked with 2% skimmed milk in HBSS at room temperature for 1 h. After washing, anti-gpVIII-HRP mAb (Amershem-Pharmacia Biotech) was added and incubated at room temperature for 1 h. TMB substrate (Sigma-Aldrich) was then added and incubated at room temperature for signal development. Optical density at 450 nm was determined after adding 1 N HCl to stop the reaction.

4.18 Detection of phage-displayed CD147ExgpVIII binding on U937 cells by immunocytochemistry

4.18.1 Preparation of silane-treated microscope slides

To improve the adhesion of cells to the microscope slide, slides were treated with silane-acetone solution (2% 3-aminopropyltriethoxysilane (Sigma-Aldrich) in anhydrous acetone) for 2 min. The slides were then quickly dipped into distilled and deionized water for 3 times. The silane-treated slides were dried at 37 ^{o}C for 2 h.

4.18.2 Immunocytochemistry

To visualize the phage-displayed CD147ExgpVIII on cell surface under microscopic examination, the immunocytochemistry was performed. Three milliliters of 10^{10} cfu/ml phage-displayed CD147ExgpVIII or VCSM13 in RPMI 1640 medium was incubated with 3 ml of 3 x 10^{5} U937 cells/ml in RPMI 1640 medium supplemented with 20% FBS and antibiotics at 37 ^{o}C for 24 h in a 5% CO_2 atmosphere. After incubation, 100 µl of 10^{6} cells/ml phage-incubated U937 cells were dropped onto the silane-treated slide and air-dried. Dropped cells were fixed with 3.7% formaldehyde in PBS pH 7.2 containing 50 mM $MgCl_2$ for 10 min. Slides were washed 3 times in PBS containing 50 mM $MgCl_2$ and blocked with 1% BSA in SSC

at room temperature for 5 min. Anti-gpVIII mAb (Amershem-Pharmacia Biotech) was added and incubated at room temperature for 1 h. After washing, Alexa680-conjugated goat anti-mouse immunoglobulins (Molecular Probes, Eugene, OR, USA) was added to the slide and incubated at room temperature for 30 min. Following washing, U937 nuclei were counterstained with 4′,6-diamidino-2-phenylindole (DAPI) (Molecular Probes). Image analysis was carried out using the Spectra Cube (Applied Spectral Imaging) on a Zeiss Axiophot 2 microscope (Zeiss) and the SKYVIEW software (Applied Spectral Imaging).

CHAPTER 5

RESULTS

5.1 Construction of pComb8-CD147Ex phagemid

The extracellular domain of CD147 cDNA was amplified from pCDM8-CD147 by PCR using primers CD147ExgpVIIIFw and CD147ExgpVIIIRev. The PCR product of 552 bp was obtained (**Figure 5.1**). The amplified product was subsequently cleaved with *Xho*I and *Spe*I, and ligated into the pComb8 phagemid treated with the same enzymes. The ampicillin-resistant *E. coli* TG1 colonies transformed with the ligated product were grown at 37 ^{o}C for plasmid minipreps. The inserted fragment of CD147Ex with the molecular weight of approximately 550 bp was retrieved from the isolated plasmid DNA after checking by restriction fragment analysis with *Xho*I and *Spe*I (**Figure 5.2**), and reamplification by PCR (**Figure 5.3**). The engineered phagemid bearing CD147 extracellular domain gene, flanked upstream by *Pel*B signal sequence and downstream by gpVIII (**Figure 5.4**), was designated as pComb8-CD147Ex.

5.2 Phage titration

To quantify the amount phage, phage titration was performed by *E. coli* infection and ELISA. By *E. coli* infection, the concentration of VCSM13 and phage-displayed CD147ExgpVIII was 4.7×10^{12} pfu./ml and 1.7×10^{12} cfu/ml, respectively. The relative amount of these phages was quantified by ELISA. The signal obtained from both phages was concordant (**Table 5.1)**.

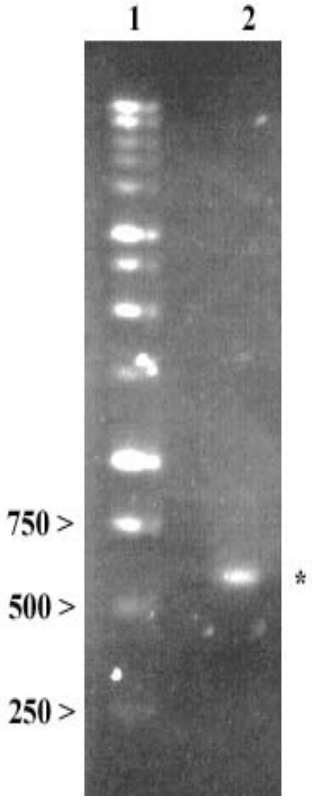

Figure 5.1 Analysis of PCR product, 552 bp (∗), of the CD147Ex amplified from pCDM8-CD147 vector using CD147ExgpVIIIFw and CD147ExgpVIIIRev primers. Samples were electrophoresed in a 1% agarose gel.

Lane 1. 1 kb DNA marker

Lane 2. Amplified product of CD147Ex

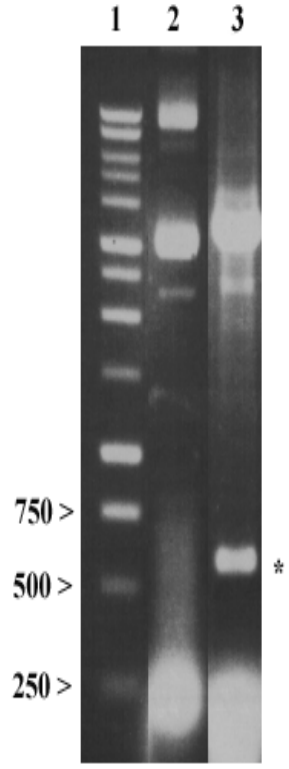

Figure 5.2 Restriction fragment analysis of pComb8-CD147Ex with *Xho*I and *Spe*I. The constructed pComb8-CD147Ex was cleaved with *Xho*I and *Spe*I. The inserted fragment of CD147Ex with the molecular weight of approximately 552 bp (*) was retrieved from the pComb8-CD147Ex (lane 3).

Lane 1. 1 kb DNA marker

Lane 2. pComb8-CD147Ex

Lane 3. *Xho*I- and *Spe*I-digested pComb8-CD147Ex

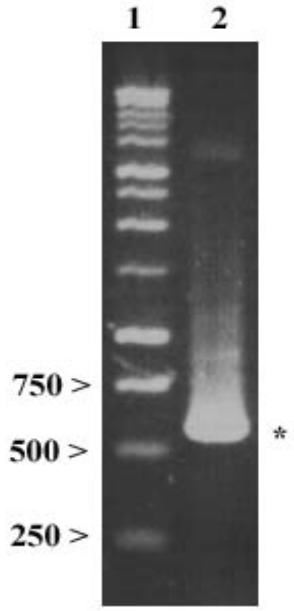

Figure 5.3 Amplified product of CD147Ex from pComb8-CD147Ex. The 552 bp amplified product (∗) from pComb8-CD147Ex template using CD147ExgpVIIIFw and CD147ExgpVIIIRev primers is shown (lane 2).

Lane 1. 1 kb DNA marker

Lane 2. Amplified product of CD147Ex

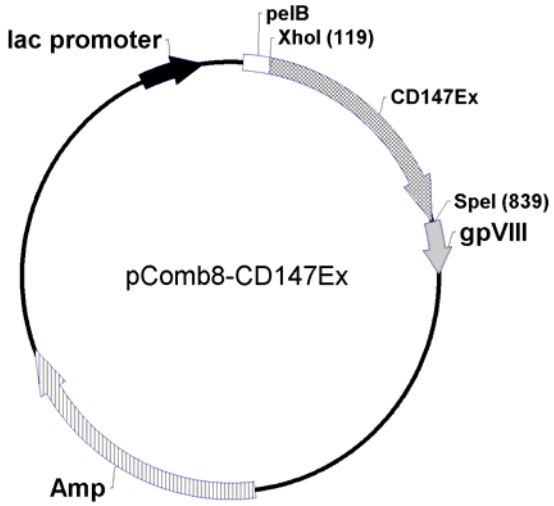

Figure 5.4 Construction of pComb8-CD147Ex phagemid. *Xho*I- and *Spe*I-cloning sites where the CD147Ex gene was inserted; *lac* promoter, the signal sequence (*PelB*), and gpVIII gene are shown.

Table 5.1 Relative amount of phage quantified by ELISA

Phage dilution	**Optical density at 450 nm**	
	VCSM13	**Phage-displayed CD147ExgpVIII**
$1{:}10^4$	1.385	1.320
$1{:}10^5$	1.055	0.982
$1{:}2 \times 10^5$	0.854	0.797

5.3 Detection of phage-displayed CD147ExgpVIII by sandwich ELISA

To study the culturing conditions for efficiently displaying of CD147Ex molecules on phage particle, the pComb8-CD147Ex-transformed TG1 was cultured and infected with the VCSM13 helper phages under five different conditions (**Figure 4.1**). The phage-displayed CD147ExgpVIII in culture supernatants obtained from various culturing conditions were compared by sandwich ELISA using a panel of anti-CD147 mAb as capture antibody. By using HRP-conjugated anti-gpVIII mAb, production of phage-displayed CD147ExgpVIII at 25 ^{o}C with IPTG-stimulation showed the highest signal with all anti-CD147 mAbs (M6-1B9, M6-1E9, M6-1D4, and M6-2F9) used (**Figure 5.5**). The second order was phage harvested from 37 ^{o}C without IPTG-, followed by 25 ^{o}C without IPTG-, and 37 ^{o}C with IPTG-stimulation when mAb M6-1B9 was used as a capture antibody. However, the second and the third rank were switched when the precipitated phages were captured by other three mAbs (M6-1E9, M6-1D4, and M6-2F9). In contrast, the recombinant phages were not recognized by an irrelevant capture antibody, mouse anti-GFP mAb.

The binding of the phage-displayed CD147ExgpVIII under 25 ^{o}C with IPTG-stimulation onto the CD147 mAb-coated wells was also demonstrated by biotinylated anti-gpIII mAb/HRP-conjugated Streptavidin detection system (**Figure 5.6**). The signaling pattern of all capture-mAbs used was corresponded to the HRP-conjugated anti-gpVIII mAb detection system.

To determine the effect of helper phage infection-period, the phage-displayed CD147ExgpVIII were produced under 25 ^{o}C with IPTG-stimulation for 0 h and 2 h before helper phage infection. The produced phages from both conditions were compared by sandwich ELISA. The recombinant phages harvested from simultaneous IPTG-stimulation and helper phage infection (0 h) was 6-11-fold higher than those harvested from which inoculation of helper phage 2 h after IPTG-stimulation (**Table 5.2**).

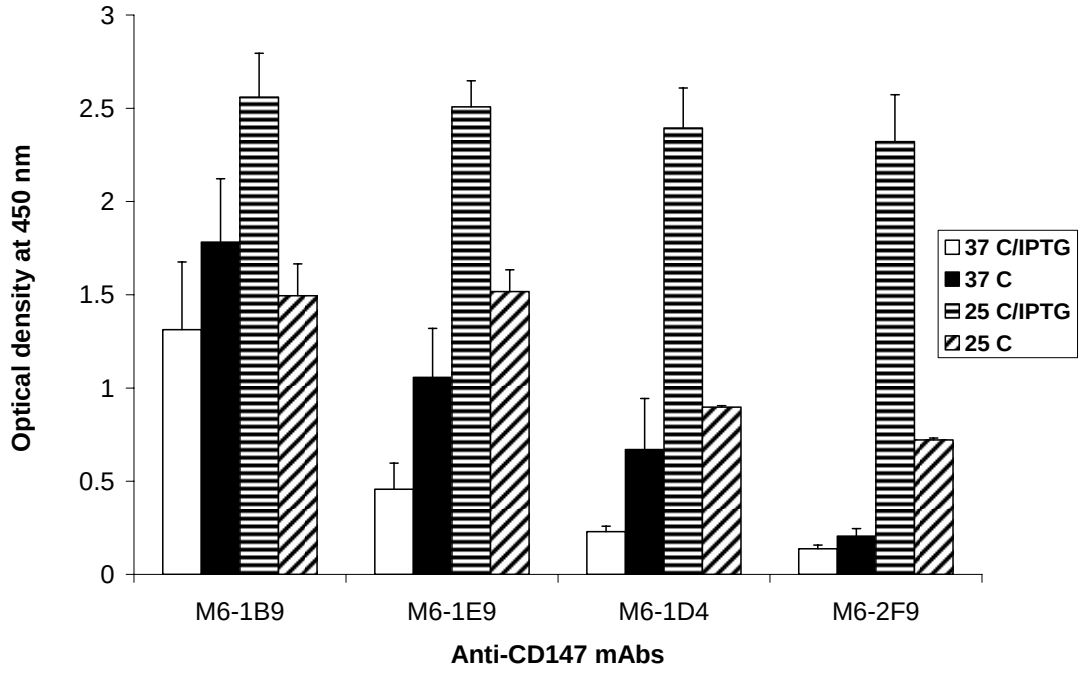

Figure 5.5 Sandwich ELISA analysis of phage-displayed CD147ExgpVIII under different growth conditions using four anti-CD147 mAbs (M6-1B9, M6-1E9, M6-1D4, and M6-2F9) as a capture and HRP/anti-gpVIII monoclonal conjugate as a tracer. The 10^{10} cfu of the construct phages under different growth conditions were used. Phage-displayed CD147Ex under 37 ^{o}C with IPTG-stimulation (no fill), 37 ^{o}C (solid bars), 25 ^{o}C with IPTG-stimulation (horizontals) and 25 ^{o}C (diagonals) were demonstrated. This experiment was done in duplicate.

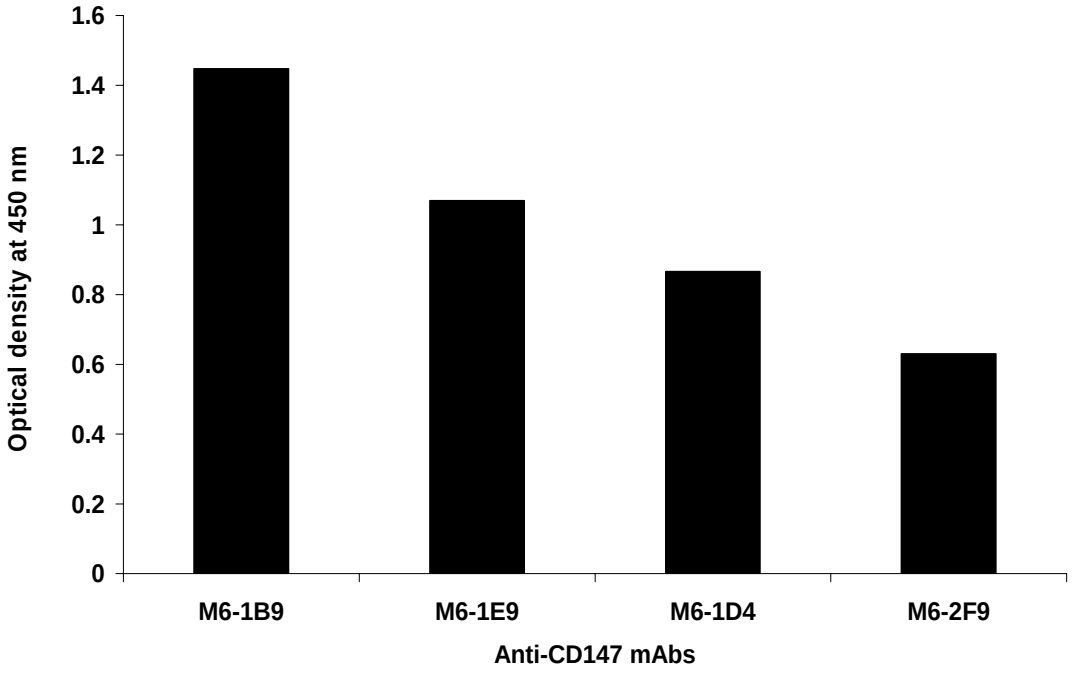

Figure 5.6 Sandwich ELISA analysis of phage-displayed CD147ExgpVIII under 25 ^{o}C with IPTG-stimulation using four anti-CD147 mAbs (M6-1B9, M6-1E9, M6-1D4, and M6-2F9) as a capture and biotinylated monoclonal anti-gpIII/Streptavidin conjugated to HRP as a tracer. The 10^{10} cfu of the construct phages were used.

Table 5.2 Comparison of helper phage infection-periods on the phage-displayed CD147ExgpVIII under 25 ^{o}C with IPTG-stimulation.

Anti-CD147 mAbs	**Optical density at 450 nm (OD450)**	
	simultaneous IPTG-stimulation	**after 2 h of IPTG-stimulation**
M6-1B9	1.684	0.289
M6-1E9	1.476	0.136
M6-1D4	1.671	0.197
M6-2F9	1.248	0.209

Note. The 10^{10} cfu of the construct phages were used. Phage-displayed CD147ExgpVIII production was assessed by sandwich ELISA using a panel of anti-CD147 monoclonal antibodies as a capture and biotinylated monoclonal anti-gpIII/Streptavidin conjugated to HRP as a tracer.

5.4 Western Immunoblotting

The protein components of the recombinant phages prepared under 25 ^{o}C with IPTG-stimulation was fractionated by SDS-PAGE under reducing conditions, blotted and probed with pooled CD147 mAbs (M6-1B9, M6-1E9, and M6-1D4). An immunoreactive protein band with the molecular weight of 28 kDa was obtained (**Figure 5.7**). No reactive band was detected in the control lane applied with phage-displayed Fo protein of respiratory syncytial virus.

5.5 Bioactive domain validation of CD147Ex incorporated on phage particle

To validate the bioactive domain of CD147Ex displayed on phage particles, U937 cells aggregation inhibition assay using the CD147 mAbs, M6-1D4 and M6-2F9, was performed. U937 cells aggregation inhibition was observed in the well added with CD147 mAb and phage-displayed CD147Ex pre-incubation in comparison to VCSM13 pre-incubation (**Figure 5.8**).

5.6 Phage-displayed CD147ExgpVIII induce morphological changes and inhibit growth of U937 cells

The generated multivalent CD147 phages were cultured with U937, Jurkat, Molt4, Sup T1 and Daudi cell lines. Among these cell types, only U937 cells exhibited morphological changes when incubated with phage-displayed CD147ExgpVIII. Morphological characteristics of apoptotic cell death such as cytoplasmic blebbing and nuclear fragmentation (114) were observed after 24 h incubation in U937 cells stimulated with recombinant phage, but not with wild-type VCSM13 (**Figure 5.9**, *A* and *B*, respectively). The cell density of U937 cells in wells containing phage-displayed CD147ExgpVIII was noticeably lower than in the control well after a 48 h of incubation (**Figure 5.10**, *A* and *B*, respectively). Cell concentrations in multivalent CD147 phage- and VCSM13 phage-added well after 48 h of incubation were $2.9 \times 10^5 \pm 0.7 \times 10^5$ and $9.5 \times 10^5 \pm 0.4 \times 10^5$ cells/ml, respectively.

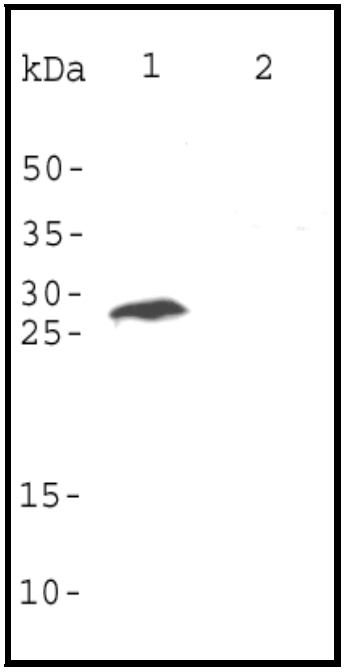

Figure 5.7 Western immunoblotting of phage-displayed CD147ExgpVIII separated by reducing SDS-PAGE. Immunological assay was performed by probing with the combination of three anti-CD147 mAbs (M6-1B9, M6-1E9, and M6-1D4). The immunoreactive bands were visualized by chemiluminescent substrate detection system. Molecular weight markers in kDa were indicated.

Lane 1. Phage-displayed CD147ExgpVIII

Lane 2. Phage-displayed Fo protein of respiratory syncytial virus

Phage-displayed CD147ExgpVIII

A

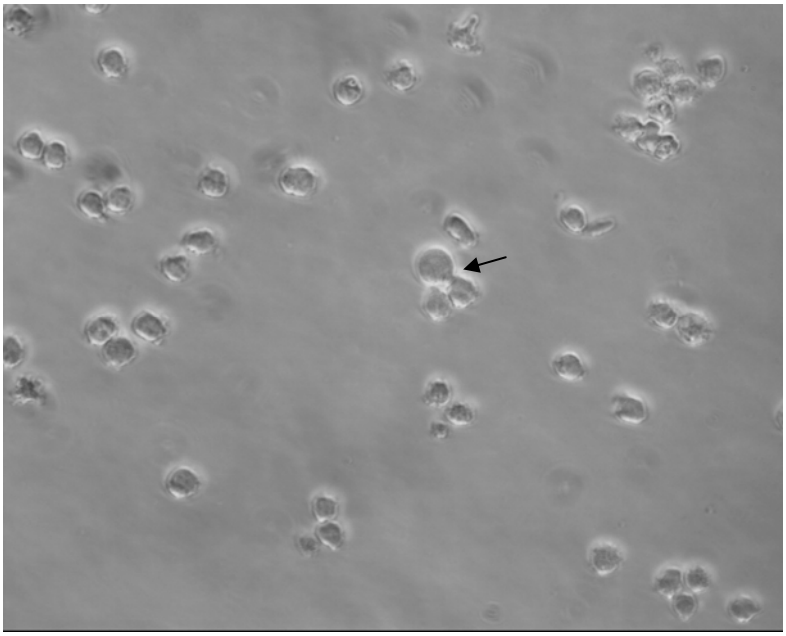

VCSM13

B

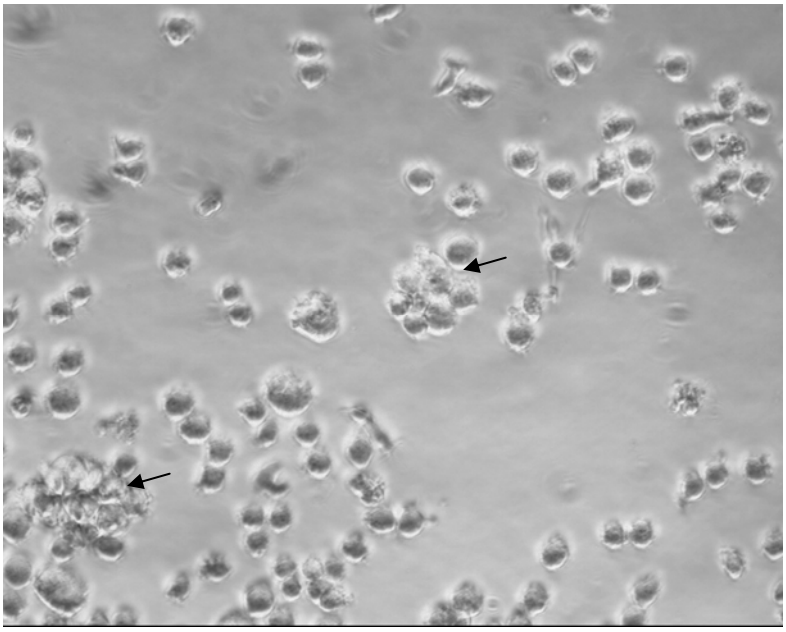

Figure 5.8 Validation of biological activity of phage-displayed CD147ExgpVIII. U937 cells aggregation inhibition was observed when anti-CD147 mAbs (M6-1D4 or M6-2F9) was pre-incubated with phage-displayed CD147Ex (*A*) comparing to VCSM13 pre-incubation (*B*).

A

Phage-displayed CD147ExgpVIII

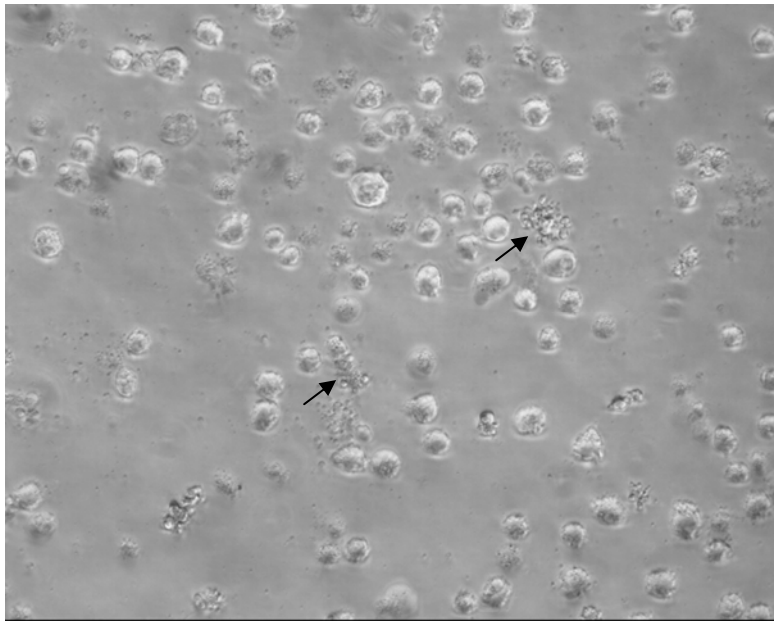

VCSM13

B

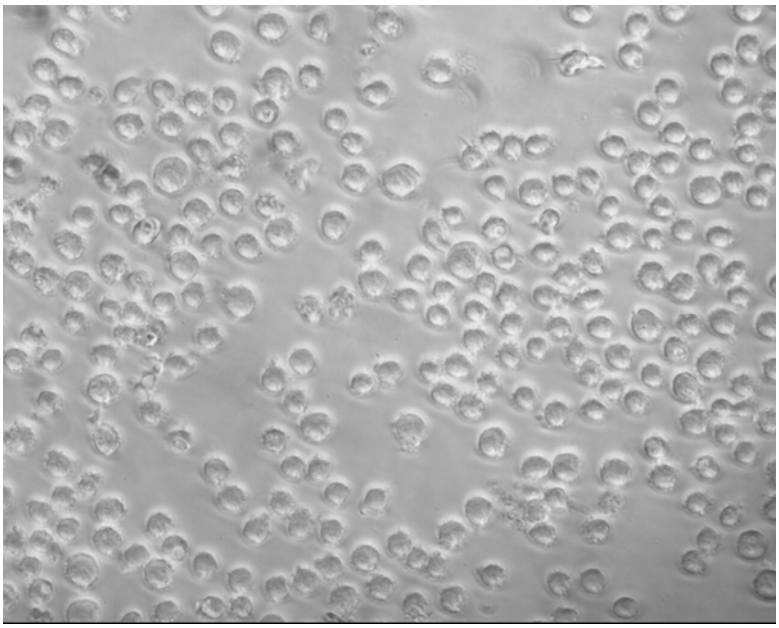

Figure 5.9 Multivalent CD147 phage induced morphological change of U937 cells. U937 cells were incubated with phage-displayed CD147ExgpVIII or VCSM13 phage and observed under inverted microscope. Morphological change of U937 cells-incubated with phage-displayed CD147ExgpVIII (*A*) was observed after 24 h incubation (arrows), in contrast to wild-type VCSM13-stimulated U937 (*B*) (200X).

Phage-displayed CD147ExgpVIII

A

VCSM13

B

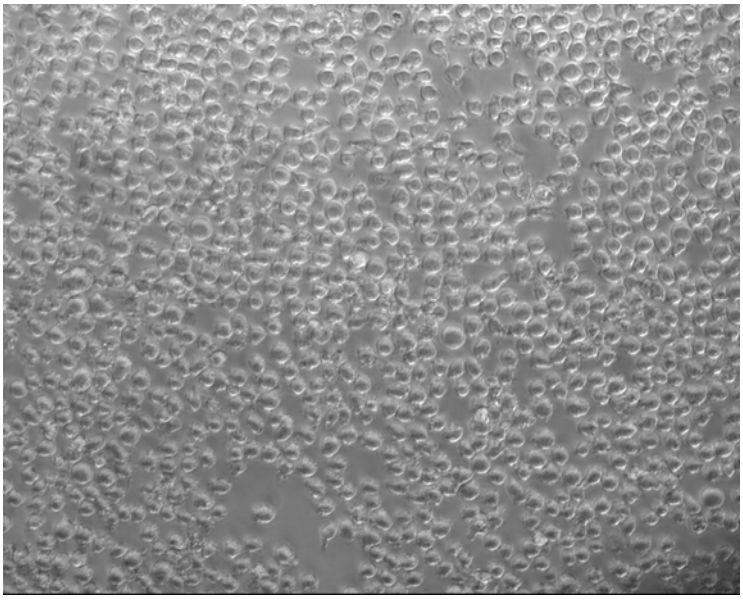

Figure 5.10 Multivalent CD147 phage induced cell cycle arrest of U937 cells. The cell density of U937 cells in wells containing phage-displayed CD147ExgpVIII (*A*) was markedly lower than in the VCSM13 added wells (*B*) after 48 h of incubation (100X).

5.7 Cytotoxic effect of phage-displayed CD147ExgpVIII on U937 cells

Since the morphological change of phage-displayed CD147ExgpVIII-incubated U937 cells indicated that cell death had occurred, vitality and cytotoxicity staining was performed. In the method employed, intracellular esterase activity in live cells converts the nonfluorescent cell-permeable calcein AM to the intensely fluorescent calcein, which is retained within live cell. Ethidium homodimer (EthD-1) enters the permeabilized plasma membranes of dead cells and undergoes a 40-fold increase in red fluorescence after binding to nucleic acids. Therefore, the nuclei of the dead cells appear red under the fluorescence microscope. Thus, cells with an active metabolism (calcein positive) that allow EthD-1 to penetrate and stain their nucleic acids most likely correspond to apoptotic cells (115). We found that double staining with calcein and EthD-1 was visualized in recombinant phage-incubated U937 cells (**Figure 5.11**, *A-C*). In contrast, VCSM13 phage-incubated U937 cells only stained positive for calcein (**Figure 5.11**, *D-F*). Fluorescence intensity in individual U937 cells incubated with recombinant phage and wild-type phage is shown in **Figure 5.12** *A* and *B*, respectively. One hundred cells were examined for the fluorescence intensity of calcein and EthD-1. Mean EthD-1 fluorescence intensity of U937 cells when incubated with phage-displayed CD147ExgpVIII was 4.4 times higher than that with VCSM13 phages, while the mean calcein fluorescence intensity from both conditions was not significantly different.

5.8 Involvement of caspase-3 activation in the mechanism of cell death of U937 cells incubated with phage-displayed CD147ExgpVIII

To assess the mechanism of cell death in phage-displayed CD147ExgpVIII-incubated U937 cells, cleaved caspase-3 was analyzed by flow cytometry using anti-cleaved caspase-3 antibody. The level of cleaved caspase-3 in recombinant phage-incubated U937 cells was higher than uninduced U937 cells and VCSM13-induced U937 cells. However, induction of cleaved caspase-3 with multivalent CD147 phages was not as high as that seen when using cisplatin as inducer (**Figure 5.13**).

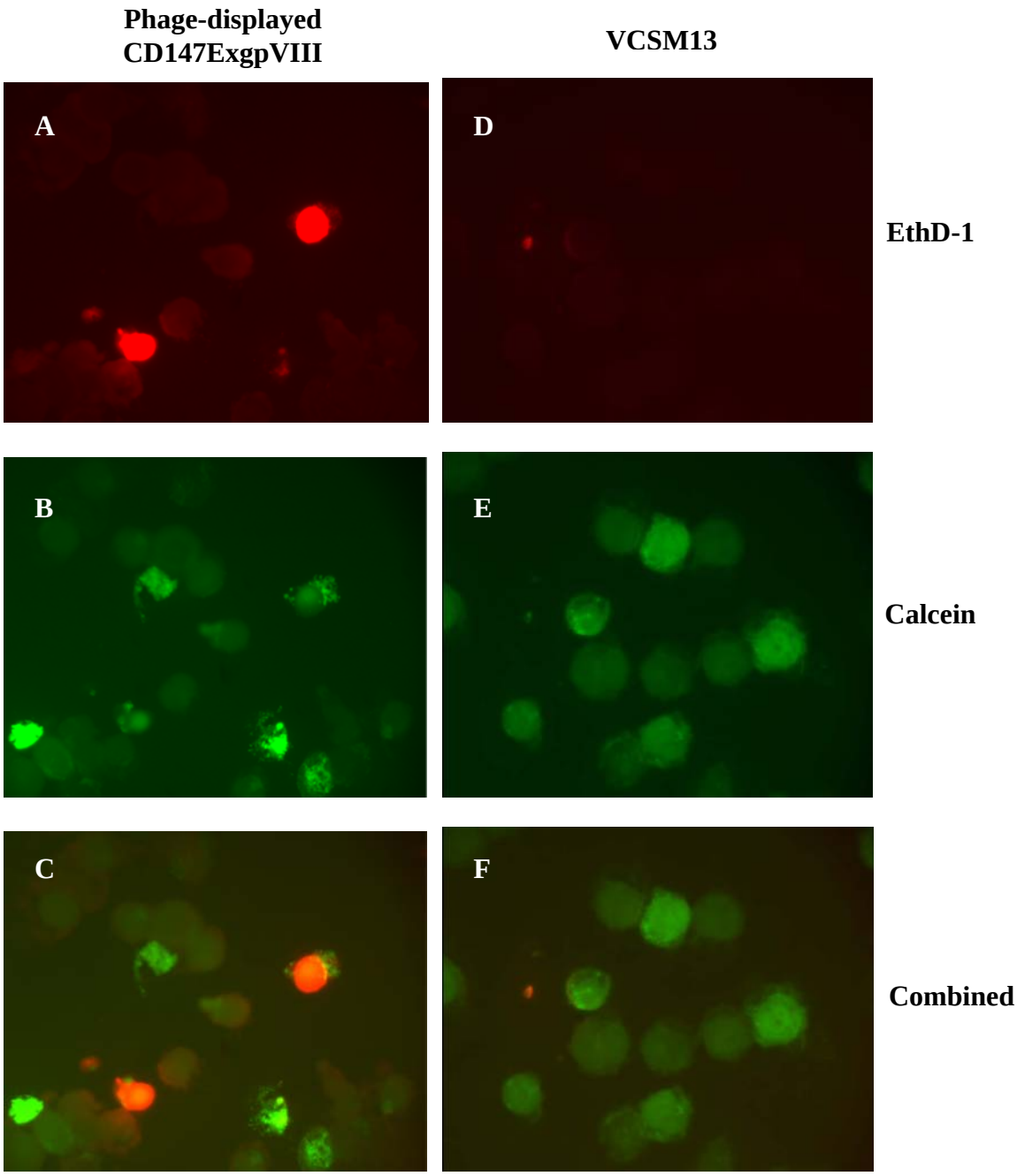

Figure 5.11 Cytotoxicity of phage-displayed CD147ExgpVIII on U937 cells. U937 cells were incubated with multivalent CD147 phage or VCSM13 phage for 48 h and stained with LIVE/DEAD Viability/Cytotoxicity Kit. Results are representative of three separate experiments.

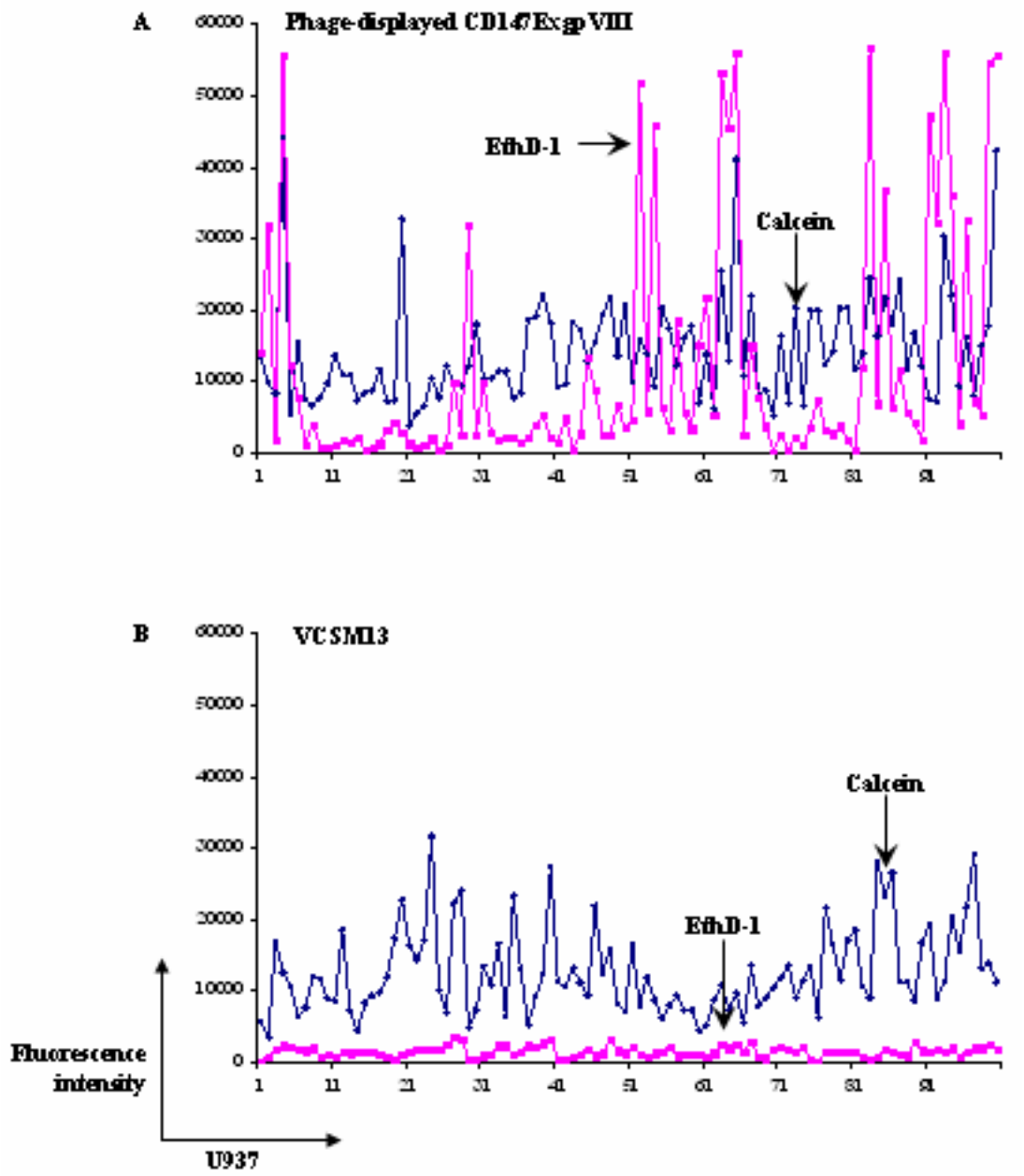

Figure 5.12 Fluorescence intensity of individual U937 cells incubated with phage-displayed CD147ExgpVIII. U937 cells were incubated with multivalent CD147 phage or VCSM13 phage for 48 h and stained with the LIVE/DEAD Viability/Cytotoxicity Kit. Individual CD147 phage-incubated U937 cells (A) and VCSM13 phage-incubated U937 cells (B) were measured the fluorescence intensity of EthD-1 and calcein. Cells double stained with EthD-1 and calcein most likely correspond to apoptotic cells. Results from one representative experiment of three are shown.

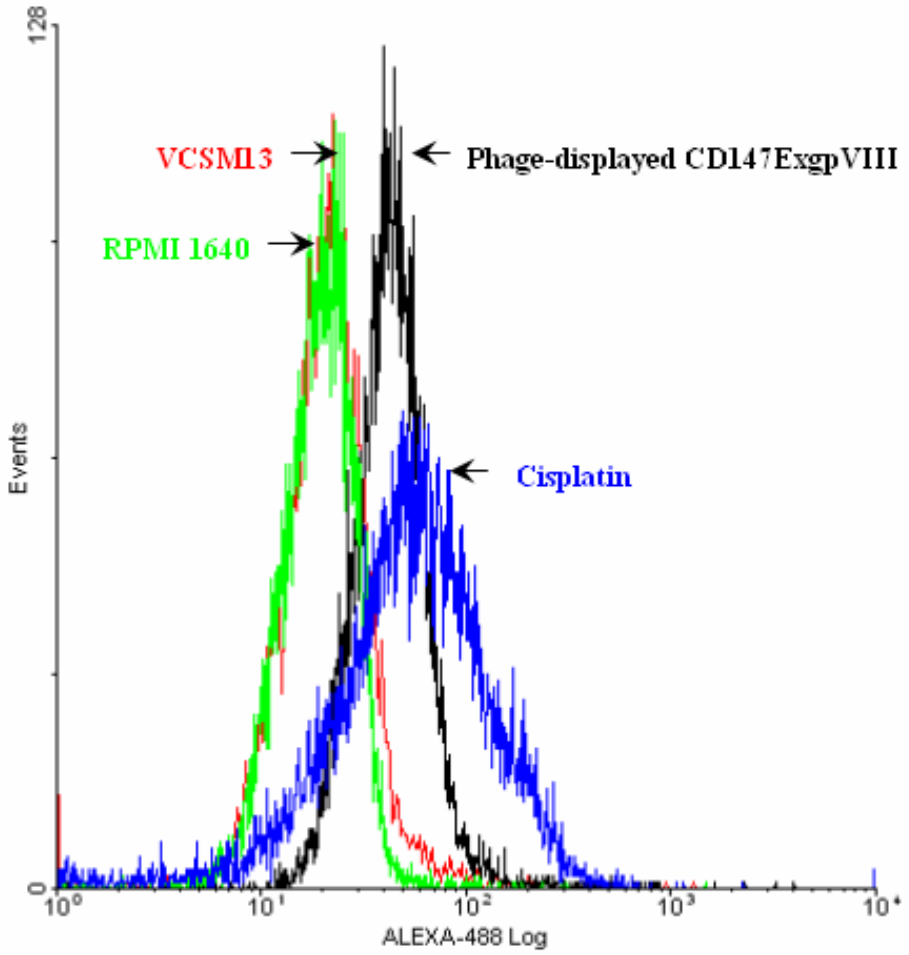

Figure 5.13 Multivalent phage-displayed CD147Ex induced U937 cell death resulted in caspase-3 activation. U937 cells were incubated with multivalent CD147 phage, VCSM13 phage, cisplatin or RPMI 1640 for 48 h. Cleaved caspase-3 was examined by flow cytometry after intracellular staining with rabbit anti-cleaved caspase-3 mAb. Results are representative of two separate experiments.

To determine whether the activation of caspase-3 in phage-displayed CD147ExgpVIII-incubated U937 cells could contribute to a low amount of cleaved caspase-3, the intracellular cleaved caspase-3 assay was then performed by immunocytochemistry. As shown in **Figure 5.14**, uninduced U937 cells and VCSM13-incubated U937 cells were negative for cleaved caspase-3, whereas induction of U937 cells by cisplatin and multivalent CD147 phage resulted in positive staining. Importantly, apoptotic cells induced by phage displaying multivalent CD147Ex showed both positive (**Figure 5.14**, *J-L*) and negative staining (**Figure 5.14**, *M-O*) with anti- cleaved caspase-3 mAb. The correlation between nuclear morphology and amount of cleaved caspase-3 in U937 cells was evaluated by arbitrarily scoring from the classified images. Scoring of staining intensity was in a scale of 0 to 3, in which 0 = negative staining, 1 = positive staining 1-5% on cell, 2 = positive staining 6-10% on cell, and 3 = positive staining > 10% on cell. As shown in **Table 5.3**, the percentage of recombinant phage-induced U937 cells harboring apoptotic nuclei was 74.3%, compared to 89.8% of cisplatin-incubated U937 cells. Interestingly, only 12.8% of multivalent phage displaying CD147Ex-induced U937 cells showed a score of 3 staining for cleaved caspase-3, whereas 41% of cisplatin-induced U937 cells exhibiting apoptotic nuclear morphology showed the same score.

Caspase-3 activation in U937 cells induced with phage-displayed CD147ExgpVIII was further investigated by Western blot analysis. As would be expected, the 17-19 kDa band of cleaved caspase-3 was not observed in protein extract from recombinant phage-incubated U937 cells, in contrast to protein extract from cisplatin-induced U937 cells (**Figure 5.15**).

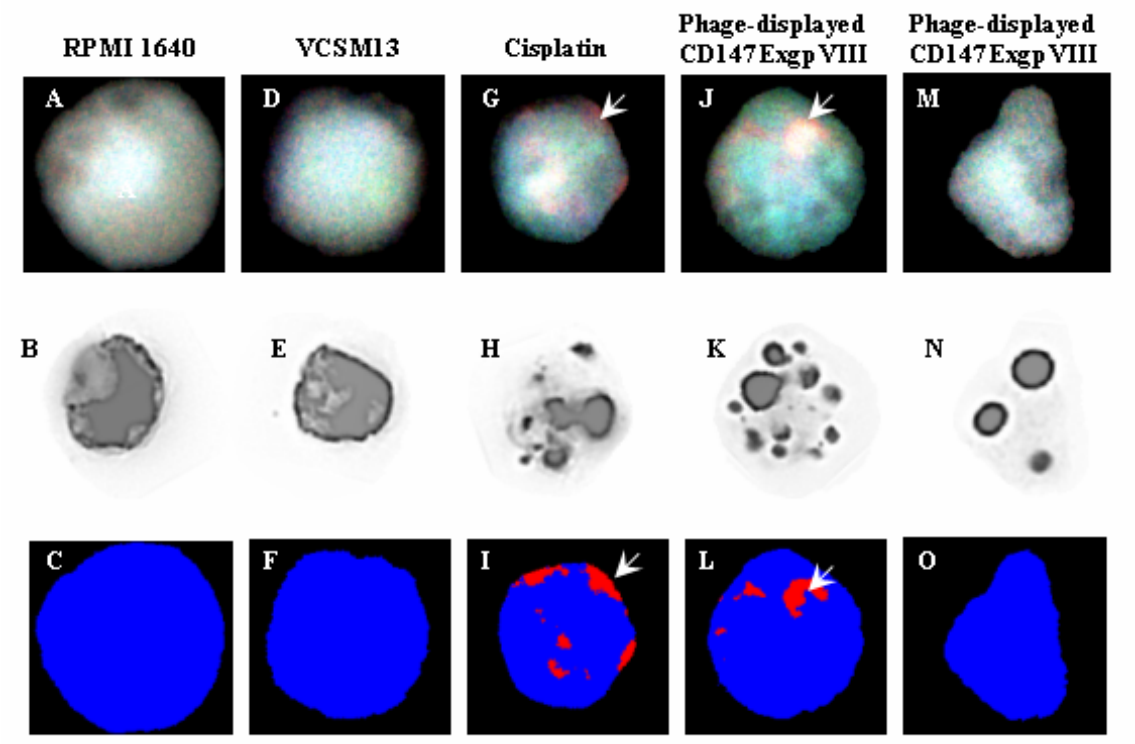

Figure 5.14 Apoptotic cell death of U937 cells in multivalent phage-displayed CD147Ex induction showed both positive and negative of cleaved caspase-3. U937 cells were incubated with multivalent CD147 phage, VCSM13 phage, cisplatin or RPMI 1640. Cleaved caspase-3 was determined by intracellular staining using rabbit anti-cleaved caspase-3 mAb and Alexa680-conjugated goat anti-rabbit immunoglobulin G. *A*, *D*, *G*, *J* and *M* represent spectral images; *B*, *D*, *H*, *K* and *N* represent inverted DAPI images; *C*, *F*, *I*, *L* and *O* represent classified images.

Table 5.3 Correlation between nuclear morphology and amount of cleaved caspase-3 in U937 cells.

Inducer	**Nuclear morphology**	**Percentage of U937 cells positive signal for cleaved caspase-3[a]**			
		-	**1+**	**2+**	**3+**
None	Apoptotic nucleus	2.4	0	0	0
	Non-apoptotic nucleus	97.6	0	0	0
Cisplatin	Apoptotic nucleus	2.6	28.2	18.0	41.0
	Non-apoptotic nucleus	0	10.2	0	0
VCSM13 phage	Apoptotic nucleus	1.8	3.6	0	0
	Non-apoptotic nucleus	62.5	30.4	1.7	0
Phage-displayed CD147ExgpVIII	Apoptotic nucleus	8.6	32.9	20.0	12.8
	Non-apoptotic nucleus	20.0	4.3	0	1.4

[a] Arbitrarily scored from classified image

0 = negative staining, 1 = positive staining 1-5% on cell, 2 = positive staining 6-10% on cell, 3 = positive staining > 10% on cell

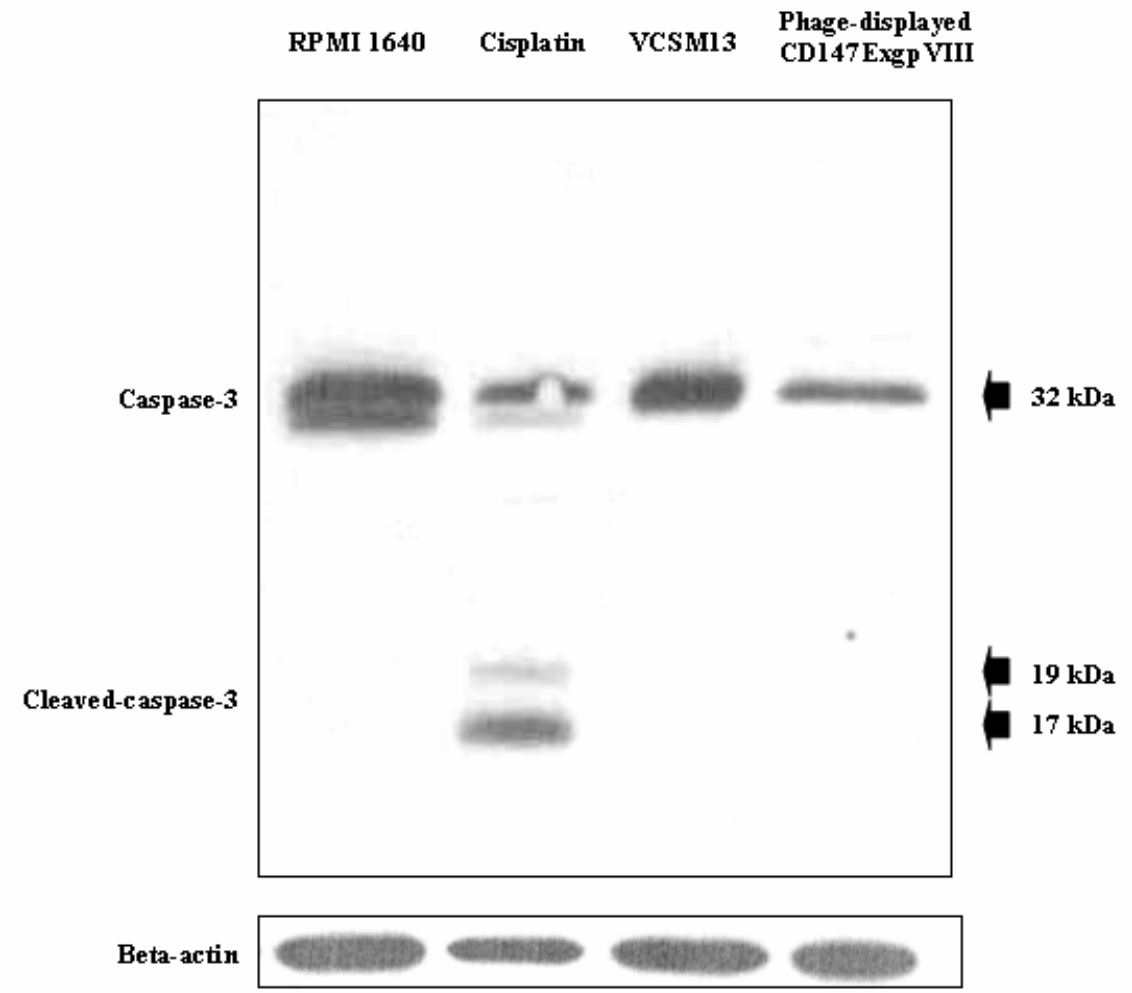

Figure 5.15 Multivalent phage-displayed CD147Ex-incubated U937 cells did not increase the amount of cleaved caspase-3 as high as cisplatin-induced U937 cells. U937 cells incubated with multivalent CD147 phage, VCSM13 phage, cisplatin or RPMI 1640. Cell lysates were analyzed by Western blot analysis using anti-caspase-3 mAbs specific for both caspase-3 and cleaved caspase-3 or anti-beta-actin mAb. One representative of four independent experiments is shown.

5.9 Phage-displayed CD147ExgpVIII binding on cell surface of U937 cells

Since some U937 cell death was noted after incubation with CD147-phage, we speculated that the change in morphology and the subsequent cell death were triggered by the interaction of multivalent CD147 molecules on phage particles and cell surface ligand (s) present on U937 cells. To examine this hypothesis, several approaches were chosen. Phage-displayed CD147ExgpVIII were incubated with U937 cells and the binding was then determined by ELISA. The recombinant phage-added well showed a 3-fold higher signal than the VCSM13-added well (**Table 5.4**). In addition, immunocytochemistry was performed to confirm the binding of multivalent CD147 phage on U937 cells. The binding of recombinant phage on individual U937 cells was also confirmed by immunocytochemistry. By our method, recombinant phage adhering on the individual U937 cell was visualized by classified image shown in red. As shown in **Figure 5.16***A* to *C*, 60% of phage-displayed CD147ExgpVIII-incubated U937 cells were positively stained with anti-gpVIII mAb. Furthermore, forty-two percent of multivalent CD147 phage-incubated U937 cells had apoptotic nuclei. In contrast, anti- gpVIII mAb did not bind to VCSM13-incubated U937 cells (**Figure 5.16**, *D-F*). These results indicate that potential CD147 ligand (s) exit on the surface of U937 cells.

Table 5.4 Detection of phage carrying multivalent CD147 via gpVIII binding on U937 cells by ELISA

Phages (10^8 cfu/well)	**Optical density at 450 nm (OD450)[a]**	
	U937-coated well (10^5 cells/well)	**None**
None	0.080 ± 0.004	ND
VCSM13	0.443 ± 0.006	0.083 ± 0.003
Phage-displayed CD147ExgpVIII	1.480 ± 0.010	0.083 ± 0.001

[a] mean ± SD of three independent experiments

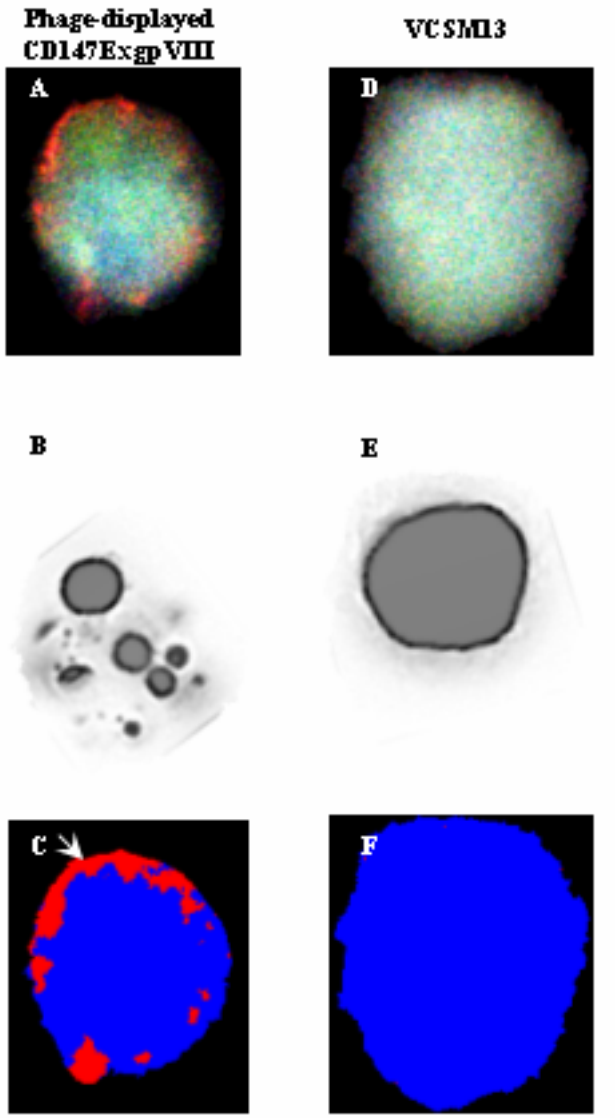

Figure 5.16 Detection of multivalent CD147 phage binding on U937 cells by immunocytochemistry. U937 cells were incubated with recombinant phages or wild-type phages for 24 h, stained with anti-gpVIII mAb and followed by Alexa680-conjugated goat anti-mouse immunoglobulins. The nuclear morphology was verified by DAPI staining. *A* and *D*, spectral image; *B* and *E*, inverted DAPI; *C* and *F*, classified image.

CHAPTER 6

DISCUSSIONS

In an attempt to investigate the molecular function of CD147Ex molecule, phage-displayed ectodomain of CD147 via gpIII was generated recently in our labs (28). However, the binding of these recombinant phages on any cell type could not be observed by indirect immunofluorescence techniques, most likely due to the level of heterologous protein displayed on phage gpIII being restricted to less than one molecule per phage particle (13). Multimeric display of CD147 on phage particles are therefore required and will be valuable in further discovering its ligand-partner on cell surface. The gpVIII of VCSM13 was previously applied for achieving the multimeric polypeptide libraries. High levels of heterologous protein display could be achieved on gpVIII, as each phage particle contains approximately 2000 copies of the protein (14, 15). The absolute binding force of these phage libraries to a certain ligand was enhanced according to the increasing copy number of each polypeptide. Moreover, multivalent CD147 on the 930 nm-length filamentous phage might overcome the limitation of CD147 anchoring to low levels of its receptor (s). The multivalent phage carrying CD147 may be valuable in functional study. Signal transferring by individual pairing with monovalent CD147 may differ from the cross-linking of cell-surface ligands with phage-displayed multivalent CD147 via gpVIII.

We decided to generate phage which displayed multivalent CD147Ex molecule on phage particles via gpVIII. However, the multivalent display of fusion protein via gpVIII on phage particles had been hindered because of a limitation on the fusion length (116). Culturing conditions during phage preparation such as temperature, IPTG-stimulation and helper phage infection-period are important factors for production of the phage expressing interested protein. In the present study, the factors mentioned were investigated to optimize the quantity of display. Filamentous

phage was employed to display CD147EX via gpVIII in TG1 *E. coli* host. By sandwich ELISA using a panel of anti-CD147 monoclonal antibodies as a capture and HRP-conjugated anti-gpVIII mAb as a tracer, the generated phages showed strong positive reactivity. The correct size of the CD147Ex-gpVIII fusion protein at 28 kDa from the generated phages was also demonstrated by western immunoblotting. This result indicated that the expression of fusion CD147-gpVIII proteins was occurred. However, a question whether the positive signal due to the secreted or the phage-bound CD147Ex-gpVIII fusion protein was raised. To address this question, the expression of CD147Ex on the surface of complete phage particles was subsequently confirmed by using the biotinylated anti-gpIII mAb/HRP-conjugated Streptavidin as a tracer in sandwich ELISA. As predicted, the generated phages showed also strong positive reactivity. The ELISA experiments indicated that the generated phages harbored CD147Ex on their surfaces.

Production of phage-displayed CD147ExgpVIII at 25 ^{o}C with IPTG-stimulation was demonstrated the most suitable condition. Reducing growth temperature, from 37 ^{o}C to 25 ^{o}C, may facilitate the correct folding and stability of the displayed protein (117-119). Although the rate of protein synthesis was low at 25 ^{o}C comparing to 37 ^{o}C, IPTG seemed to compensate this disadvantage. The reduction in cultivating temperature and addition of IPTG may have a complementary effect on phage propagation and on the fusion protein incorporation resulting in the high density display per phage particle.

Phage harvested from 37 ^{o}C without IPTG-stimulation was demonstrated to be the second effective order when M6-1B9 mAb was used as a capture antibody. In surprising contrast, when other three mAbs (M6-1E9, M6-1D4, and M6-2F9) were used as capture antibodies, the second rank was changed to phage harvested from 25 ^{o}C without IPTG-stimulation. These results could be speculated that the folding of CD147 epitope recognized by M6-1B9 mAb on recombinant phage produced at 37 ^{o}C without IPTG-stimulation was more proper than phages produced at 25 ^{o}C without IPTG-stimulation. Regarding the previous study in our lab (28), the epitopes recognized by M6-1B9 and M6-1E9 mAbs were overlapped. The variation in exposing of these epitopes in the different culturing conditions indicated the

proximate but non-identical epitopes recognized by M6-1B9 and M6-1E9 mAbs. The recombinant phage harvested from 37 ^{o}C with IPTG-stimulation was given the lowest signal in all anti-CD147 mAbs used. This result was consistent with the experiment of antibody-gpVIII phage production (25). Insoluble protein accumulation and degradation of the recombinant protein in the periplasm by host proteases might be facilitated at higher growth temperatures (118). Apparently, high expression level of fusion protein by IPTG-stimulation rendered the formation of inclusion bodies which decreased the incorporating efficiency of CD147Ex-gpVIII into phage particles (117-119).

One proposed strategy for increasing the amount of recombinant protein displayed on phage particles via gpVIII was by delaying the infection-period of helper phage after IPTG-stimulation (120). However, the controversial result was obtained in this study. The phage-displayed CD147ExgpVIII produced at 25 ^{o}C with IPTG-stimulation at the same time of helper phage infection were higher than those obtained by infection of helper phages 2 h later. A plausible explanation of this result was that, after 2-h induction, *E. coli* produced an excess amount of CD147ExgpVIII which was prone to form aggregation before the phage packaging components were synthesized. In summary, multivalent CD147Ex phage produced at 25 C with IPTG stimulation at the same time of helper phage infection is the most suitable tool for studying the molecular function of CD147Ex molecules on various hematopoietic cell lines which is not fully understood.

In order to produce high density phages, various sophisticate techniques have been developed. Sidhu increased the display of human growth hormone by mutating the amino acid residues on the gpVIII fusion partner (121). More recently, a novel gpVIII display system, in which every copy of gpVIII was modified, was reported (27). The gpVIII was expressed from the phagemid and the helper phage used to rescue the phagemid had been deficient in gpVIII production. In contrast, we established here a simple method for increasing of the multimeric CD147Ex expression on phage particles. Apart from the major parameters i.e. temperature and IPTG-stimulation which were formerly investigated (20, 25), the influence of helper

phage infection-period after IPTG-stimulation on enhancing the CD147Ex displaying, particularly, demonstrated a high impact of this study.

After the discovery of the CD147 protein, there was no concrete evidence describing the role of CD147 in triggering the membrane bound molecule. Although recombinant CD147 could be expressed on the surface of other cell types *in vitro*, it is not suitable for studying CD147 function, as other pairs of membrane-protein interactions may interfere with the absolute signal originating from CD147 induction. In contrast to the previous study using monovalent CD147 phage (28), the present study shows the anchoring of multivalent CD147Ex phage on U937 cells as demonstrated by immunological techniques, i.e. ELISA and immunocytochemistry. These results suggest the presence of CD147 counter-receptor (s) on the U937 cell surface. Implicit in the display system was the notion that multivalent CD147 enhanced the binding efficiency of CD147 to its counter-receptor (s).

The physical association between CD147 and β1 integrin in the membrane has been reported (72, 73). Berditchevski *et al*. (72) suggested that association of $\alpha^3\beta_1$ integrin and $\alpha^6\beta_1$ integrin with CD147 is in lateral fashion, similar to interaction of β_3 integrins with CD47, another immunoglobulin superfamily proteins (74, 75). It has been reported that CD147 also serves as a signaling receptor for extracellular cyclophilin A (76-78). Recently, the cyclophilin-binding region in CD147 molecule has been identified (122). The specific binding was observed with full-length CD147 and CD147 external-transmembrane domain constructs. No binding was detected with CD147 external domain and CD147 external-cytoplasmic domain. These results speculated that the extracellular domain of CD147 was not bound to cyclophilin A. Indeed, transmembrane domain of CD147 was necessary and sufficient for CD147 binding to cyclophilin A. Similar results were obtained using cyclophilin B-coated beads, suggested that interaction of cyclophilins with the CD147 transmembrane domain may involve the active site common to all cyclophilins. This report was also demonstrated the proline residue located at position 211 in transmembrane domain was identified as the critical residue responsible for the intracellular interaction of cyclophilins and CD147 (122). Interaction between the lactate transporter MCT1 and CD147 has been reported (71, 123). The tightly association between MCT1 and a

hybrid protein of the extracellular domain of CD2 and the transmembrane and cytoplasmic domains of CD147 has been reported (71). This study also suggested that transmembrane and cytoplasmic domains of CD147 are important for MCT-CD147 interaction (71). Implication with this study, the counter-receptor of multivalent CD147Ex phage on U937 cells may be other cell surface molecules, not be integrins, cyclophilins and MCTs. The possibility that CD147 could be a receptor for itself has been mentioned (1). COS cells transiently expressing full-length CD147 adhered moderately well to immobilized CD147 extracellular domain-Fc fusion protein (1). However, in our attempts to mimic the homophilic interaction of CD147 using the fusion protein of CD147Ex- (BCCP) and multivalent CD147EX phage we have been unable to demonstrate the binding of these proteins by ELISA (data not shown). Thus, homophilic interaction of CD147 is still controversial.

The bound phage displaying CD147 is hypothesized to induce the signal transduction into the U937 cells. Accordingly, these multivalent CD147 phages induced morphological changes in U937 cells, in contrast to Jurkat, Molt4, SupT1 and Daudi cells. Engagement of cell surface receptors by multivalent ligands might be necessary for this cellular change. A similar phenomenon has been reported in a study that showed IgE dimers were less effective than larger IgE oligomers in stimulating cellular responses (124). Dependency of cellular responses on receptor aggregates also has been observed for related receptors, such as the B-cell receptor (125, 126) and T-cell receptor (127, 128). Thus, signal transduction by individual binding of monovalent CD147 may differ from the cross-linking of cell surface-ligands with multivalent CD147 phage. Herein, the molecular interaction of multivalent phage displaying CD147 and its counter-receptor (s) on U937 cells mediated the morphological changes characteristic of apoptotic cell death. Interactions between recombinant CD147 phage and its receptor (s) on U937 cells might consequently lead to sending death signals into cells. The death of CD147 phage-incubated U937 cells did not result from chemical toxicity in phage preparation because this phenomenon was not observed in VCSM13-incubated U937 cells. In addition, the cell death was specifically observed in U937 cells but not other tested cell lines. Time-dependent cell death of U937 cells incubated with multivalent CD147 phage was also observed. In

addition to CD147 phage-induced apoptotic morphological change of U937 cells, growth arrest of U937 cells was observed after 48 h of incubation.

The morphological features of apoptotic cell death and double staining with calcein and EthD-1 visualized in U937 cells incubated with multivalent CD147Ex phage suggest a possible involvement of caspase activation in this phenotype. To address this question, the presence of cleaved caspase-3 in U937 cells incubated with multivalent CD147 phage was examined by flow cytometry, immunocytochemistry and Western blot analysis. By flow cytometry, the level of cleaved caspase-3 in U937 cells incubated with multivalent CD147Ex phage was higher than uninduced or wild-type phage-incubated U937 cells. However, it was not as remarkable as levels of cleaved caspase-3 seen in cisplatin-induced U937 cells. When individual U937 cells were analyzed by immunocytochemistry, the percentage of recombinant phage-induced U937 cells harboring apoptotic nuclei was 74.3%, with only 12.8% scoring 3+ for cleaved caspase-3 positive staining by immunocytochemistry. Correspondingly, by Western blot analysis the 17-19 kDa of cleaved caspase-3 was not observed in protein extract from U937 cells incubated with phage-displayed CD147ExgpVIII. It is feasible that the apoptotic cell death of multivalent CD147 phage-stimulated U937 cells is only partially associated with an enhancement in cleaved caspase-3 level. Initiation of caspase-dependent and -independent cell death in response to a given stimulus has been recently reported (129, 130). Triggering of HLA class I molecules on Jurkat T lymphoblasts was implicated in cell death induction of two parallel pathways (130). Our data indicate that a caspase-independent pathway may also be involved in cell death mediated by multivalent CD147.

In summary, we introduce here a useful strategy in applying phage display technique for cell signaling studies. Multivalent CD147 phages were generated and applied for functional study of the CD147 molecule. Production of multivalent CD147Ex on phage particles was achieved in TG1 *E. coli* when growing the pComb8-CD147Ex–transformed TG1 at 25 ^{o}C with IPTG-stimulation at the same time of helper phage infection. To study the interaction of CD147Ex displayed on phage particles and cell surface molecule (s) on hematopoietic cell lines, the multivalent CD147Ex phage was incubated with various hematopoietic cell lines. Among these

cell lines, morphological change of cells incubated with these constructed phages was observed after 24 h of incubation in U937 cells only and cell propogation of U937 cells was ceased at 48 h of incubation. The caspase-3-dependent of multivalent CD147Ex phage-incubated U937 cells plays a partial role in U937 cell death. In addition, the anchoring of these constructed phages on cell surface of U937 cells was demonstrated which is coordinated with apoptotic nuclei. A novel function of CD147 in triggering apoptotic cell death in U937 cells was identified. Since this phenomenon specifically occurred with U937 cells, which is a monocytic cell line, the involvement of CD147 in immune regulation of specific lineage and developmental stages will be the focus of future studies.

CHAPTER 7

CONCLUSION

A useful strategy in applying phage display technique is introduced for studying the molecular function of extracellular domain of leukocyte surface molecule, CD147. The DNA fragment coding for extracellular domain of CD147 was inserted in between the Sec signal sequence and the gpVIII gene of the bacteriophage VCSM13 in a phagemid vector, pComb8, named pComb8-CD147Ex. This recombinant vector was transformed and the fusion gene was inducible expressed in *Escherichia coli* TG-1. The CD147Ex were successfully expressed via the major coated protein, gpVIII, on phage particles under 25 ^{o}C with simultaneous isopropyl-β-D-thiogalactopyranoside (IPTG) stimulation and VCSM13 phage infection. The multivalent CD147Ex phages in culture supernatant were harvested by PEG-NaCl precipitation. The harvested phages were examined for the display of CD147Ex on phage particle by sandwich ELISA using a panel of anti-CD147 mAb as capture antibody. Phage-displayed CD147ExgpVIII is recognized using HRP-conjugated anti-gpVIII mAb as a tracer. In contrast, the recombinant phages were not recognized by an irrelevant capture antibody. The CD147Ex-gpVIII fusion protein at 28 kDa from these multivalent phages was demonstrated by Western blot analysis. The generated phages harbored CD147Ex on their surfaces was subsequently confirmed using the biotinylated anti-gpIII mAb/HRP-conjugated Streptavidin as a tracer in sandwich ELISA.

These multivalent CD147Ex phages were applied for the functional study of CD147Ex molecule. A novel function of CD147 in triggering the apoptotic cell death in only U937 cells, not other hematopoietic cell lines used, was identified. By immunocytochemistry, flow cytometry and Western blot analysis, the apoptotic cell death of multivalent CD147 phages-induced U937 cells is only partially associated with an enhancement in cleaved caspase-3 level. However, the precise mechanism of

apoptotic cell death of U937 cells induced by multivalent phage-displayed CD147Ex is still unknown. Further investigations on a mechanism of multivalent CD147Ex phages-stimulated U937 cell death may lead to a better understanding of the involvement of CD147 and immune regulation which may provide the new avenue for clinical application.

REFERENCES

1. Sun J, Hemler ME. Regulation of MMP-1 and MMP-2 production through CD147/ extracellular matrix metalloproteinase inducer interactions. Cancer Res 2001;61(5):2276-81.
2. Bowen MA, Bajorath J, Siadak AW, Modrell B, Malacko AR, Marquardt H, et al. The amino-terminal immunoglobulin-like domain of activated leukocyte cell adhesion molecule binds specifically to the membrane-proximal scavenger receptor cysteine-rich domain of CD6 with a 1:1 stoichiometry. J Biol Chem 1996;271(29):17390-6.
3. Vilardell C, Juan M, Miralles A, Barcelo JJ, Esparza J, Palou E, et al. Isolation of two CD50 (ICAM-3)-negative Jurkat T-cell clones and their application for analysis of CD50 function. Tissue Antigens 1998;51(5):509-19.
4. Martinez-Pomares L, Crocker PR, Da Silva R, Holmes N, Colominas C, Rudd P, et al. Cell-specific glycoforms of sialoadhesin and CD45 are counter-receptors for the cysteine-rich domain of the mannose receptor. J Biol Chem 1999;274(49):35211-8.
5. Guo H, Li R, Zucker S, Toole BP. EMMPRIN (CD147), an inducer of matrix metalloproteinase synthesis, also binds interstitial collagenase to the tumor cell surface. Cancer Res 2000;60(4):888-91.
6. Prager E, Sunder-Plassmann R, Hansmann C, Koch C, Holter W, Knapp W, et al. Interaction of CD31 with a heterophilic counterreceptor involved in downregulation of human T cell responses. J Exp Med 1996;184(1):41-50.
7. Koch C, Staffler G, Huttinger R, Hilgert I, Prager E, Cerny J, et al. T cell activation-associated epitopes of CD147 in regulation of the T cell response, and their definition by antibody affinity and antigen density. Int Immunol 1999;11(5):777-86.

8. Smith GP. Filamentous fusion phage: novel expression vectors that display cloned antigens on the virion surface. Science 1985;228(4705):1315-7.
9. Scott JK, Smith GP. Searching for peptide ligands with an epitope library. Science 1990;249(4967):386-90.
10. Cwirla SE, Peters EA, Barrett RW, Dower WJ. Peptides on phage: a vast library of peptides for identifying ligands. Proc Natl Acad Sci U S A 1990;87(16): 6378-82.
11. Wrighton NC, Farrell FX, Chang R, Kashyap AK, Barbone FP, Mulcahy LS, et al. Small peptides as potent mimetics of the protein hormone erythropoietin. Science 1996;273(5274):458-64.
12. Fairbrother WJ, Christinger HW, Cochran AG, Fuh G, Keenan CJ, Quan C, et al. Novel peptides selected to bind vascular endothelial growth factor target the receptor-binding site. Biochemistry 1998;37(51):17754-64.
13. Bass S, Greene R, Wells JA. Hormone phage: an enrichment method for variant proteins with altered binding properties. Proteins 1990;8(4):309-14.
14. Petrenko VA, Smith GP, Gong X, Quinn T. A library of organic landscapes on filamentous phage. Protein Eng 1996;9(9):797-801.
15. Iannolo G, Minenkova O, Gonfloni S, Castagnoli L, Cesareni G. Construction, exploitation and evolution of a new peptide library displayed at high density by fusion to the major coat protein of filamentous phage. Biol Chem 1997;378(6):517-21.
16. Larocca D, Kassner PD, Witte A, Ladner RC, Pierce GF, Baird A. Gene transfer to mammalian cells using genetically targeted filamentous bacteriophage. Faseb J 1999;13(6):727-34.
17. Legendre D, Soumillion P, Fastrez J. Engineering a regulatable enzyme for homogeneous immunoassays. Nat Biotechnol 1999;17(1):67-72.
18. Legendre D, Laraki N, Graslund T, Bjornvad ME, Bouchet M, Nygren PA, et al. Display of active subtilisin 309 on phage: analysis of parameters influencing the selection of subtilisin variants with changed substrate specificity from libraries using phosphonylating inhibitors. J Mol Biol 2000;296(1):87-102.

19. Ponsard I, Galleni M, Soumillion P, Fastrez J. Selection of metalloenzymes by catalytic activity using phage display and catalytic elution. Chembiochem 2001;2(4):253-9.

20. Chappel JA, He M, Kang AS. Modulation of antibody display on M13 filamentous phage. J Immunol Methods 1998;221(1-2):25-34.

21. Nygaard FB, Harlow KW. Heterologous expression of soluble, active proteins in Escherichia coli: the human estrogen receptor hormone-binding domain as paradigm. Protein Expr Purif 2001;21(3):500-9.

22. O'Brien PM, Maxwell G, Campo MS. Bacterial expression and purification of recombinant bovine Fab fragments. Protein Expr Purif 2002;24(1):43-50.

23. Soltes G, Barker H, Marmai K, Pun E, Yuen A, Wiersma EJ. A new helper phage and phagemid vector system improves viral display of antibody Fab fragments and avoids propagation of insert-less virions. J Immunol Methods 2003;274(1-2):233-44.

24. Tayapiwatana C, Kasinrerk W. Construction and characterization of phage-displayed leukocyte surface molecule CD99. Appl Microbiol Biotechnol 2002;60(3):336-41.

25. Kretzschmar T, Geiser M. Evaluation of antibodies fused to minor coat protein III and major coat protein VIII of bacteriophage M13. Gene 1995;155(1):61-5.

26. Wang L, Radic MZ, Siegel D, Chang T, Bracy J, Galili U. Cloning of anti-Gal Fabs from combinatorial phage display libraries: structural analysis and comparison of Fab expression in pComb3H and pComb8 phage. Mol Immunol 1997;34(8-9):609-18.

27. Legendre D, Fastrez J. Construction and exploitation in model experiments of functional selection of a landscape library expressed from a phagemid. Gene 2002;290(1-2):203-15.

28. Tayapiwatana C, Arooncharus P, Kasinrerk W. Displaying and epitope mapping of CD147 on VCSM13 phages: influence of Escherichia coli strains. J Immunol Methods 2003;281(1-2):177-85.

29. Mason D, Andre P, Bensussan A, Buckley C, Civin C, Clark E, et al. CD antigens 2001: aims and results of HLDA Workshops. Stem Cells 2001;19(6):556-62.

30. Mason D, Andre P, Bensussan A, Buckley C, Civin C, Clark E, et al. CD Antigens 2001. Mod Pathol 2002;15(1):71-6.

31. Gottesman MM, Pastan I. The multidrug transporter, a double-edged sword. J Biol Chem 1988;263(25):12163-6.

32. Abbas AK. Cellular and molecular immunology. 5th ed. Philadelphia: Saunders; 2003.

33. Lowin B, Hahne M, Mattmann C, Tschopp J. Cytolytic T-cell cytotoxicity is mediated through perforin and Fas lytic pathways. Nature 1994; 370(6491):650-2.

34. Armitage RJ, Tough TW, Macduff BM, Fanslow WC, Spriggs MK, Ramsdell F, et al. CD40 ligand is a T cell growth factor. Eur J Immunol 1993;23(9):2326-31.

35. Kanzaki M, Shibata H, Mogami H, Kojima I. Expression of calcium-permeable cation channel CD20 accelerates progression through the G1 phase in Balb/c 3T3 cells. J Biol Chem 1995;270(22):13099-104.

36. Shipp MA, Look AT. Hematopoietic differentiation antigens that are membrane-associated enzymes: cutting is the key! Blood 1993;82(4):1052-70.

37. Deterre P, Gelman L, Gary-Gouy H, Arrieumerlou C, Berthelier V, Tixier JM, et al. Coordinated regulation in human T cells of nucleotide-hydrolyzing ecto-enzymatic activities, including CD38 and PC-1. Possible role in the recycling of nicotinamide adenine dinucleotide metabolites. J Immunol 1996;157(4): 1381-8.

38. Wang TF, Guidotti G. CD39 is an ecto-(Ca2+,Mg2+)-apyrase. J Biol Chem 1996; 271(17):9898-901.

39. Guan JL, Chen HC. Signal transduction in cell-matrix interactions. Int Rev Cytol 1996;168:81-121.

40. Schwartz MA, Schaller MD, Ginsberg MH. Integrins: emerging paradigms of signal transduction. Annu Rev Cell Dev Biol 1995;11:549-99.

41. Springer TA. Traffic signals for lymphocyte recirculation and leukocyte emigration: the multistep paradigm. Cell 1994;76(2):301-14.
42. Springer TA. Adhesion receptors of the immune system. Nature 1990;346(6283): 425-34.
43. Gumbiner BM. Cell adhesion: the molecular basis of tissue architecture and morphogenesis. Cell 1996;84(3):345-57.
44. Buckley CD, Rainger GE, Bradfield PF, Nash GB, Simmons DL. Cell adhesion: more than just glue (review). Mol Membr Biol 1998;15(4):167-76.
45. Aplin AE, Howe AK, Juliano RL. Cell adhesion molecules, signal transduction and cell growth. Curr Opin Cell Biol 1999;11(6):737-44.
46. Hogg N, Landis RC. Adhesion molecules in cell interactions. Curr Opin Immunol 1993;5(3):383-90.
47. Gahmberg CG, Nortamo P, Li R, Valmu L. Leukocyte cell adhesion proteins: from molecular dissection to clinical applications. Ann Med 1992;24(5):329-35.
48. Yong K, Khwaja A. Leucocyte cellular adhesion molecules. Blood Rev 1990; 4(4): 211-25.
49. Ross GD. Regulation of the adhesion versus cytotoxic functions of the Mac-1/CR3/ alphaMbeta2-integrin glycoprotein. Crit Rev Immunol 2000;20(3):197-222.
50. Patarroyo M. Adhesion molecules mediating recruitment of monocytes to inflamed tissue. Immunobiology 1994;191(4-5):474-7.
51. Ebnet K, Kaldjian EP, Anderson AO, Shaw S. Orchestrated information transfer underlying leukocyte endothelial interactions. Annu Rev Immunol 1996;14:155-77.
52. Shimizu Y, van Seventer GA, Horgan KJ, Shaw S. Roles of adhesion molecules in T-cell recognition: fundamental similarities between four integrins on resting human T cells (LFA-1, VLA-4, VLA-5, VLA-6) in expression, binding, and costimulation. Immunol Rev 1990;114:109-43.
53. Picker LJ. Control of lymphocyte homing. Curr Opin Immunol 1994;6(3):394-406.
54. Kasinrerk W, Fiebiger E, Stefanova I, Baumruker T, Knapp W, Stockinger H. Human leukocyte activation antigen M6, a member of the Ig superfamily,

is the species homologue of rat OX-47, mouse basigin, and chicken HT7 molecule. J Immunol 1992;149(3):847-54.

55. Miyauchi T, Masuzawa Y, Muramatsu T. The basigin group of the immunoglobulin superfamily: complete conservation of a segment in and around transmembrane domains of human and mouse basigin and chicken HT7 antigen. J Biochem (Tokyo) 1991;110(5):770-4.
56. Biswas C, Zhang Y, DeCastro R, Guo H, Nakamura T, Kataoka H, et al. The human tumor cell-derived collagenase stimulatory factor (renamed EMMPRIN) is a member of the immunoglobulin superfamily. Cancer Res 1995;55(2):434-9.
57. Kirsch AH, Diaz LA, Jr., Bonish B, Antony PA, Fox DA. The pattern of expression of CD147/neurothelin during human T-cell ontogeny as defined by the monoclonal antibody 8D6. Tissue Antigens 1997;50(2):147-52.
58. Fossum S, Mallett S, Barclay AN. The MRC OX-47 antigen is a member of the immunoglobulin superfamily with an unusual transmembrane sequence. Eur J Immunol 1991;21(3):671-9.
59. Altruda F, Cervella P, Gaeta ML, Daniele A, Giancotti F, Tarone G, et al. Cloning of cDNA for a novel mouse membrane glycoprotein (gp42): shared identity to histocompatibility antigens, immunoglobulins and neural-cell adhesion molecules. Gene 1989;85(2):445-51.
60. Miyauchi T, Kanekura T, Yamaoka A, Ozawa M, Miyazawa S, Muramatsu T. Basigin, a new, broadly distributed member of the immunoglobulin superfamily, has strong homology with both the immunoglobulin V domain and the beta-chain of major histocompatibility complex class II antigen. J Biochem (Tokyo) 1990;107(2):316-23.
61. Nehme CL, Cesario MM, Myles DG, Koppel DE, Bartles JR. Breaching the diffusion barrier that compartmentalizes the transmembrane glycoprotein CE9 to the posterior-tail plasma membrane domain of the rat spermatozoon. J Cell Biol 1993;120(3):687-94.

62. Seulberger H, Lottspeich F, Risau W. The inducible blood--brain barrier specific molecule HT7 is a novel immunoglobulin-like cell surface glycoprotein. Embo J 1990;9(7):2151-8.

63. Fadool JM, Linser PJ. 5A11 antigen is a cell recognition molecule which is involved in neuronal-glial interactions in avian neural retina. Dev Dyn 1993;196(4):252-62.

64. Schlosshauer B, Herzog KH. Neurothelin: an inducible cell surface glycoprotein of blood-brain barrier-specific endothelial cells and distinct neurons. J Cell Biol 1990;110(4):1261-74.

65. Spring FA, Holmes CH, Simpson KL, Mawby WJ, Mattes MJ, Okubo Y, et al. The Oka blood group antigen is a marker for the M6 leukocyte activation antigen, the human homolog of OX-47 antigen, basigin and neurothelin, an immunoglobulin superfamily molecule that is widely expressed in human cells and tissues. Eur J Immunol 1997;27(4):891-7.

66. Kaname T, Miyauchi T, Kuwano A, Matsuda Y, Muramatsu T, Kajii T. Mapping basigin (BSG), a member of the immunoglobulin superfamily, to 19p13.3. Cytogenet Cell Genet 1993;64(3-4):195-7.

67. Kasinrerk W, Tokrasinwit N, Phunpae P. CD147 monoclonal antibodies induce homotypic cell aggregation of monocytic cell line U937 via LFA-1/ICAM-1 pathway. Immunology 1999;96(2):184-92.

68. Stockinger H. Interaction of GPI-anchored cell surface proteins and complement receptor type 3. Exp Clin Immunogenet 1997;14(1):5-10.

69. Staffler G, Stockinger H. Cd147. J Biol Regul Homeost Agents 2000;14(4):327-30.

70. Schuster VL, Lu R, Kanai N, Bao Y, Rosenberg S, Prie D, et al. Cloning of the rabbit homologue of mouse 'basigin' and rat 'OX-47': kidney cell type-specific expression, and regulation in collecting duct cells. Biochim Biophys Acta 1996;1311(1):13-9.

71. Kirk P, Wilson MC, Heddle C, Brown MH, Barclay AN, Halestrap AP. CD147 is tightly associated with lactate transporters MCT1 and MCT4 and facilitates their cell surface expression. Embo J 2000;19(15):3896-904.

72. Berditchevski F, Chang S, Bodorova J, Hemler ME. Generation of monoclonal antibodies to integrin-associated proteins. Evidence that alpha3beta1 complexes with EMMPRIN/basigin/OX47/M6. J Biol Chem 1997;272(46):29174-80.

73. Cho JY, Fox DA, Horejsi V, Sagawa K, Skubitz KM, Katz DR, et al. The functional interactions between CD98, beta1-integrins, and CD147 in the induction of U937 homotypic aggregation. Blood 2001;98(2):374-82.

74. Brown E, Hooper L, Ho T, Gresham H. Integrin-associated protein: a 50-kD plasma membrane antigen physically and functionally associated with integrins. J Cell Biol 1990;111(6 Pt 1):2785-94.

75. Lindberg FP, Gresham HD, Reinhold MI, Brown EJ. Integrin-associated protein immunoglobulin domain is necessary for efficient vitronectin bead binding. J Cell Biol 1996;134(5):1313-22.

76. Pushkarsky T, Zybarth G, Dubrovsky L, Yurchenko V, Tang H, Guo H, et al. CD147 facilitates HIV-1 infection by interacting with virus-associated cyclophilin A. Proc Natl Acad Sci U S A 2001;98(11):6360-5.

77. Yurchenko V, O'Connor M, Dai WW, Guo H, Toole B, Sherry B, et al. CD147 is a signaling receptor for cyclophilin B. Biochem Biophys Res Commun 2001;288(4):786-8.

78. Yurchenko V, Zybarth G, O'Connor M, Dai WW, Franchin G, Hao T, et al. Active site residues of cyclophilin A are crucial for its signaling activity via CD147. J Biol Chem 2002;277(25):22959-65.

79. Ellis SM, Nabeshima K, Biswas C. Monoclonal antibody preparation and purification of a tumor cell collagenase-stimulatory factor. Cancer Res 1989;49(12):3385-91.

80. Muraoka K, Nabeshima K, Murayama T, Biswas C, Koono M. Enhanced expression of a tumor-cell-derived collagenase-stimulatory factor in urothelial carcinoma: its usefulness as a tumor marker for bladder cancers. Int J Cancer 1993;55(1):19-26.

81. Polette M, Gilles C, Marchand V, Lorenzato M, Toole B, Tournier JM, et al. Tumor collagenase stimulatory factor (TCSF) expression and localization

in human lung and breast cancers. J Histochem Cytochem 1997;45(5):703-9.

82. Bordador LC, Li X, Toole B, Chen B, Regezi J, Zardi L, et al. Expression of emmprin by oral squamous cell carcinoma. Int J Cancer 2000;85(3):347-52.
83. Basset P, Bellocq JP, Wolf C, Stoll I, Hutin P, Limacher JM, et al. A novel metalloproteinase gene specifically expressed in stromal cells of breast carcinomas. Nature 1990;348(6303):699-704.
84. Majmudar G, Nelson BR, Jensen TC, Johnson TM. Increased expression of matrix metalloproteinase-3 (stromelysin-1) in cultured fibroblasts and basal cell carcinomas of nevoid basal cell carcinoma syndrome. Mol Carcinog 1994;11(1):29-33.
85. Caudroy S, Polette M, Nawrocki-Raby B, Cao J, Toole BP, Zucker S, et al. EMMPRIN-mediated MMP regulation in tumor and endothelial cells. Clin Exp Metastasis 2002;19(8):697-702.
86. Yang JM, Xu Z, Wu H, Zhu H, Wu X, Hait WN. Overexpression of extracellular matrix metalloproteinase inducer in multidrug resistant cancer cells. Mol Cancer Res 2003;1(6):420-7.
87. Muramatsu T, Miyauchi T. Basigin (CD147): a multifunctional transmembrane protein involved in reproduction, neural function, inflammation and tumor invasion. Histol Histopathol 2003;18(3):981-7.
88. Noguchi Y, Sato T, Hirata M, Hara T, Ohama K, Ito A. Identification and characterization of extracellular matrix metalloproteinase inducer in human endometrium during the menstrual cycle in vivo and in vitro. J Clin Endocrinol Metab 2003;88(12):6063-72.
89. Kuno N, Kadomatsu K, Fan QW, Hagihara M, Senda T, Mizutani S, et al. Female sterility in mice lacking the basigin gene, which encodes a transmembrane glycoprotein belonging to the immunoglobulin superfamily. FEBS Lett 1998;425(2):191-4.
90. Igakura T, Kadomatsu K, Kaname T, Muramatsu H, Fan QW, Miyauchi T, et al. A null mutation in basigin, an immunoglobulin superfamily member,

indicates its important roles in peri-implantation development and spermatogenesis. Dev Biol 1998;194(2):152-65.

91. Igakura T, Kadomatsu K, Taguchi O, Muramatsu H, Kaname T, Miyauchi T, et al. Roles of basigin, a member of the immunoglobulin superfamily, in behavior as to an irritating odor, lymphocyte response, and blood-brain barrier. Biochem Biophys Res Commun 1996;224(1):33-6.
92. Renno T, Wilson A, Dunkel C, Coste I, Maisnier-Patin K, Benoit de Coignac A, et al. A role for CD147 in thymic development. J Immunol 2002; 168(10):4946-50.
93. Khunkeawla P, Moonsom S, Staffler G, Kongtawelert P, Kasinrerk W. Engagement of CD147 molecule-induced cell aggregation through the activation of protein kinases and reorganization of the cytoskeleton. Immunobiology 2001;203(4):659-69.
94. Staffler G, Szekeres A, Schutz GJ, Saemann MD, Prager E, Zeyda M, et al. Selective inhibition of T cell activation via CD147 through novel modulation of lipid rafts. J Immunol 2003;171(4):1707-14.
95. Hoess RH. Protein design and phage display. Chem Rev 2001;101(10):3205-18.
96. Winter G, Griffiths AD, Hawkins RE, Hoogenboom HR. Making antibodies by phage display technology. Annu Rev Immunol 1994;12:433-55.
97. Sidhu SS. Engineering M13 for phage display. Biomol Eng 2001;18(2):57-63.
98. Holliger P, Riechmann L. A conserved infection pathway for filamentous bacteriophages is suggested by the structure of the membrane penetration domain of the minor coat protein g3p from phage fd. Structure 1997;5(2):265-75.
99. Fulford W, Model P. Gene X of bacteriophage f1 is required for phage DNA synthesis. Mutagenesis of in-frame overlapping genes. J Mol Biol 1984;178(2):137-53.
100. Smith GP, Schultz DA, Ladbury JE. A ribonuclease S-peptide antagonist discovered with a bacteriophage display library. Gene 1993;128(1):37-42.
101. Lowman HB, Bass SH, Simpson N, Wells JA. Selecting high-affinity binding proteins by monovalent phage display. Biochemistry 1991;30(45):10832-8.

102. Pasqualini R, Ruoslahti E. Organ targeting in vivo using phage display peptide libraries. Nature 1996;380(6572):364-6.

103. Pasqualini R, Koivunen E, Ruoslahti E. Alpha v integrins as receptors for tumor targeting by circulating ligands. Nat Biotechnol 1997;15(6):542-6.

104. Smith GP, Petrenko VA, Matthews LJ. Cross-linked filamentous phage as an affinity matrix. J Immunol Methods 1998;215(1-2):151-61.

105. Richins RD, Kaneva I, Mulchandani A, Chen W. Biodegradation of organophosphorus pesticides by surface-expressed organophosphorus hydrolase. Nat Biotechnol 1997;15(10):984-7.

106. Li B, Tom JY, Oare D, Yen R, Fairbrother WJ, Wells JA, et al. Minimization of a polypeptide hormone. Science 1995;270(5242):1657-60.

107. Jones P. Display of antibody chains on filamentous bacteriophage. Methods Mol Biol 1998;80:449-59.

108. Hoogenboom HR. Overview of antibody phage-display technology and its applications. Methods Mol Biol 2002;178:1-37.

109. Ballinger MD, Jones JT, Lofgren JA, Fairbrother WJ, Akita RW, Sliwkowski MX, et al. Selection of heregulin variants having higher affinity for the ErbB3 receptor by monovalent phage display. J Biol Chem 1998;273(19):11675-84.

110. Soumillion P, Jespers L, Bouchet M, Marchand-Brynaert J, Sartiaux P, Fastrez J. Phage display of enzymes and in vitro selection for catalytic activity. Appl Biochem Biotechnol 1994;47(2-3):175-89; discussion 189-90.

111. Soumillion P, Jespers L, Bouchet M, Marchand-Brynaert J, Winter G, Fastrez J. Selection of beta-lactamase on filamentous bacteriophage by catalytic activity. J Mol Biol 1994;237(4):415-22.

112. Mannervik B, Cameron AD, Fernandez E, Gustafsson A, Hansson LO, Jemth P, et al. An evolutionary approach to the design of glutathione-linked enzymes. Chem Biol Interact 1998;111-112:15-21.

113. Bradford MM. A rapid and sensitive method for the quantitation of microgram quantities of protein utilizing the principle of protein-dye binding. Anal Biochem 1976;72:248-54.

114. Zheng TS, Schlosser SF, Dao T, Hingorani R, Crispe IN, Boyer JL, et al. Caspase-3 controls both cytoplasmic and nuclear events associated with Fas-mediated apoptosis in vivo. Proc Natl Acad Sci U S A 1998;95(23):13618-23.

115. Kluza J, Lansiaux A, Wattez N, Mahieu C, Osheroff N, Bailly C. Apoptotic response of HL-60 human leukemia cells to the antitumor drug TAS-103. Cancer Res 2000;60(15):4077-84.

116. Malik P, Terry TD, Gowda LR, Langara A, Petukhov SA, Symmons MF, et al. Role of capsid structure and membrane protein processing in determining the size and copy number of peptides displayed on the major coat protein of filamentous bacteriophage. J Mol Biol 1996;260(1):9-21.

117. Knappik A, Krebber C, Pluckthun A. The effect of folding catalysts on the in vivo folding process of different antibody fragments expressed in Escherichia coli. Biotechnology (N Y) 1993;11(1):77-83.

118. Wall JG, Pluckthun A. Effects of overexpressing folding modulators on the in vivo folding of heterologous proteins in Escherichia coli. Curr Opin Biotechnol 1995;6(5):507-16.

119. Bothmann H, Pluckthun A. Selection for a periplasmic factor improving phage display and functional periplasmic expression. Nat Biotechnol 1998;16(4): 376-80.

120. Kang AS, Barbas CF, Janda KD, Benkovic SJ, Lerner RA. Linkage of recognition and replication functions by assembling combinatorial antibody Fab libraries along phage surfaces. Proc Natl Acad Sci U S A 1991;88(10): 4363-6.

121. Sidhu SS, Weiss GA, Wells JA. High copy display of large proteins on phage for functional selections. J Mol Biol 2000;296(2):487-95.

122. Yurchenko V, Pushkarsky T, Li JH, Dai WW, Sherry B, Bukrinsky M. Regulation of CD147 cell surface expression: involvement of the proline residue in the CD147 transmembrane domain. J Biol Chem 2005.

123. Wilson MC, Meredith D, Halestrap AP. Fluorescence resonance energy transfer studies on the interaction between the lactate transporter MCT1 and

CD147 provide information on the topology and stoichiometry of the complex in situ. J Biol Chem 2002;277(5):3666-72.

124. Hlavacek WS, Perelson AS, Sulzer B, Bold J, Paar J, Gorman W, et al. Quantifying aggregation of IgE-FcepsilonRI by multivalent antigen. Biophys J 1999;76(5):2421-31.

125. Dintzis HM, Dintzis RZ, Vogelstein B. Molecular determinants of immunogenicity: the immunon model of immune response. Proc Natl Acad Sci U S A 1976;73(10):3671-5.

126. Dintzis RZ, Middleton MH, Dintzis HM. Studies on the immunogenicity and tolerogenicity of T-independent antigens. J Immunol 1983;131(5):2196-203.

127. Sloan-Lancaster J, Shaw AS, Rothbard JB, Allen PM. Partial T cell signaling: altered phospho-zeta and lack of zap70 recruitment in APL-induced T cell anergy. Cell 1994;79(5):913-22.

128. Kersh EN, Shaw AS, Allen PM. Fidelity of T cell activation through multistep T cell receptor zeta phosphorylation. Science 1998;281(5376):572-5.

129. Konopleva M, Tsao T, Estrov Z, Lee RM, Wang RY, Jackson CE, et al. The synthetic triterpenoid 2-cyano-3,12-dioxooleana-1,9-dien-28-oic acid induces caspase-dependent and -independent apoptosis in acute myelogenous leukemia. Cancer Res 2004;64(21):7927-35.

130. Daniel D, Opelz G, Mulder A, Kleist C, Susal C. Pathway of apoptosis induced in Jurkat T lymphoblasts by anti-HLA class I antibodies. Hum Immunol 2004;65(3):189-99.

APPENDIX

APPENDIX A

CHEMICALS AND INSTRUMENTS

1. Chemicals and antibodies

All chemicals used as in this study were analytical grade reagents.

Chemical name	Source
3,3′,5,5′-tetramethylbenzidine (TMB)	Sigma-Aldrich, St. Louis, MO, USA
3-aminopropyltriethoxysilane	Sigma-Aldrich, St. Louis, MO, USA
4′,6-diamidino-2-phenylindole (DAPI)	Molecular Probes, Eugene, OR, USA
Acrylamide	BDH Laboratory Supplies, UK
Agarose (electrophoresis grade)	Sigma-Aldrich, St. Louis, MO, USA
Ammonium persulfate	Amersham Pharmacia Biotech, Buckinghamshire, UK
Ampicillin	Sigma-Aldrich, St. Louis, MO, USA
Anti-beta-actin mAb	Sigma-Aldrich, St. Louis, MO, USA
Anti-gpIII mAb	Exalpha Biologicals, Watertown, MA, USA
Anti-gpVIII mAb	Amersham Pharmacia Biotech, Buckinghamshire, UK
Anti-rabbit Igs-Alexa488	Molecular Probes, Eugene, OR, USA
Anti-rabbit Igs-Alexa680	Molecular Probes, Eugene, OR, USA
Biotinylated anti-gpIII mAbs	Exalpha Biologicals, Watertown, MA
Bis-acrylamide	BDH Laboratory Supplies, UK
Bromophenol blue	Sigma-Aldrich, St. Louis, MO, USA

Chemical name	Source
Chemiluminescent detection system	Amersham Pharmacia Biotech, Buckinghamshire, UK
Cisplatin	Sigma-Aldrich, St. Louis, MO, USA
EDTA	Sigma-Aldrich, St. Louis, MO, USA
Ethanol	Merck, Darmstadt, Germany
Ethidium bromide	Sigma-Aldrich, St. Louis, MO, USA
Fetal bovine serum (FBS)	Gibco, Grand Island, NY, USA
Formaldehyde	Sigma-Aldrich, St. Louis, MO, USA
Glacial acetic acid	BDH Laboratory Supplies, UK
Glycerol	Sigma-Aldrich, St. Louis, MO, USA
HRP-conjugated anti-gpVIII	Amersham Pharmacia Biotech, Buckinghamshire, UK
Hybond-C membrane	Amersham Pharmacia Biotech, Buckinghamshire, UK
IPTG	Amresco, Solon, OH, USA
LIVE/DEAD Viability/Cytotoxicity kit	Molecular Probes, Eugene, OR, USA
Methanol	Merck, Darmstadt, Germany
NaCl	Sigma-Aldrich, St. Louis, MO, USA
NaOH	Sigma-Aldrich, St. Louis, MO, USA
PEG MW 8000	Sigma-Aldrich, St. Louis, MO, USA
Plasmid Mini Kit	QIAGEN, Hilden, Germany
Polyvinylidene-fluoride (PVDF) membrane	PALL, East Hills, NY, USA
ProofStart DNA polymerase	QIAGEN, Hilden, Germany

Chemical name	Source
QIAprep spin Miniprep kit	QIAGEN, Hilden, Germany
QIAquick Gel Extraction kit	QIAGEN, Hilden, Germany
QIAquick PCR purification Kit	QIAGEN, Hilden, Germany
Rabbit anti-caspase-3 (8G10) mAb	Cell Signaling, Beverly, MA, USA
Rabbit anti-cleaved caspase-3 (ASP175) (5A1) mAb	Cell Signaling, Beverly, MA, USA
Rabbit anti-mouse IgG-HRP	Dako, Dakopatts, High Wycombe, UK
Rainbow Marker	Amersham Pharmacia Biotech, Buckinghamshire, UK
RPMI 1640 medium	Gibco, Grand Island, NY, USA
SDS	Sigma-Aldrich, St. Louis, MO, USA
Skimmed milk	Difco Laboratories, Detroit MI, USA
Sodium chloride	Merck, Darmstadt, Germany
*Spe*I	Promega, Medison, WI, USA
Streptavidin-HRP	ZYMED Laboratories, San Franscisco, CA, USA
T_4 ligase enzyme	Roche Molecular Biochemicals, Manheim, Germany
TEMED	BioRad, Hercules, CA, USA
Tween20	Fluka, Buchs, Switzerland
*Xho*I	Promega, Medison, WI, USA

2. Instruments

Instruments	Source
37 °C incubator	JP Selecta, Barcelona, Spain
37 °C CO_2 incubator EG 115 IR	Jouan GmbH, Unterhaching, Germany
Beckman Coulter EPICS ALTRA	Beckman Coulter, Fullerton, CA, USA
BECKMAN L-60 ultracentrifuge	Beckman Coulter, Fullerton, CA, USA
BIO-KINETICS READER EL 340 MICROPLATE	Bio-Tek Instruments, Winooski, WT, USA
Electrophoretic power supply 3000Xi	BioRad, Hercules, CA, USA
Fluo-Link UV transluminator	Vilber Lourmat, Marne-la-Vallée Cedex, France
Fluorescence microscope	Carl Zeiss Canada Ltd., Toronto, ON, Canada
Inverted microscope	Carl Zeiss Canada Ltd., Toronto, ON, Canada
Microcentrifuge	Eppendorf AG, Hamburg, Germany
Microplate	NUNC, Roskilde, Denmark
MiniVE vertical electrophoresis system	Amersham Pharmacia Biotech, Buckinghamshire, UK
MRX-150 Refrigerated microcentrifuge	Tomy Tech USA Inc., CA, USA
MyLab orbital shaker OS-20	BioSan Ltd., Riga, Latvia
Northern Eclipse 5.0	Empix Imaging Inc., Missisauga, ON, Canada
RT 6000 D refrigerated centrifuge	Sorvall, Kendro Laboratory Products GmbH, Langenselbold, Germany

Instruments	Source
SKYVIEW software	Applied Spectral Imaging, Carlsbad, CA, USA
Spectra Cube	Applied Spectral Imaging, Carlsbad, CA, USA
Thermal cycler	Eppendorf AG, Hamburg, Germany
UV spectrophotometer	Shimadzu Scientific Instruments Inc, Kyoto, Japan
UV transilluminator	Fotodyne incorporated, Hartland, WI, USA
Vortex-Genie K-550-GE	Scientific Industries Inc, Bohemia, NY, USA
Zeiss Axiophot 2 microscope	Carl Zeiss Canada Ltd., Toronto, ON, Canada

3. Microorganisms

Microorganism	Source
Escherichia coli TG1	kindly provided by Dr. A.D. Griffiths, MRC Cambridge, UK
VCSM13 filamentous phage	Stratagene Corporate, La Jolla, CA, USA

4. Cell lines

Cell line	Cell type	Origin
Daudi	B cell line	Burkitt's lymphoma
Jurkat	T cell line	Acute lymphoblastic leukemia
Molt4	T cell line	Acute lymphoblastic leukemia
SupT1	T cell line	Acute lymphoblastic leukemia
U937	Monocytic cell line	Histiocytic lymphoma

APPENDIX B

REAGENT PREPARATIONS

1. 50× Tris-acetate/EDTA electrophoresis buffer (TAE)

Tris-base	242	gm
Glacial acetic acid	57.1	ml
0.5 M EDTA, pH 8.0	100	ml

Dissolved all ingredients in deionized distilled water and filled up to 1,000 ml.

Sterilized by autoclave and kept at room temperature.

2. 0.5 M EDTA, pH 8.0

EDTA	14.65	gm
Distilled water	100	ml

Dissolved and adjusted pH to 8.0 with 1 M NaOH.

3. 1or 2 % Agarose gel

Agarose	1 or 2	gm
1× TAE	100	ml

Melted by microwave oven.

4. Ethidium bromide working solution (10 mg/ml)

Ethidium bromide	1.0	gm
Distilled water	100	ml

Dissolved and kept in dark bottle at 4 °C.

5. 6× gel loading buffer

Bromphenol blue	0.25	%
Glycerol	30	%

Mixed thoroughly and stored at -20 °C.

6. Phosphate buffer saline (PBS), pH 7.2

NaCl	8.00	gm
KCl	0.20	gm
Na_2HPO_4	1.15	gm
KH_2PO_4	0.20	gm

Dissolved all ingredients in deionized distilled water and filled up to 900 ml.

Adjusted pH to 7.2 with 1 N HCL or 1 N NaOH.

Added distilled water to adjust the volume to 1,000 ml and kept at room temperature.

7. Reagents for SDS-polyacrylamide gel electrophoresis (SDS-PAGE)

7.1 1.5 M Tris-HCl, pH 8.8

Tris-base	18.15	gm

Dissolved in 75 ml deionized distilled water.

Adjusted pH to 8.8 with concentrated HCL.

Adjusted the volume to 100 ml with deionized distilled water and stored at 4 °C.

7.2 0.5 M Tris-HCL, pH 6.8

Tris-base	6.0	gm

Dissolved in 75 ml deionized distilled water.

Adjusted pH to 6.8 with concentrated HCL.

Adjusted the volume to 100 ml with deionized distilled water and stored at 4 °C.

7.3 Running buffer

Tris-base	1.51	gm
Glycine	7.20	gm
Sodium dodesyl sulfate	0.5	gm

Dissolved in 500 ml deionized distilled water and kept at 4 °C.

7.4 Blotting buffer

Tris-base	3.03	gm
Glycine	14.41	gm
SDS	0.5	gm

Added deionized distilled water to 700 ml and mixed well.

Added 200 ml of methanol

Adjusted the volume to 1,000 ml with deionized distilled water and kept at 4 °C.

8. LB broth

Yeast extract	5.0	gm
Tryptone	10.0	gm
NaCl	10.0	gm

Dissolved all ingredients in 1,000 ml distilled water.

Sterilized by autoclave, poured on Petri dish (plate) and kept at 4 °C.

9. LB agar

LB agar	15	gm

Dissolved all ingredients in 1,000 ml distilled water.

Sterilized by autoclave, poured on Petri dish (plate) and stored at 4 °C.

10. 0.1 M $CaCl_2$

$CaCl_2$	1.11	gm

Dissolved in 100 ml distilled water.

Sterilized by autoclave and kept at 4 °C.

11. 85% glycerol

Glycerol	42.5	ml

Added distilled water to 100 ml.

Mixed well, sterilized by autoclave and stored at room temperature.

12. 2×TY broth

Tryptone	16	gm
Yeast extract	10	gm
NaCl	5	gm

Dissolved in 1,000 ml distilled water.

Sterilized by autoclave and kept at 4 °C.

13. 50% glucose

D-glucose	5	gm

Added distilled water to 10 ml and boiled in boiling water.

Filtered through 0.2 μ Millipore filter and stored at 4 °C.

14. TYE

Tryptone	10	gm
Yeast extract	5	gm
NaCl	8	gm

Dissolved in 1,000 ml distilled water.

Sterilized by autoclave and kept at 4 °C.

15. Solid TYE medium

Tryptone	10	gm
Yeast extract	5	gm
NaCl	8	gm
Agar	10	gm

Dissolved in 1,000 ml distilled water.

Sterilized by autoclave, poured on Petri dish (plate) and kept at 4 °C.

16. 0.05 M carbonate buffer, pH 9.6

Na_2CO_3	0.159	gm
$NaHCO_3$	0.293	gm

Dissolved all ingredients in deionized distilled water and filled up to 90 ml.

Adjusted pH to 9.6.

Adjusted the volume to 100 ml with deionized distilled water and kept at room temperature.

17. 0.05% Tween20 in PBS (washing buffer for ELISA and Western blot)

Tween20	0.5	ml

Dissolved in 1,000 ml PBS.

Mixed well and stored at room temperature.

18. 2% solution of 3-aminoprppultriethoxysilane in anhydrous acetone

3-aminopropyltriethoxysilane	3	ml

Added anhydrous acetone to 150 ml.

Mixed well.

Prepared freshly before used.

19. Incubation buffer for cleaved caspase-3 analysis using flow cytometry

Bovine serum albumin (BSA)	0.5	gm

Dissolved in 100 ml PBS.

Stored at 4 °C.

20. Hank's balanced salt solution (HBSS)

NaCl	4	gm
KCl	0.2	gm
KH_2PO_4	0.3	gm
D-glucose	0.5	gm
Na_2HPO_4	0.2393	gm
$NaHCO_3$	0.175	gm

Dissolved all ingredients in 1,000 ml deionized distilled water and kept at room temperature.

APPENDIX C

PRESENTATION AND PUBLICATIONS

List of Presentation

1. Effects of temperature, IPTG and helper phage infection-period on incorporation of CD147ExgpVIII to phage particle. BioThailand 2003: Technology for life at Pattaya, Thailand

List of publications

1. Intasai N, Arooncharus P, Kasinrerk W, Tayapiwatana C. Construction of high-density display of CD147 ectodomain on VCSM13 phage via gpVIII: effects of temperature, IPTG, and helper phage infection-period. Protein Expr Purif 2003;32(2):323-31.
2. Intasai N, Mai S, Kasinrerk W, Tayapiwatana C. Binding of multivalent CD147 phages on U937 cells induces apoptosis. Intl Imm (manuscript in preparation) 2005.

BIOGRAPHY

NAME Miss Nutjeera Intasai

DATE OF BIRTH 11 March 1973

PLACE OF BIRTH Chiang Rai, Thailand

INSTITUTIONS ATTENDED Chiang Mai University, 1991-1995

Bachelor of Science (Medical Technology)

Chiang Mai University, 1997-2000

Master of Science (Medical Technology)

Mahidol University, 2001-2005

Doctor of Philosophy (Medical Technology)

FELLOWSHIP/ RESEARCH GRANT

The Scholarship under the Commission on Higher Education Thai Staff, Ministry of University Affair, Thailand

Supported in part by

Canadian Institutes of Health Research Strategic Training Program "Innovative Technologies in Multidisciplinary Health Research Training", Canada

Supported in part by

The Thailand Research Fund, Thailand

Supported in part by

The National Center for Genetic Engineering and Biotechnology (BIOTEC), Thailand.

POSITION & OFFICE

Department of Medical Technology, Faculty of Associated Medical Sciences, ChiangMai University

Chiang Mai, Thailand

Position: Instructor

Tel. 053 949237

E-mail: nutjeera@chiangmai.ac.th

HOME ADDRESS

110/197 Intawarorote Rd. Sripoom, Mueng, Chiang Mai, Thailand 50200

Tel. 053-947203